THE UNIVERSITY OF SHEFFIELD

Improved Brain-Computer Interface Methods with Application to Gaming

by

James Henshaw

A thesis submitted in partial fulfillment for the
degree of Doctor of Philosophy

in the
Faculty of Engineering
Department of Electronic and Electrical Engineering

June 2018

THE UNIVERSITY OF SHEFFIELD

Abstract

Faculty of Engineering

Department of Electronic and Electrical Engineering

Doctor of Philosophy

by James Henshaw

Brain-computer interfaces (BCIs) are real-time communication systems which bridge the gap between human and machine, extracting useful neural signals from the brain and converting them into commands which allow the user to interact with computers or devices using their thoughts. BCIs have a wide range of applications, including gaming, research and entertainment. And they can also be used as part of an assistive device for disabled users.

This PhD thesis focuses on two BCI types: the steady-state visually evoked potential (SSVEP) BCI, which is operated using gaze control, and the motor imagery-based BCI, which responds to imagined limb movements. Contained within are novel methods designed to improve each BCI type with respect to performance and user experience. New normalisation methods are found to improve SSVEP-BCI performance. A new three-dimensional SSVEP-BCI game *SnookerMaze* is created, along with the Predicted Optimal Colour (POC) SSVEP-BCI, which automatically selects the optimal stimulus colours for a user in order to exploit differences in the way the brain responds to different coloured stimuli. And a feasibility study is conducted where we implement a new method for training users to operate a motor imagery-based BCI, and investigate predictors of BCI performance.

Acknowledgements

Contents

Contents

Contents

Contents

List of Figures

List of Tables

Abbreviations

AgCl	Silver Chloride
BC-CCA	Baseline-Corrected Canonical Correlation Analysis
BCI	Brain Computer Interface
CAR	Common Average Reference
CCA	Canonical Correlation Analysis
CSP	Common Spatial Pattern
DFT	Discrete Fourier Transform
DoF	Degrees of Control
DoF	Degrees of Freedom
ECoG	Electrocorticography
EEG	Electroencephalography
EKG	Electrocardiography
EMG	Electromyography
EOG	Electrooculography
EP	Evoked Potential
ERD	Event-Related Desynchronisation
ERP	Event-Related Potential
ErrP	Error-Related Potential
ERS	Event-Related Synchronisation
FBCSP	Filter Bank Common Spatial Pattern
FES	Functional Electrical Stimulation
FFT	Fast Fourier Transform
fMRI	functional Magnetic Resonance Imaging
FN	False Negative

FP	**F**alse **P**ositive
hBCI	**h**ybrid **B**rain **C**omputer **I**nterface
IDFT	**I**nverse **D**iscrete **F**ourier **T**ransform
IIR	**I**nfinite **I**mpulse **R**esponse
ITR	**I**nformation **T**ransfer **R**ate
KL	**K**ullback-**L**iebler
LCD	**L**iquid **C**rystal **D**isplay
LDA	**L**inear **D**iscriminant **A**nalysis
LED	**L**ight-**E**mmiting **D**iode
MEG	**M**agneto**e**ncephalo**g**raphy
MI	**M**otor **I**magery
POC	**P**redicted **O**ptimal **C**olour
PSDA	**P**ower **S**pectral **D**ensity **A**nalysis
RVS	**R**epetitive **V**isual **S**timulus
SMR	**S**ensori**m**otor **R**hythms
SNR	**S**ignal-to-**n**oise **R**atio
SQUID	**S**uperconducting **Q**uantum **I**nference **D**evice
SSVEP	**S**teady-**S**tate **V**isually **E**voked **P**otential
SVM	**S**upport **V**ector **M**achine
TCP/IP	**T**ransmission **C**ontrol **P**rotocol/**I**nternet **P**rotocol
U-DP	**U**se-**D**ependent **P**lasticity
UDP	**U**ser **D**atagram **P**rotocol
VEP	**V**isually **E**voked **P**otential

For Heidi, and my family. . .

List of Contributions

Henshaw, J., Liu, W., & Romano, D. (2014). Problem solving using hybrid brain-computer interface methods: A review. In *Cognitive Infocommunications (CogInfoCom), 2014 5th IEEE Conference on* (pp. 215-219). IEEE.

Henshaw, J., Liu, W., & Romano, D. (2017). Improving SSVEP-BCI Performance Using Pre-Trial Normalization Methods. In *Cognitive Infocommunications (CogInfoCom), 2017 8th IEEE Conference on*, In Press. Winner of "Best Paper Award"

Chapter 1

Introduction

1.1 What is a BCI?

A brain-computer interface, or BCI, is a communication system which allows users to send commands to external electronic devices such as computer, using signals directly from their brain. These signals bypass the usual system of peripheral muscles [1], and therefore, BCIs are often described as systems which provide an additional communication channel.

BCIs have been used in a wide variety of applications and fields: gaming and entertainment; intelligent mobility devices for disabled users; rehabilitation methods for disabled users; neurofeedback devices; and used in research across a multitude of disciplines. More details on BCI applications can be found in Chapter 3.

Work in this thesis focuses primarily upon two types of BCI: the steady-state visually evoked potential (SSVEP) BCI, which is operated using the brain's response to repetitively flickering visual stimuli, and the motor imagery BCI, which is operated using the brain's responses that are elicited when the user imagines moving their limbs. More details on both of these BCI types can be found in Chapter 2.

1.2 Limitations of the BCI

The BCI suffers from several limitations, both in how it functions and how it is set up. Most BCI-types are fatigue-inducing, meaning they cannot be comfortably

operated for long periods. Motor imagery-based BCIs in particular require large amounts of training sessions, as well as calibration data on the day of use, in order to be operated effectively. They also suffer from somewhat unreliable classification accuracy, and a low information transfer rate. Another issue is 'BCI deficiency', also known as 'BCI illiteracy', which is when a user is unable to control a type of BCI to any reasonable standard, and despite research into the topic, it is not particularly well understood.

1.3 Thesis Motivation

Brain-computer interfacing is an exciting research area that is still in its relative infancy. It has potential multidisciplinary applications to a huge number academic and commercial fields; any field involving human behaviour has a potential overlap with BCI research. As will be discussed in Chapter 3, promising research demonstrates the positive impact that BCIs can have on disabled users, as well as the strong technological advancements that have been made with gaming BCIs. Despite the wide potential impact of BCIs, there is still a lot to do in the field; BCI systems are currently used mainly as a research tool rather than a widely-available, affordable piece of technology that can easily be used in one's own home. Commercial BCIs are currently available, therefore the focus should be on developing automatic methods that require minimal user input. Despite the application to gaming, most of the challenges undertaken in this thesis are relevant to non-gaming areas of BCI research as well.

1.4 Contribution to Knowledge

This thesis contributes to knowledge in several ways; Firstly, in terms of automaticity, by providing automatic methods that can be applied to improve BCI performance without requiring expert input. This work will help to push BCIs further towards being used in the home more easily. Additionally, it contributes new methods which improve SSVEP-BCI performance both technologically and from a user-centred viewpoint. Finally, it contributes a new multi-layered approach to training users to operate a BCI using imagined movements.

1.4.1 Summary of Findings and Achievements

1. Two novel normalisation methods, Baseline-Corrected CCA (BC-CCA) and Scaled CCA, are found to improve SSVEP-BCI performance without calibration data

2. The Predicted Optimal Colour (POC) SSVEP-BCI is introduced, which automatically selects the best combination of stimulus colours for the user

3. The POC SSVEP-BCI is evaluated and found to improve users' gaming performance, and improve their mood

4. A new SSVEP-BCI game is developed

5. A novel approach to training participants to operate an SMR-BCI is employed

6. Correlations between resting alpha and BCI performance are found both in an existing single-session dataset, and in our participant across a large number of BCI training sessions.

1.5 Thesis Objectives

This thesis focuses on gaming BCIs, and the motivation behind the work is to alleviate many of the inherent limitations of BCIs in order to improve gaming BCIs both in terms of performance and user experience. The topics investigated include: improving BCI performance using normalisation; improving the gaming BCI by using stimulus colour information; creating a BCI controlled by imagined movements that takes both a technology- and user-centred approach; and predictors of BCI performance while training to use a motor imagery BCI.

1.5.1 Solving the SSVEP-BCI Stimulus Selection Problem

One of the main limitations of the SSVEP-BCI is the restrictions related to stimulus selection. Factors such as stimulus size, proximity, colour, and frequency can have a large impact on SSVEP performance, the effects of which may vary from user to user. For the SSVEP-BCI to successfully become part of a commercial

gaming device that users can easily enjoy in their own homes, rather than perpetually existing as a research application, solutions must be found to the stimulus selection problem. Additionally, any solutions should ideally work automatically without any expert input, and work without negatively affecting the BCI too greatly. Due to the magnitude of the problem, this thesis will focus on two main areas of SSVEP stimulus selection:

1. **Stimulus frequency selection:** Chapter 4 explores the problem of frequency selection. Two novel solutions are proposed and evaluated.

2. **Stimulus colour selection:** In Chapter 5 the problem of frequency selection is addressed. A new SSVEP-BCI with automatic stimulus colour selection, the Predicted Optimal Colour (POC) SSVEP-BCI, is proposed and evaluated.

1.5.2 A User-Centric BCI that Improves User Experience

Loup-Escande et al. [2] distinguish between a 'technocentric' and 'anthropocentric' approaches to creating a gaming BCI. BCI research generally focuses on improving one of these areas: either taking a technocentric approach by focusing on increasing accuracy or speed for example, or taking the anthropocentric approach of improving user experience. However, these approaches are actually complementary — a good user experience would be expected to produce a good performance, and vice versa — therefore, this thesis will use an approach which focuses on improving both areas simultaneously.

Chapter 3 reviews BCI applications in order to assess the current technocentric and anthropocentric state-of-the-art in BCI research, in order to fully understand what can be expected from a modern BCI.

The POC-SSVEP-BCI, introduced in Chapter 5, is aimed at increasing BCI performance and improving user experience. Several measures of user-experience are taken, and the results contextualised both in terms of how both aspects of BCI usage can be improved.

Chapter 6 details the design and evaluation of a user-centred BCI, controlled using imagined movements. This chapter also investigates predictors of performance

accuracy for new users as well as for a longtime user as they learn to use the BCI over time, forming a feasibility study for this longitudinal approach.

The desired outcome of this approach is to advance knowledge on creating a BCI that is both technocentrically and anthropocentrically sound.

1.6   Outline of the Thesis

Chapter 2 gives a detailed review of methods used in brain-computer interfacing, including brief introductions to: brain function, neural imaging, signal processing, and machine learning methods used in BCI research. Chapter 3 summarises BCI applications in rehabilitation and gaming, as well as research into normalisations methods used in SSVEP-BCI research, the influence of stimulus colour on the SSVEP-BCI performance, and the relationship between psychological factors (mood and fatigue) and BCI performance. Chapter 4 proposes and evaluates normalisation techniques aimed at improving the performance of the SSVEP-BCI. Chapter 5 details the creation of an SSVEP-BCI controlled three-dimensional game, and investigates whether stimulus colour information can be exploited to improve SSVEP-BCI performance. Chapter 6 details the process of training a user to operate a gaming BCI using imagined movements. Lastly, Chapter 7 contains the thesis conclusions and plans for future work.

Chapter 2

Technical Background

2.1 Introduction

This chapter covers the background material relevant to designing and implementing a brain-computer interface, and includes an introduction to the brain's structure and functionality, reviews various recording and signal processing methods required to produce a usable signal, and discusses BCI classification methods. Fig. 2.1 briefly outlines these steps, which include:

- **Brain Signal Acquisition:** Recording neural data

- **Preprocessing:** Applying signal processing methods such as filtering and artifact removal, to improve signal quality

- **Feature Extraction:** Identifying and extracting informative features from the recorded neural data

- **Classification:** Using the extracted features to create a classifier that can distinguish between different cognitive states

- **Device Control:** Using the classifier outputs as a communication channel that can directly interact with an external device

- **Feedback:** Providing real-time feedback to the user, which allows them to adapt their strategy if necessary, to improve performance
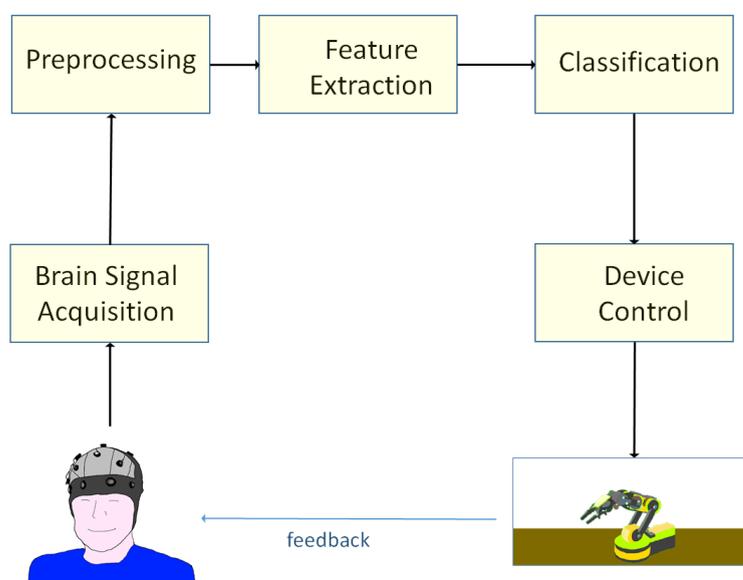
FIGURE 2.1: BCI block diagram

2.2 Definitions

2.2.1 Synchronous or Asynchronous BCI

A BCI can be either synchronous or asynchronous. When operating a synchronous BCI, a user has no control over when a command is sent, and instead have to adjust their actions to coincide with the BCI's timing to achieve the best performance; for example, minimising blinking and muscle movements whenever leading up to the active period. Asynchronous BCIs, also known as self-paced BCIs, allow the user to regulate the pace of the BCI, and voluntarily cease sending commands to the BCI if desired. Technically, asynchronous BCIs are harder to implement than synchronous BCIs. This is mainly due to difficulties detecting the brain's so-called 'idle' state, which is something of a misnomer, as the brain is constantly active. As a result, it is difficult to know when the user *does not* want to sent a command. However, several methods have been devised to achieve this asynchronicity, including: using thresholding, where commands are only sent when the user's brain activity surpasses a predetermined threshold; using a so-called 'brain-switch', where a neural command is used to start or stop the BCI sending commands; or even using muscle movements or blinks as a trigger to start or stop BCI functions.

2.2.2 Invasive or Non-invasive BCI

A BCI can be classified as invasive or non-invasive, based on whether or not it penetrates the skin. They also differ in terms of the type of signals they acquire: invasive BCIs measure local field potentials (LFP) directly by penetrating brain tissue [3], whilst non-invasive BCIs measure scalp potentials from the surface of the head. More details on invasive and non-invasive methods can be found in 2.4.

2.3 Neurophysiological Underpinnings of the BCI

Due to the complexity of the brain it is impractical to give a detailed summary of its functions; instead, this section will outline aspects relevant to brain-computer interfacing, and the work contained within this thesis, including: neuronal function, and an overview of the brain's structure.

2.3.1 The Brain

The brain is a powerful organ made up of an estimated 86 billion neurons and 85 billion non-neuronal cells [4]. The largest part of the brain is know as the cerebrum, which contains an outer layer of tightly-packed neurons known as the cerebral cortex. The cerebral cortex is divided into four main lobes (Fig. 2.2):

- Frontal lobe: associated with maintaining working memory and the selection of goals [5], as well as movement [6]

- Parietal lobe: plays a role in episodic memory retrieval [7] and directing visual attention [8]

- Temporal lobe: associated functions include spatial awareness [9] and auditory perception

- Occipital lobe: plays a large role in visual processing [10]
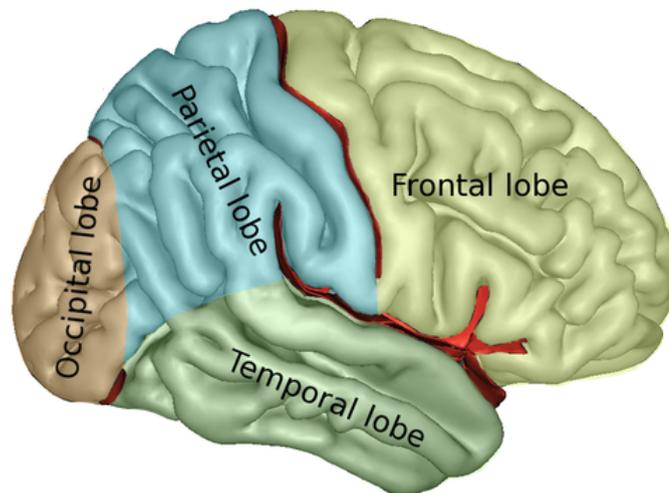
FIGURE 2.2: Lobes of the cerebral cortex by Sebastian023 (licensed under CC BY 3.0)

2.3.2 Neuronal Function

Neurons (Fig. 2.3) are the individual brain cells responsible for communication within the brain, whose activity make brain function possible. Neurons communicate via electrical impulses and chemical transmissions; when enough neurotransmitters (chemical messengers) are received at the neuron's tree-like dendritic branches, it triggers an action potential (large voltage change) which travels from the soma, along the axon, to the axon terminal, where it can trigger the release of neurotransmitters.

2.4 Recording Methods

Methods for recording brain activity can be broadly grouped into two classes: *invasive methods*, which require some components to be inserted into the body, and *non-invasive methods*, which do not. This section outlines the most popular methods available.
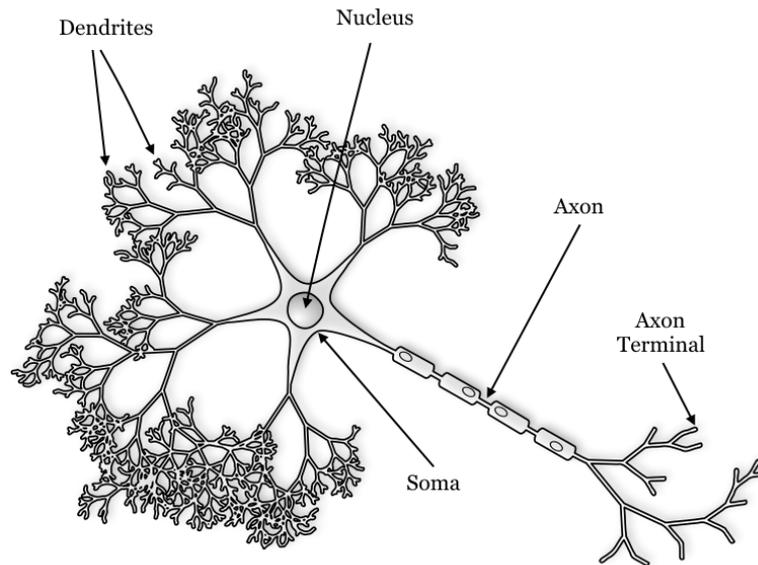
FIGURE 2.3: Neuron diagram by Nicolas Rougier (licensed under CC BY 3.0)

2.4.1 Invasive Methods

Intracortical microelectrodes arrays implanted into the brain's cerebral cortex give an extremely high spatial and temporal resolution. Researchers have demonstrated their potential for use in a number of BCI studies; Collinger et al. [11] and Hochberg et al.'s [12] studies demonstrated that tetraplegic users could learn to control a robotic arm with 7 degrees of freedom. The main disadvantages of intracortical electrodes are that they require surgery, and that the brain can recognise them as a foreign body, often leading to inflammatory responses such as 'glial scarring' [13].

Electrocorticography (ECoG) involves measuring cortical field potentials using electrode placed upon the outer surface of the brain, the cerebral cortex. Technically, ECoG could be classed as *partially-invasive*, as it is implanted below the skull but outside of the brain. ECoG has the benefit of having both high temporal and spatial resolution. The main disadvantage is that surgery is required to implant the electrodes.

FIGURE 2.4: Dry EEG

2.4.2 Non-invasive Methods

Electroencephalography (EEG), which will be the main method of use in this thesis, measures differences in electrical potential which are caused by neural activity within the brain. EEG signals are acquired via electrodes on the surface of the scalp. Extracting a signal strong enough for use requires the synchronised action of thousands or millions of cortical neurons [14], mainly because EEG scalp potentials become blurred as they pass through the brain, skull, and scalp tissues. Scalp electrodes are usually placed according to the 10-20 system, where electrode spacing between adjacent electrodes is either 10 or 20% of the skull's diameter, from front-to-back or left-to-right [15]. Electrode locations are generally labelled based on which brain area they are situated above, with Fp, F, C, P, and O representing the frontopolar, frontal, central, parietal, and occipital brain regions, respectively. EEG electrodes can be water-based, gel-based, or dry (Fig. 2.4). Gel electrodes can be time-consuming to apply, and require that participants have gel applied to their hair, which some users may find unpleasant. Dry electrodes are much quicker to apply, albeit at the expense of signal quality, as they have been found to lead to increased impedance, as well as increased broad-band noise [16].

Magnetoencephalography (MEG) measures the magnetic disturbance caused by neuronal activity. MEG signals are acquired using superconducting quantum inference devices (SQUIDs [17]), which are placed in an array over the scalp.

Functional magnetic resonance imaging (fMRI) detects changes in blood oxygenation level; these changes are associated with neuronal activity. fMRI is performed

in an fMRI machine, and works by creating a magnetic field which alters the state of protons in the body. The different rates of 'relaxation' (the time required for protons to return to their initial state) allow researchers to calculate the blood oxygenation level in any part of the brain at a particular moment.

Near-infrared spectroscopy (NIRS) is also used to measure neural changes related to blood oxygenation levels. Near-infared light is able to pass through skin and bone on the surface of the head, and is absorbed by haemoglobin. Measuring the absolute change in oxyhaemoglobin (HbO_2) and deoxyhaemoglobin (Hb) gives researchers the ability to monitor the changes in haemoglobin, thereby monitoring the oxygenation and haemodynamic activity associated with neural activity [18].

The aforementioned methods all differ in terms of strengths and weaknesses: EEG has a high temporal resolution, which is on the order of milliseconds, but poor spatial resolution (order: cm^3); MEG has high temporal resolution (milliseconds) and spatial resolution which is poor but superior to EEG; fMRI has poor temporal resolution (1-2 seconds) and good spatial resolution (order: $64mm^3$) [19]. Near-infrared spectroscopy (NIRS) methods can potentially achieve a spatial resolution on the order of centimetres, but this comes with a poor depth resolution [20] .

2.5   Signal Production

BCI signal production is where the user produces brain activity that can be used to operate a BCI. There are many different methods for producing this brain activity, only some of which are utilised in this thesis. Therefore, in this section we discuss the most relevant and most influential BCI signal production methods.

2.5.1   Evoked Potentials

Evoked potentials (EPs) refer to a group of signals that are elicited involuntarily by external stimuli. EPs evoked by visual, auditory, or somatosensory stimuli have all been used to operate a BCI.

Steady-State Visually Evoked Potentials (SSVEP): The steady-state visually evoked potential (SSVEP) refers to a type of visually evoked potential (VEP), a brain response that is elicited by visual stimulus. The SSVEP is phase-locked

and can be elicited by a repetitive visual stimulus (RVS) such as a flickering light [21], or a reversing pattern [22], and becomes 'steady' if the stimulus presentation rate is above a certain frequency. SSVEP responses are detected mainly by electrodes placed above the occipital and parietal lobes [23], and have a wave-like spatial structure [24] with similar frequency characteristics to that of the triggering input. The RVS initiates the selection of a cortical network that can oscillate at that same frequency [25], meaning the response matches the input with a good signal-to-noise ratio. SSVEP-BCIs are popular due to their short training time, high classification rate [26], and the fact that they can be detected using non-invasive neuroimaging methods such as EEG. They have been used in a diverse range of BCI types, including BCI-controlled exoskeletons [27], [28], wheelchairs [29], [30], and robotic humanoids [31]. As with all other signal production methods, the overall goal is to maximize the signal-to-noise ratio (SNR) using various methods. Researchers can determine which stimulus is being observed by searching the brain signals for specific frequencies related to the RVS frequency. While the brain has been found capable of producing SSVEP responses to RVS frequencies ranging from 1-90 Hz [21], optimal stimulation frequencies are found within the range of 5.6-15.3 Hz, with a strongest response at 12 Hz [22]. Bakardjian et al. [22] reported that selection between 8 commands yielded a mean classification accuracy of 98% (96-100%) and a mean command recognition delay of 3.4s (2.5-4.2s). The main advantage of using an SSVEP-based BCI is the high signal-to-noise ratio (SNR) and therefore high accuracy. The main disadvantage is that viewing the RVS carries an epilepsy risk [32], and long sessions can cause the user to become fatigued [33].

2.5.2 Neural Rhythms

Brain oscillations are usually categorised into specific frequency bands (Fig. 2.5); delta: < 4 Hz, theta: 4-7 Hz, alpha: 8-12 Hz, beta: 12-30 Hz, and gamma: > 30 Hz [26]. Oscillations recorded from the somatosensory and motor cortices are referred to as sensorimotor rhythms (SMRs) [34], and the alpha rhythm is referred to as the mu rhythm. Changes in the amplitude of SMRs can be used to make inferences about the user's cognitive state, and is known as an SMR-BCI.

(a) Delta rhythm

(b) Theta rhythm

(c) Alpha rhythm

(d) Beta rhythm

(e) Gamma rhythm
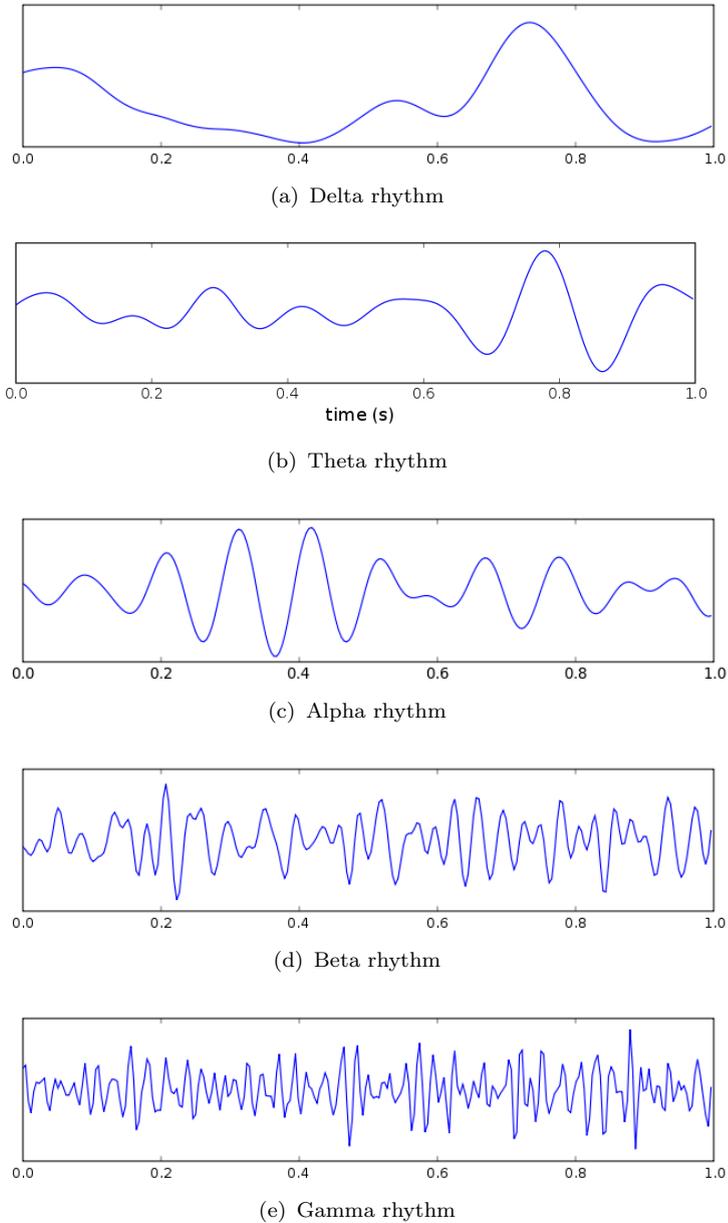
FIGURE 2.5: Brain waves recorded over one-second (credit: Hugo Gamboa)

2.5.3 Event-Related Desynchronisations/Synchronisations

Event-related desynchronisations (ERD) and event-related synchronisations (ERS) are detectable changes in SMRs that accompany imagined or actual motor tasks. The ERD is a decrease in power in the upper alpha (mu) band and lower beta band, occurring in the contralateral hemisphere approximately two seconds before movement onset, and becoming bilaterally symmetrical immediately before movement onset [14]. The ERS is an increase in power which appears after completion of the motor task. The ERS can also occur simultaneously with the ERD, but

15
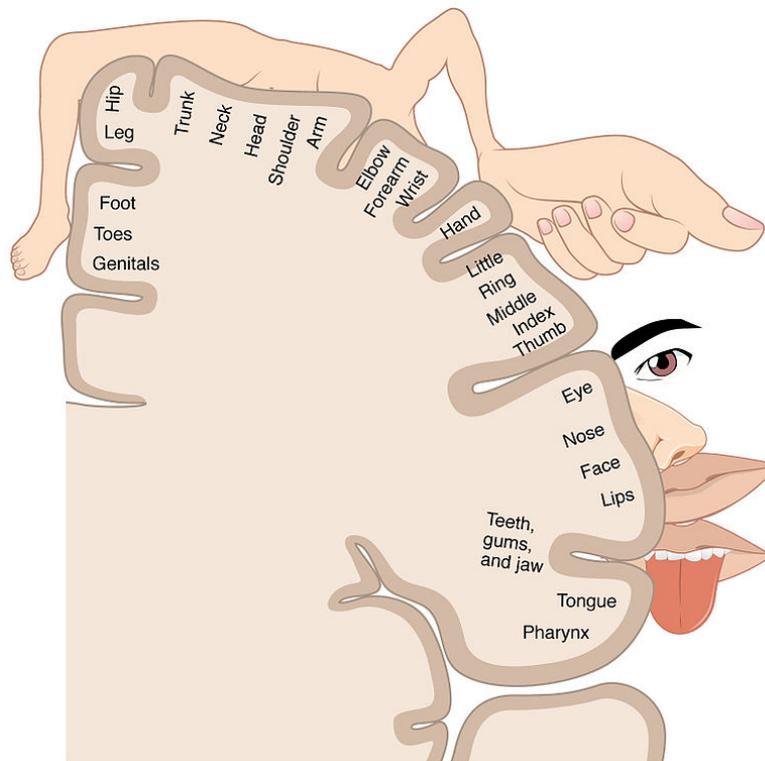
FIGURE 2.6: A 2-D cortical sensory homunculus, by OpenStax College (licensed under CC BY 3.0)

in this case it occurs in a different cortical area [35]. ERD/ERS are produced topographically with respect to the homuncular organisation of the sensorimotor cortices (Fig. 2.6). This means that ERD and ERS activity generated in relation to foot movement will appear most prominently over the foot region of the sensorimotor cortex. The homuncular organisation also means that current non-invasive BCIs struggle to distinguish between movements from the two feet, as they are located close together (both are located approximately between the brain's medial longitudinal fissure), as well as between individual finger movements. They can, however, distinguish between foot, right-, and left-hand movements due to their large distance from one another.

2.5.4 Event-Related Potentials

Event-related potentials (ERPs) are brain responses that are elicited by some event, and show a stable relationship with this event. The definition of ERPs is similar to, and sometimes used interchangeably with that of EPs [36]; however, the
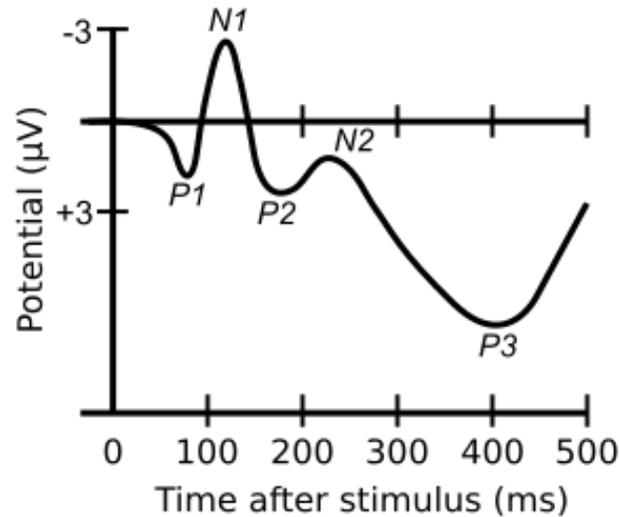
ERP can essentially be seen as something that produces a measurable waveform following an event's onset.

P300: A P300 evoked potential (also known as P3b) is a positive peak registered in the parietal cortex which occurs 300ms after stimulus onset, and is an example of an ERP. It was discovered by Sutton et al. [37] and is elicited when unlikely events occur between events with high probability. The P300's main use in BCI research is in the 'P300 speller' [38], which is a grid of letters (typically 6×6) from which a user can select individual letters by focusing their gaze upon them. The letters flash randomly, however, the BCI is time-locked to these flashes (termed, the 'oddball paradigm' [39]), and letter selection is based upon P300 wave generation. Guger et al. [40] tested the P300 signal's ability to be used for spelling, finding an overall classification accuracy of 91%. Also, 72.8% of participants could use the P300 signal to spell words with 100% accuracy, while less than 3% demonstrated complete BCI deficiency with the P300. The main advantages of using a P300-based BCI are the relatively short training times, and the high accuracy. The main disadvantage is its lack of speed.

Error-related Potentials: Error-related potentials (ErrP) [41] refer to a brain's response to the user detecting a mistake, which can be used to operate a BCI, usually for automatic error correction.

17

Artefact	Characteristic	Cause	Removal
EOG	High amplitude deflections in 3-4 Hz range	Eye movements/ blinking	ICA, eye channel
EMG	Mainly in the > 30 Hz range	Bodily movements, e.g. head/face neck	Filtering high frequency data
Signal distortion	Signal drift	Skin conductance change, e.g. sweating	-
EKG	Very low frequency artefacts	Heart beat	Low-pass filtering (e.g. 0.5 Hz)

TABLE 2.1: Common EEG artifacts

2.6 Preprocessing

The goal of the preprocessing stage is to improve the signal-to-noise ratio (SNR) and spatial resolution through the removal of artifacts. Artifacts are unwanted additions to the signal which can contribute positively or negatively to a BCI's performance, and can be removed using methods such as referencing and filtering the data. Sanei and Chambers [42] identify a number of possible artifact sources, including muscles (electromyogram, EMG), eyes (electrooculogram, EOG), interference from electrical sources, and cable defect artifacts. To remove artifacts the signal must be amplified and filtered. A list of common EEG artifacts is available in Table 2.1. Another artifact removal technique is thresholding, where a threshold is set for an input signal (e.g. EOG) and epochs where the signal's amplitude exceeds the threshold are deemed to be contaminated and are removed.

2.6.1 Downsampling

Due to the complexity of brain activity, EEG data is extremely high-dimensional, which, as a result makes it inherently difficult to classify. Downsampling is a form of dimensionality reduction that reduces the sampling rate. EEG recorded at 1000 Hz can be downsampled to 500 Hz by discarding every other sample. This reduces complexity, and can improve BCI performance if used correctly.

2.6.2 Temporal Filtering

Discrete Fourier Transform Filters

The Discrete Fourier Transform (DFT) is a method for converting a signal from the time domain into the frequency domain, removing all temporal information from the signal and representing it as a sum of sinusoids instead. DFT filtering of a signal x_n is a three-step process, which involves: transforming the signal into the frequency domain; setting all coefficients outside of desired range to 0; and then transforming the signal back to the time domain. DFT filtering can be performed using:

$$X_k = \sum_{n=0}^{N-1} x_n e^{-\frac{2\pi i}{N} kn} \tag{2.1}$$

where N is the number of samples, k reflects the sinusoidal frequency at k/N samples, e is Euler's constant, and i is an imaginary number with $i^2 = -1$. After setting all coefficients outside of the target frequencies to zero, the signal is transformed back to the temporal domain using the inverse DFT (IDFT):

$$x_n = \frac{1}{N} \sum_{k=0}^{N-1} X_k e^{\frac{i2\pi kn}{N}} \tag{2.2}$$

Finite Impulse Response Filters

A finite impulse response (FIR) filter is a linear filter whose response to an input is of finite length. The FIR response is calculated based upon the last M samples of unfiltered signal $s(n)$. Filtered signal $y(n)$ is found using:

$$y(n) = \sum_{k=0}^{M} b_k s(n-k) \tag{2.3}$$

where b_k is a vector containing the feedforward filter coefficients, $s(n)$ is the raw unfiltered signal.

Infinite Impulse Response Filters

Infinite impulse response (IIR) filters are recursive digital filters whose response to an input is of infinite length. The IIR response is based on both the last M samples of $s(n)$, as well as the outputs of the previous P filter operations. Filtered signal $y(n)$ is found using:

$$y(n) = \sum_{k=0}^{M} b_k s(n-k) + \sum_{k=1}^{P} a_x y(n-k) \tag{2.4}$$

where a_x is a vector containing the feedback filter coefficients.

Temporal Filter Applications

High-pass filtering: Low-frequency signals are often associated with artifacts, such as those that accompany breathing, amplifier drift, and changes in skin resistance due to sweat. Most can be removed by a high-pass filter with a cut-off frequency of around 0.5-1 Hz. Electrocardiogram (ECG) artifacts may also be detectable by EEG [43]; however, the effects of this low-frequency signal can also be reduced using a high-pass filter.

Low-pass filtering: High-frequency noise is often removed using low-pass filters with a cut-off frequency around 50-70 Hz [42].

Band-pass filtering: Band-pass filters can be used to extract various useful frequency bands, which can be those associated with motor imagery such as mu and beta bands. Even BCIs that do not rely on spectral information, such as the P300-BCI, are usually filtered before detection. P300-BCI signal detection usually involves band-pass filtering between 0.1-20 Hz.

Notch filtering: Notch filters are a type of band-stop filter which is typically of a very high order. They can be used to remove 50 or 60 Hz line noise.

Zero-phase filtering: Zero-phase filters apply a time reversal to data during the filtering process in order to prevent phase distortions and signal delay. The filter works by initially filtering the data, reversing and filtering again, and then reversing the data again. Despite the benefits of zero-phase filtering, it is generally reserved for offline data, as it is non-causal, and relies on future inputs.

2.6.3   Spatial Filtering

2.6.3.1   Reference Electrodes

In EEG BCIs, reference electrodes are used to find the voltage for each channel. The voltage, which is the difference in electrical potential between two points, is found by placing the reference electrode on a nearby location and then calculating the difference. The mastoid bone (behind the ear) is the most common reference location [44–46]; however, tactical reference placement can yield significant advantages.

2.6.3.2   Scalp Reference

Choosing a scalp electrode as a reference removes noise that is common to that part of the brain. This has been used in numerous studies, for example in SSVEP studies using references in central and parietal locations [47–49] to isolate the SSVEP activity, which is usually best detected by electrodes above the occipital lobe.

2.6.3.3   Bipolar Reference

Subtracting s_j, the signal from channel j, from s_i, the signal from channel i, produces a new bipolar channel $\tilde{s}_{i,j}$.

$$\tilde{s}_{i,j} = s_i - s_j \qquad (2.5)$$

2.6.3.4   Common Average Reference

Common average reference (CAR) works by subtracting the average signal of all electrodes from each electrode, at each time point. This method is good at reducing noise that is common to all electrodes (e.g. 50 or 60 Hz power source noise), and at enhancing signals contained in a small number of electrodes. However it is not good at reducing noise that is common only to a few electrodes, such as EOG, or EMG. For this reason CAR is usually used in conjunction with other methods to

remove other artifacts. Applying CAR to an electrode montage with N electrodes uses:

$$\tilde{s}_i = s_i - \frac{1}{N} \sum_{i=1}^{N} s_i \qquad (2.6)$$

where N is the number of channels, and $\tilde{s}_i$ is a single spatially filtered channel.

2.6.3.5 Surface Laplacian

Laplacian reference works by adjusting the signal at each electrode, subtracting the average of the four neighbouring electrodes ('small Laplacian') [50] or the four next closest ('large Laplacian') [51]. This method is useful for reducing noise that is specific to a certain region.

$$\tilde{s}_i = s_i - \frac{1}{4} \sum_{i \in \Theta} s_i, \qquad (2.7)$$

where Θ represents the electrodes of the small or large Laplacian reference.

Numerous referencing methods can be applied, individually or in some cases, together. The goal is to apply methods that remove the most noise without removing too much useful information from the signals of interest.

2.6.3.6 Common Spatial Pattern (CSP)

CSP is a technique which finds spatial filters that maximise the variance between EEG signals from two conditions. Its use in BCI research was popularised by Ramoser et al. [52], and since then it has had numerous adaptations [53] and expansions for multiclass classification [54].

Common Spatial Pattern (CSP) works by finding spatial filters w which maximise variance in one class, and minimise variance in the other. A fully trained CSP spatial filter filters the data into a form where the top row's activity corresponds mostly to one class, whilst the bottom row's activity corresponds mostly to the other class. CSP is particularly effective in BCIs based on oscillatory activity,

for example, classifying between left and right hand motor imagery. Data is initially bandpass filtered into a relevant band, such as 8-30 Hz (which includes both the alpha and beta rhythms). Next, the EEG's normalised spatial covariance is obtained, using:

$$C = \frac{EE^T}{trace(EE^T)}, \tag{2.8}$$

where E is the bandpass filtered EEG data of size $N \times T$, where N represents the number of channels and T represents the number of samples. $(\cdot)^T$ denotes the transpose operator, while $trace(\cdot)$ is the sum of the diagonal elements of a square matrix. Next, taking the average over trials of C for each class gives the spatial covariance $\bar{C}_d, \in [l, r]$. The composite spatial covariance is therefore:

$$C_c = \bar{C}_l + \bar{C}_r. \tag{2.9}$$

C can be expressed in terms of eigenvalues and eigenvectors:

$$C_c = U_c \lambda_c U_c^T, \tag{2.10}$$

where λ_c is the diagonal matrix of eigenvalues, and U_c is the eigenvector matrix. Next, variances within U_c are equalised using the whitening transform:

$$P = \sqrt{\lambda_c^{-1} U_c^T}. \tag{2.11}$$

By transforming $\bar{C}_l$ and $\bar{C}_r$, so that:

$$S_l = P\bar{C}_l P^T \quad \text{and} \quad S_r = P\bar{C}_r P^T \tag{2.12}$$

it can be shown that S_l and S_r share common eigenvectors. If:

$$S_l = B\lambda_l B^T, \quad \text{then} \quad S_r = B\lambda_r B^T, \quad \text{and} \quad \lambda_l + \lambda_r = I, \tag{2.13}$$

where I is the identity matrix, and B represents the eigenvectors. Two corresponding eigenvalues sum to one, meaning that an eigenvector with a large eigenvalue

for S_l will have a small eigenvalue for S_r, which gives the CSP algorithm its ability to separate the variances between classes so effectively. Finally, the projection matrix $W = (B^T P)^T$ is used to perform the spatial filtering:

$$Z = WE, \tag{2.14}$$

where Z is the spatially filtered single trial. Details on how this method can be used to extract useful class-relevant features from EEG are described in 2.9.

2.6.4 Source Localisation

Activity at EEG sensors placed over a certain brain location is not necessarily representative of activity occurring at that brain location. EEG electrodes cover a large area, and the signal must also pass through layers of bone, skin, and hair. Source Localisation (SL) is a source reconstruction method which uses multichannel EEG data to model the spatiotemporal processes of the brain's neural currents. SL works by mapping EEG onto a higher dimensional source grid [55] where dipoles represent individual source activity. Performing SL usually requires an MRI image of the user's head, from which an anatomical model can be created although a standardised model can be adapted to match the user's head if this is not possible. There are two main aims of SL: either forward modeling, which aims to reconstruct EEG data, given the source activity; or inverse modeling, which aims to estimate the current source locations and strengths that produce a given set of EEG data.

2.7 Feature Extraction

The aim of feature extraction is to select features that characterise the user's current activity and represent them as a feature vector. EEG data is too complex and high-dimensional to control a BCI without being reduced; feature extraction effectively discards unwanted data and retains data that is relevant to making the BCI function. There are many different forms of feature extraction used in BCI. They can be separated into several groups, including: time-domain, frequency-domain, and spatial features. Switching between the time and frequency domains can be

achieved through decomposition methods such as the Discrete Fourier transform (DFT) and the inverse discrete Fourier transform (IDFT), via efficient algorithms known as fast Fourier transforms (FFTs) which allow the DFT to be calculated much faster. Analysing a signal plotted in the time-domain shows how the signal varies over time and therefore allows one to view time-dependent phenomena, for example the P300 wave, which appears 300ms after stimulus onset, would only be visible in the time-domain. Analysing an EEG signal in the frequency-domain produces no temporal information, but instead shows how much of a signal lies in a particular frequency band with regards to a number of given frequencies. This can be used to identify SSVEPs, assuming an appropriately sized time window is selected.

2.7.1 Amplitude Features

The amplitude of a signal can be used to train a classifier, for example, with detection of the P300 wave in the P300 speller.

2.7.2 Band power Features

The average power of a signal within a particular frequency band can be used as a feature, known as a band power feature. This is found by bandpass filtering the signal and taking the average of the absolute value within that band. A new type of feature can be made by applying the log-transform to these features [56], which approximates normal distribution, and produces what are sometimes known as log-band power features. Either type of feature can be used to train a classifier for use in a BCI.

2.7.3 Power Spectral Density Features

The process of transforming a signal into the frequency domain using the DFT can be used to produce usable BCI features. Power spectral density (PSD) features can be found by squaring the power spectrum and using the values at the frequency of interest to train a classifier. This method can be used in motor imagery, SSVEP [57–59], and many other BCI types.

2.7.4 Canonical Correlation Analysis

CCA detects the underlying correlation between two multidimensional variables, and can be used to perform unsupervised SSVEP detection on EEG data [60–64]. Given two multidimensional variables $\boldsymbol{X}$ and $\boldsymbol{Y}$ with weighted linear combinations $\boldsymbol{x} = \boldsymbol{X}^T\boldsymbol{W_X}$ and $\boldsymbol{y} = \boldsymbol{Y}^T\boldsymbol{W_Y}$, CCA finds weight vectors $\boldsymbol{W_X}$ and $\boldsymbol{W_Y}$ which maximise the correlation between $\boldsymbol{x}$ and $\boldsymbol{y}$. This is achieved by solving the following optimisation problem:

$$
\begin{aligned}
\max_{\boldsymbol{W_X},\boldsymbol{W_Y}} \rho(\boldsymbol{x},\boldsymbol{y}) &= \frac{E[\boldsymbol{xy}]}{\sqrt{E[\boldsymbol{xx}]E[\boldsymbol{yy}]}} \\
&= \frac{E[\boldsymbol{W_X^T X Y^T W_Y}]}{\sqrt{E[\boldsymbol{W_X^T X X^T W_X}]E[\boldsymbol{W_Y^T Y Y^T W_Y}]}},
\end{aligned}
\tag{2.15}
$$

where $E[x]$ is the expected value of x, and ρ is the correlation value, which is maximised with respect to weight vectors $\boldsymbol{W_X}$ and $\boldsymbol{W_Y}$, thereby calculating the canonical correlation between $\boldsymbol{X}$ and $\boldsymbol{Y}$.

During SSVEP detection, $\boldsymbol{X} \in R^{C \times S}$ is the multidimensional EEG signal with C channels and S samples. $\boldsymbol{Y}_f \in R^{2N_h \times S}$ is the set of multidimensional reference signals based on stimulus frequency f, with $2N_h$ individual sine waves and S samples, where N_h is the number of harmonics. The sine waves are assembled into a matrix [60]:

$$
Y_f = \begin{bmatrix} \sin(2\pi f t) \\ \cos(2\pi f t) \\ ... \\ \sin(2\pi N_h f t) \\ \cos(2\pi N_h f t) \end{bmatrix},
\tag{2.16}
$$

where t is the time in seconds. By performing CCA on $\boldsymbol{X}$ and $\boldsymbol{Y_f}$ for all f, the stimulation frequency with the maximal canonical correlation value can be identified, which is selected as the estimated SSVEP frequency.

2.7.5 Common Spatial Pattern Features

The method outlined in 2.6.3.6 details how to train spatial filter W, which filters EEG data into spatially filtered signal Z. As the rows of Z are separated, maximally in terms of variance between classes one and two, the outer m rows are selected. Taking the signals Z_p $(p = 1, ..., m)$, the log-variance features can be extracted using:

$$f_p = \log \left(\frac{var(Z_p)}{\sum_{i=1}^{2m} var(Z_i)} \right), \tag{2.17}$$

where f_p is the $(1 \times 2m)$ feature vector. Using the log-transformation provides an approximation of normal distribution, and the features can be used to train a classifier and predict the class of new data.

2.8 Feature Selection

Feature vectors created using feature extraction often require further reduction, which can be achieved using feature selection algorithms. This reduces the effects of a problem known as the "curse of dimensionality" [65], where the amount of training data required increases exponentially relative to the size of the feature vector. Other benefits include reduced training times, reduced storage requirements, improved prediction performance, and the facilitation of data visualisation [66]. Feature selection algorithms can be categorised into *filters*, which select subsets of variables as a preprocessing step, and *wrappers*, which assess different subsets of variables using the classifier of choice [67]. Filter methods attempt to identify the best individual features using methods such as calculating the correlation between the variable and the target. Wrappers assess subsets of features, meaning they take into account interactions between features. Effective use of both methods leads to a model which can correctly classify a large subset of the data without 'overfitting' [67], with overfitting referring to the phenomenon that occurs when a trained model is too fixated on a small number of data points to accurately classify new data. Forwards and backwards stepwise selection are two popular implementations of wrapper methods. In forward selection the model either begins with one

feature, and sequentially adds one variable at a time as long as it improves accuracy [67]. Backwards stepwise selection works identically but in reverse, starting with a full feature set, removing one at a time.

2.9 Classification

Classification uses the feature vectors created during feature extraction to make inferences about a user's current state. Classification methods can be placed into two groups: supervised learning, where an algorithm is shown labelled samples of each class and then learns the classes to identify them at a later point in time, and unsupervised learning, where the algorithm is given the unlabelled data and decides which categories best represent the data. For BCI-controlled robots, classification leads to a pre-determined action (e.g. movement). Many methods for classification exist, including artificial neural networks, support vector machines, linear discriminant classifiers, and many more. In BCI literature some the most commonly used classification algorithms are linear discriminant analysis (LDA [68]) and support vector machine (SVM [69]).

2.9.1 Linear Discriminant Analysis

Linear discriminant analysis is a popular supervised learning algorithm which separates classes using hyperplanes which maximise class separability. LDA states that the separation of classes is equal to the ratio of between class variance to within class variance [68]. LDA functions by finding the weight vector w which maximises:

$$J(w) = \frac{w^T S_B w}{w^T S_W w} \tag{2.18}$$

where S_B represents the between class scatter matrix, and S_W represents the within class scatter matrix. LDA assumes normal distribution and equal class covariance.
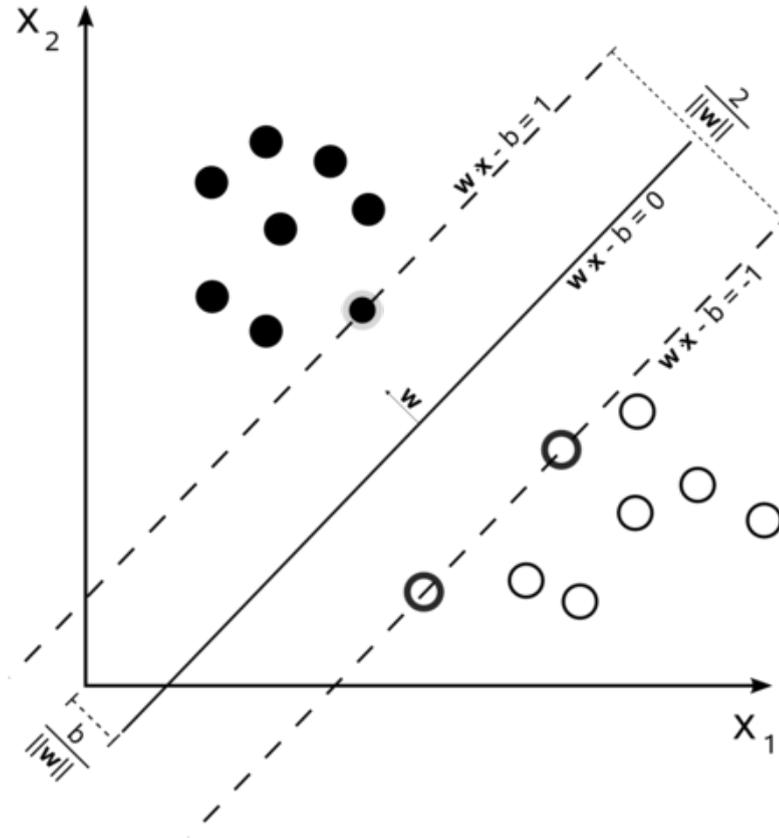
FIGURE 2.7: SVM hyperplane

2.9.2 Support Vector Machine

A support vector machine (SVM [69]) is another supervised classification method which separates classes using a hyperplane, however, the focus is on maximising the distance between the outer margins and the nearest training data points on either side of the hyperplane (Fig. 2.7), known as the support vectors. While initially used as a linear classification method, SVM can be extended to non-linear classification by using the 'kernel trick' [70].

2.10 BCI Performance Assessment

2.10.1 Classification Accuracy

Classification accuracy measures the percentage of correct classifications made, tested on a set of evaluation data or the whole dataset.

2.10.2 Cross-Validation Accuracy

Cross-validation involves systematically separating a dataset into training and evaluation sets of pre-determined size, in order to train the classifier repeatedly and assess its performance. Numerous cross-validation methods exist [71], and can be selected based on the situation:

- **Holdout:** Here, the data is split into a training set with approximately two-thirds of the data, and a 'holdout' set with approximately one-third of the data. This method uses random sub-sampling to select data, evaluates the classifier using the holdout data. The method can be repeated k times, averaging accuracy across runs.

- **k-fold cross-validation:** This method sees the data split into k random, mutually exclusive, and approximately equally-sized subsets, known as *folds*. The model is trained and evaluated k times, designating one fold as the evaluation set and all others as the training folds, evaluating the classifier, repeating for each fold, and averaging the accuracy across total number of folds.

- **Leave-one-out:** This fits a classifier using all but one of the observations, and attempts to classify the remaining observation. The process is repeated for all observations, meaning it is useful for small datasets, but can be computationally demanding.

2.10.3 Information Transfer Rate

Information transfer rate (ITR) [72] is a useful metric for comparing different BCI speeds whilst taking the variability of BCIs in terms of accuracy and number of possible commands, into account.

The ITR B (bits/symbol) can be found using:

$$B = \log_2 N + P\log_2 P + (1 - P)\log_2\left[\frac{(1 - P)}{N - 1}\right] \tag{2.19}$$

where N is the number of possible classifier outputs, and P is the classifier accuracy. The bit rate in bits per minute usually preferred for BCIs:

$$B_t = B * (60/T) \qquad (2.20)$$

where T is the time in seconds per symbol required to send one symbol

The ITR makes the assumption that classes are equally likely to be selected, which is not always true. Additionally its use is not always appropriate, for example with asynchronous BCIs or offline BCI studies [73].

2.10.4 Cohen's Kappa

Cohen's Kappa (κ) [74] is a criterion for assessing classifier performance based on the classification accuracy and the accuracy that could be achieved by chance alone. The κ coefficient can be found using:

$$\kappa = \frac{p_0 - p_e}{1 - p_e} \qquad (2.21)$$

where p_0 is the accuracy, and p_e is the expected result by chance. Both p_0 and p_e are proportions, existing between 0 and 1.

2.11 Hybrid BCIs

A hybrid BCI (hBCI) refers to a system that combines at least two types of input signals, with at least one signal originating from a BCI. The other signal or signals can either come from: another BCI signal from the same modality, creating a system known as a 'pure' hBCI; another BCI signal from a different modality, such as combining EEG and fMRI; physiological signals such as heart rate or EMG, although it could be debated whether using EMG constitutes a true hBCI; or from an intelligent device such as an eye tracker or intelligent wheelchair. Pure hBCIs can be categorised as either sequential or simultaneous: sequential hBCIs perform a function from one modality at a time, whilst simultaneous hBCIs perform actions from multiple modalities in parallel. Numerous combinations of hBCIs have been demonstrated to work, such as P300 and SSVEP [75], ERD and SSVEP [76], and ERD and P300 [77] among others. The main advantage of hBCIs is their

Study	Hybrid	Problem	Solution
[75]	P300/ SSVEP	Poor user performance	Simultaneous: hBCI that uses two modalities simultaneously to improve accuracy
[79]	P300/ SSVEP/ ERD	Standard BCIs have limited control commands	Sequential: Increases DoF by mapping commands to P300 and SSVEP, switches between them using ERD
[78]	P300/ SSVEP	Low ITR	Simultaneous Improves BCI by calculating horizontal and vertical axes with different BCI types, before cross-referencing location
[76]	SSVEP/ MI	Multi-dimensional control required	Simultaneous: Shares commands amongst two different BCI types simultaneously
[80]	SSVEP/ ERD	Multi-dimensional control required	Simultaneous: Shares commands amongst two different BCI types simultaneously
[41]	P300/ ErrP	Low ITR	Simultaneous: Monitors brain to detect errors, which it removes automatically
[77]	P300/ ERD	Multiple tasks to perform	Both: used a sequential setup with simultaneous processing at each stage, creating an accurate hBCI with enough DoF

TABLE 2.2: Hybrid BCIs designed to improve upon standard BCIs

ability to compensate for deficiencies that exist within the modality or modalities. Examples of improvements hBCIs can make to standard BCIs include increasing the available degrees of control (DoC) [76], increasing the ITR [78], and improving accuracy [75]. Table 2.2 summarises the outcomes of several pure hBCI studies.

2.12 Conclusion

This chapter reviewed detailed the underlying processes that allow a BCI to function, and the various methods for implementing a BCI. There are a wide variety of BCI types, and approaches can vary in terms of methods of signal detection and production, feature extraction and selection, classification, and translation; each with their own strengths and weaknesses. While several BCI-capable neuroimaging methods exist, EEG is the most convenient due to its relatively low cost, and portability. For a fast responsive BCI, SSVEP-BCIs are preferred due to the strength of the SSVEP response, and CCA-based detection methods are ideal for this purpose due to their accuracy and the lack of training data needed.

However, motor imagery BCIs have the benefit of requiring no external input, and can be detected using CSP-based methods.

Chapter 3

The Current State of the Art

This chapter reviews the applications of BCIs, as well as establishing the current state of the art.

3.1 Rehabilitation BCI

Arguably one of the most important applications for BCIs is in rehabilitation for disabled users. Rehabilitation BCI can be grouped under two main categories: motor recovery, which seeks to restore motor function to the disabled user, and motor substitution, which seeks to replace the missing function using technology.

3.1.1 Motor Recovery

The most popular motor recovery method in BCI literature involves coupling a BCI with a device to give participants added artificial control over their limbs. Controlling this with a BCI is hypothesised to aid motor recovery because it allows the brain to exert control over the muscle groups with reduced function, and according to the principles of Hebbian learning ("cells that fire together, wire together" [81] [p.21]), this could potentially promote use-dependent plasticity (U-DP), strengthening the remaining connections between the brain's motor area and the affected area.

Of the motor recovery studies reviewed, all were non-invasive, with a strong preference shown for EEG. Pfurtscheller et al. [82] performed a feasibility study with

a spinal cord injury (SCI) patient with tetraplegia (paralysis affecting all limbs) is trained to use an EEG-BCI with functional electrical stimulation (FES), where the nerves are stimulated to give the patient extra limb control. The patient used imagined foot movements to generate beta oscillations in the sensorimotor cortex (SMC), which act as a 'brain-switch' that activates a FES device attached to the malfunctioning hand, thus aiding grasping function. The patient was then able to grasp a cylinder while the FES device was active. One criticism is that this study (and many other motor recovery studies) attempts to use activation from one limb type to control a different limb type (imagined foot movements to control hand movements). It is not clear as to whether this would promote neuronal reorganisation through Hebbian learning, because, due to the topographical arrangement of the motor cortices, representations of hands and feet are located a relatively large distance from one another, meaning there is less chance of overlapping activation to trigger U-DP. Future work should use control groups to determine whether BCI/FES gives preferable or inferior results to FES alone. Studies by Gollee et al. [83] and Do et al. [84] demonstrate that BCI with FES can be used successfully in different areas: namely respiration control and lower extremity control. Gollee et al. used the SSVEP response as a control signal, while Do et al. used EEG-BCI with real foot movements. Both use multiple participants (12 and 5 Ps, respectively) and report excellent classification rates for the BCI controlling the FES (90% and 85.1 - 97.6%, respectively). Both showed minimal training times; SSVEP typically requires little or no training, whereas Do et al.'s use of real foot movements required only 23 minutes of training and calibration time. However, both studies were restricted to neurologically healthy participants, which creates two main problems: firstly, it cannot be taken for granted that these results are transferable to a target demographic comprised of individuals whose brains may have been damaged through stroke or traumatic brain injury; and secondly, these studies cannot report whether these interventions actually improve symptoms.

Shindo et al. [85] did not utilise FES. Participants were eight stroke outpatients demonstrating hemiparesis (unilateral weakness often associated with stroke). This study coupled EEG-BCI and motor imagery (MI), allowing participants to control sensorimotor rhythms (SMRs) using neurofeedback, a real-time display of information relevant to the user's brain activity. Successful MI activated an orthotic device which extended the fingers. Five participants reported improved finger function, with 3 of these showing reduced arm paresis. Measuring participant's voluntary surface EMG activity before and after the intervention showed that four

participants had significantly increased voluntary EMG activity. A lack of a control group means it is impossible to disentangle the effects of the BCI, the orthotic device, and the physical therapy, where applicable. Daly et al. [86] used EEG-BCI with FES to restore hand function in a stroke patient, using nine training sessions. This is one of the few early studies that involves actual patients and reports clinical outcome. In this study the patient reportedly regained some volitional control over their fingers. This is a positive result, though it is low in power due to having only one patient.

Overall, research shows that BCI provides a fairly reliable method of controlling the FES. It appears that some progress is being made, as the application of BCI+FES is spreading to different parts of the body. However, more research needs to be conducted using actual patients and reporting the clinical outcome, as well as including a control group to separate the effects of the BCI from the FES. More studies need to test whether these interventions create significant U-DP; initiating U-DP is the central premise behind using BCI in motor recovery, and should therefore be subjected to falsification testing.

3.1.2 Non-Invasive Motor Substitution

Using healthy participants in motor substitution studies carries fewer drawbacks than in motor recovery, as the main goal is simply to produce an effective motor substitute rather than producing clinical improvements. Consequently, all non-invasive studies reviewed used healthy participants. BCI-controlled robotic movement studies can be separated into two main types: 'Goal selection' is when the BCI is used to select a discrete output. The robot will then usually perform a predefined action or set of actions, based on this output. Alternatively, 'kinematic control' is when BCI outputs are used to create continuous outputs, giving the user finer control over the robot. In this section we will review both non-invasive and invasive motor substitution BCI studies.

Millán et al. [87] created an early demonstration of robotic control using non-invasive BCI. Two healthy participants used EEG-BCI to drive a wheelchair-like robot through a house-like environment (Fig. 3.1) using goal selection, operating the BCI using mental tasks of their choice. The users entered one of four mental states, for example by imagining themselves counting, relaxing, or rotating a cube. The BCI converted this signal into a goal selection output to control the robot.

The researchers demonstrated that this method works, and found high classification accuracy (over 98%). Manual control with a joystick was found to be faster by approximately 25%. It should be noted that this robot had extremely high level commands (for example, "turn left at next available chance"); however, this should not distract from the high classification accuracy obtained from this study. Rebsamen et al. [88] demonstrated that this can be performed using P300-based VEPs attaining 95% classification accuracy, and that stopping can be performed by generating mu- or beta-rhythms in the SMC. Due to the slow reaction time when registering a stop signal (5-6s) it may be dangerous to use the BCI to control stopping. Bell et al. [31], and Muller-Putz and Pfurtscheller's [89] participants performed assistive tasks using high-level goals, selected using EEG-BCIs. Bell et al used P300-based ERPs to control an assistive robotic humanoid, reporting 98% classification accuracy for selecting objects and then the area to transport them to (number of false activations not reported). Similarly to Millán et al.'s [87] robot, Bell et al.'s robot also requires high level commands, and for this reason would not be useful outside of a structured environment. Muller-Putz and Pfurtscheller used SSVEPs to control a prosthetic arm and found varying success rates, with participants attaining 44-88% accuracy. This study is notable because it allowed asynchronous control of the robot, and could feasibly lead to performing tasks in an unstructured environment due to the low-level nature of the input commands (i.e. rotate wrist, grasp). One issue to overcome is the number of false activations; from the reported figures we are able to calculate that false positives (FP) were experienced at an average rate of 6.75 FPs/min (with a four second refractory period) during the no-control condition, while false negatives (FN) were experienced at an average rate of 25%, meaning one in four commands was incorrect. Due to the use of ERPs and SSVEPs both studies required 10 minutes training or less. These studies show that motor substitution tasks can be performed using non-invasive BCI; however current studies rely on goal selection, and accuracy is greatest when commands are high-level, reducing the potential for use in an unstructured environment.

3.1.3 Invasive Motor Substitution

Hochberg et al.'s [90] early work with a SCI patient used invasive methods to record local field potentials through a 96-electrode array (as do all the invasive studies included in this review). The patient performed grasping actions using the
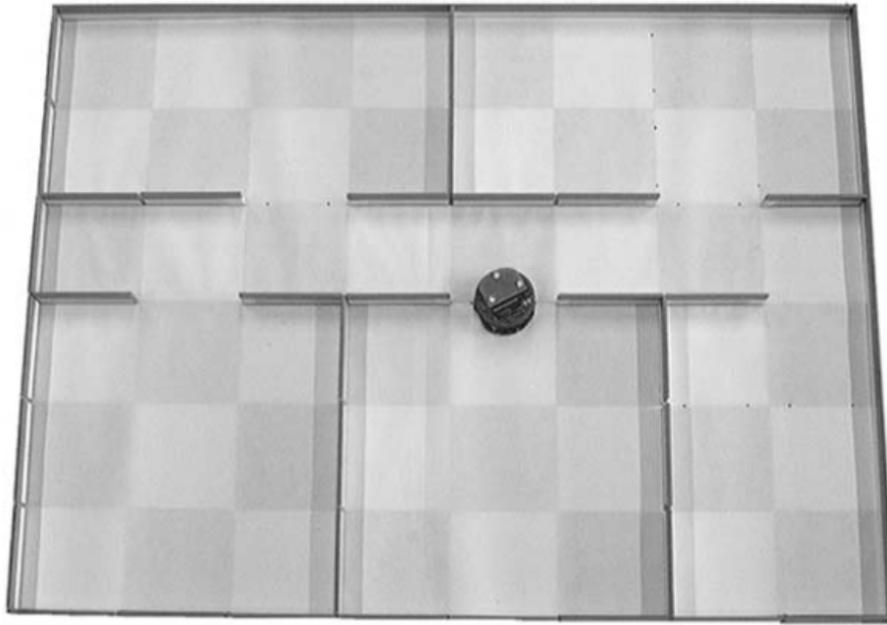
FIGURE 3.1: Early non-invasive robotic control experiment by Millán et al. Image from [87]

neurally-controlled prosthetic, demonstrating that these actions can be performed. In Hochberg et al.'s later work [12], two brainstem stroke patients were trained to perform grasping tasks with a BCI-controlled prosthesis in near-weekly sessions, using kinematic control. This produced a range of successful performances (21.3%-62.2%) that were significantly higher than chance alone. A performance of 21.3% success may sound poor compared to some of the previously discussed research; however, these tasks took place using kinematic control and many degrees of control. To overcome this, researchers should report the probability of performing one sequence of the task by chance alone. For example, in a goal selection task with 4 possible outcomes this probability would be 0.25 (25%); the success of the test should be assessed with regards to this. This would be less useful in studies using kinematic control, where the probability would always be very small. Instead we suggest devising a standard set of tests, which would allow direct comparison across kinematic control studies. Collinger et al. [11] taught a spinocerebellar degeneration patient to control a robotic arm with seven degrees of control, using only invasive BCI. The patient was trained using observation-based calibration, which is when the user watches the robot performing pre-determined movements while visualising themselves controlling the robot. After 13 weeks of training the patient was able to perform reach and grasp tasks, and cone-stacking

tasks, among others. Results showed the participant reaching 91.6% completion of target-based reaching tasks, and also that the number of neurons that were tuned to seven degrees of control had increased linearly over the course of training. This is undoubtedly the most positive result of all studies reviewed. Also, the increase of neuronal tuning gives insight to the nature of adaptation that takes place while using the BCI. It is unfortunate that studies with one patient have so little power, however, considering the costs incurred it may have been unavoidable.

To summarise, motor substitution is being investigated using both invasive and non-invasive methods; however, non-invasive BCIs appear to be primarily used for goal selection outputs, while the latest invasive studies have had success with kinematic control with up to seven degrees of control. The use of goal selection has produced useful assistive devices which work well, but are primarily designed for specific structured environments; however, the current aim of non-invasive studies in this area should therefore be to make assistive devices that use simple signals more effectively to produce complex yet controlled behaviours.

3.2 SSVEP BCI Gaming

Previous research has analysed various aspects of BCI games: studies have investigated the performance of games across different BCI modalities [91, 92], and investigated the game design choices made by developers [93]. The current section takes a different approach and investigates the game control mechanics used in SSVEP-BCI games, focusing particularly on the BCI translation methods (kinematic control or goal selection) used and the pacing methods (synchronous or asynchronous) used. A brief summary of these results can be seen in Table 3.1

3.2.1 Synchronous SSVEP-BCI Gaming

From the synchronous SSVEP-BCI games reviewed, each used goal selection. Lalor et al.'s [104] 'MindBalance' was an early synchronous two-class SSVEP BCI game where the player must correct the avatar's balance on a tightrope by selecting the appropriate target. The RVS was triggered at fixed intervals, and classification was performed after a pre-determined length of time. Some BCI games can be classed as synchronous due to external input pacing the BCI: Mühl et al.'s [103]

Study	Year	Method	Anthrop.	Techno.	Synchronicity
[94]	2015	GS		✓	A
[95]	2015	GS		✓	A
[96]	2015	GS		✓	A
[97]	2013	GS	✓	✓	S
[98]	2013	KC	✓	✓	A
[99]	2013	GS		✓	S
[100]	2012	GS		✓	A
[101]	2011	GS	✓		S
[102]	2010	KC		✓	A
[103]	2010	GS	✓	✓	S
[104]	2005	GS		✓	S

TABLE 3.1: Game control methods used for SSVEP BCIs

'Bacteria Hunt', and Hakvoort et al.'s [101] 'Mind the Sheep!' were both hBCIs which used mouse or keyboard inputs to pace the BCI, as well as being two of the only four games to take an anthropocentric approach during their evaluation. Bacteria Hunt, a hBCI utilising keyboard input, alpha waves, and the SSVEP response, used one-class SSVEP classification to 'eat' targets that were within range of the avatar after approaching using the keyboard. User's game experience was assessed across various metrics, including: pleasantness, naturalness, and enjoyability. 'Mind the Sheep!', a hBCI utilising mouse input and the SSVEP response, used three-class SSVEP classification to select which avatar to herd sheep characters with. This study found that the BCI component significantly increased immersion in four out of five categories: cognitive, dissociation, emotional, and control, without a significant increase in challenge. Parafita et al.'s [99] spacecraft game was controlled by selecting a direction using two-class classification, with the authors reporting 96% accuracy and an ITR of 15 bits/min. Chumerin et al. [97] performed the final synchronous gaming SSVEP-BCI reviewed, with their game 'The Maze' (Fig. 3.2); they used a "decision queue" method where incoming EEG data was classified every 200ms within a decision queue of predetermined length, the weighted outputs were summed after this time had passed, giving a movement command in the direction of the highest overall output.
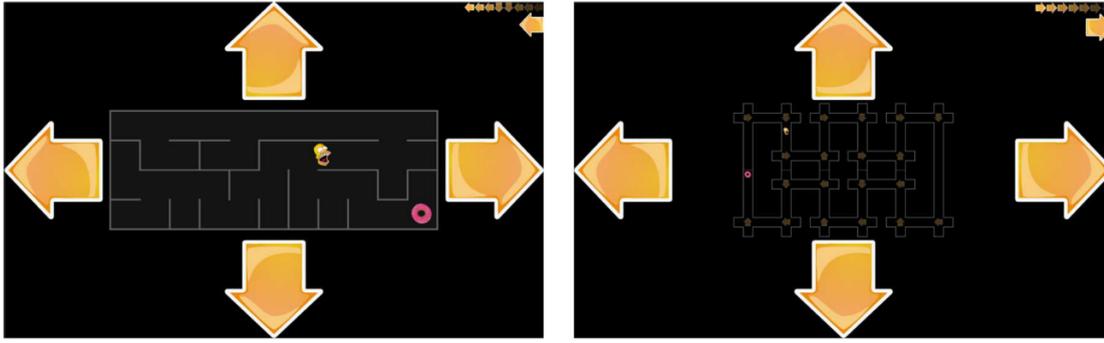
FIGURE 3.2: BCI game 'The Maze' by Chumerin et al. Image from [97]

3.2.2 Asynchronous SSVEP-BCI Gaming

The only two games reviewed that used kinematic control were both asynchronous BCIs: Mehta et al.'s [102] shooter game updated classification every 500ms to give the user a precise level of control, while Legény et al.'s [98] own SSVEP shooter adjusted the feedback level on the cannon based upon the intensity of the user's SSVEP response. Asynchronous control in Mehta et al.'s shooter was accomplished through a method where a fixed number of consecutive classifications are required before movement translation takes place. Legény et al achieved control using log-bandpower features extracted using a one-second time window with a 100ms overlap, although the exact method for achieving asynchronous control is not explicitly stated. Whilst evaluating the game they found that participants prefer gaming BCIs to use context-dependent controls, such as removing the RVS when not in use, or locking controls to prevent unnecessary misclassification. Asynchronous BCIs using goal selection included van Vliet et al. [100] and Ali et al. [95], who both utilised thresholding techniques to achieve asynchronous control. Van Vliet et al. calculating the thresholds automatically based on mean amplitudes detected from calibration data during RVS fixation and RVS-free periods. Ali et al. used fixed predetermined thresholds for all participants, and combined it with the 'consecutive classifications' method so that satisfying either condition could trigger translation. Other games that utilised the consecutive classifications method include Koo et al. [94] (Fig. 3.3), whose four-class maze games returned a CCA classification every 500ms, and required three consecutive classifications to perform translation. The authors reported an ITR of 25.58 bits per minute; and Wong et al.'s [96] which similarly used CCA and three consecutive classifications to elicit translation.
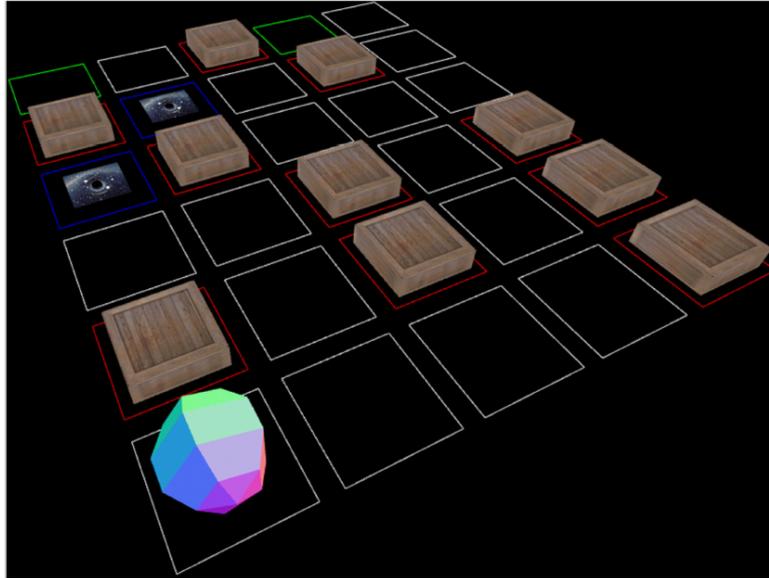
FIGURE 3.3: A 3D virtual reality BCI game by Koo et al. Image from [94]

There are a number of consistencies across SSVEP-BCI games: they generally use a small number of RVS (< 5); goal selection strategies are used a lot more frequently than kinematic control; while older games were more likely to use synchronous control, as advances are being made in BCI research asynchronous control is becoming more popular; and studies were generally technologically centred, with fewer studies focused on user-experience. Regarding the technological state of the art, SSVEP-BCI games are generally accurate and responsive, with a large number of different available approaches for achieving asynchronous control. The studies have also shown that regarding user-experience, the BCI increases the level of immersion.

3.3 Motor Imagery BCI Gaming

Unlike SSVEP-BCI gaming, where different games often use similar methods, there is a tremendous amount of variability in motor imagery BCI gaming methods. The regular use of calibration data, and increased training periods create additional sources of variability in terms of amount of data to use, and duration of training.

Hasan et al. [105] Hasam et al. developed an asynchronously controlled BCI version of Hangman, the popular game where participants must guess a word one letter at a time. Incorrectly selecting a letter draws one individual part of

Hangman, with the game ending either when the word is correctly guessed or when the whole picture has been drawn. The game itself used two classes to select letters: one class to select the letter, and the other to move the selection to the next letter. Both a static and adaptive LDA classifier were available for this game. The gaming BCI functions by recording EEG activity from electrodes positioned above the sensorimotor cortex, extracting features from the whole mu band (8-12 Hz) and part of the beta band (13-16 Hz) at each electrode. Calibration involved collecting data from four classes (right hand, left hand, left or right foot, and idle) and selecting the two most separable classes for online classification. The adaptive classifer performed unsupervised adaptation by adapting the LDA classifier based upon the average number of movements used to select a word. Testing the classifier with healthy participants ($n = 5$) showed an improved the True-False rate. This study took a technocentric approach in that it focused heavily on the methods, finding that adaptive classification reduced the average amount of time required to complete a task, when compared to static classification.

Asensio-Cubero et al. [106] tested their three-command endless running game using motor imagery. The commands used were stride left, stride right, and jump, and used left hand, right hand, and feet motor imagery, respectively. Motor imagery features were extracted after applying a wavelet lifting transform and CSP to EEG data filtered between 8 and 30 Hz. The number of number of CSP features were selected using five-fold crossvalidation on 30 trials of training data per class, before real-time classification using an LDA classifier. In this game the researchers found a strong training accuracy (71%), but weaker accuracies during online control (53%).

Zhao et al. [107] controlled a game called 'Mind-Driven Car' in a 3D virtual environment using motor-imagery BCI. The game had two options: 1. steering the car along a straight road, avoiding the traffic cones, and 2. steering the car along a curved road, avoiding the road border. The game itself used four classes to generate commands: motor imagery from the right hand, left hand, and feet, as well as relaxation for the fourth class. Information from these four classes allows the user to control the car's speed and direction. The BCI implementation used common spatial frequency patterns (CSFP [107]) and an LDA classifier, which was trained using several three-minute training runs. CSFP is an extension of CSP which allows the optimisation of spatial and frequency filters for improved performance. Acceleration was initiated using foot MI, and steering direction

was controlled by hand motor imagery (with right hand MI initiating a right turn, and left MI initiating a left turn). MI duration was used as an additional control parameter, with the turn output cumulating incrementally as the duration increased. A trial was defined as 'relaxation' (and therefore no output sent) if the confidence of the classifier was below a pre-determined threshold, such as 90%. Due to the small sample size (n=4), it is difficult to draw any strong conclusions, however, three out of the four participants gained control over 75%, with two of these reaching 91%.

Leeb et al. [108] modified the game 'PPRacer' to be operated by their MI-BCI and tested it with 14 participants. The game itself involves steering a penguin avatar down a snowy mountain, and jumping to catch fish. Jumping was performed using foot dorsiflexion, as a one-class classification problem. Features were extracted as log-bandpower features taken from non-overlapping 2 Hz frequency windows from 6 to 40 Hz, and these features were reduces using Distinction Sensitive Learning Vector Quantization (DSLVQ [109]) for feature selection. DSLVQ approximates the optimal between-class borders using labeled reference data (codebook vectors) and a weighted distance function.

Bonnet et al. [110] developed a two-player BCI football game called 'BrainArena', where players use two-class classification to control the ball right or left (right hand and left hand MI respectively). For each of the twenty participants, the CSP algorithm was used to create subject-specific spatial filters, which were trained on 40 trials containing five seconds MI data, with each trial filtered between the 8-30 Hz range. The game contained solo, cooperative, and competitive modes, and the experimenters looked at several aspects of user experience, including: difficulty, fun, motivation, and global appreciation. It was found that collaborative mode was significantly more fun and motivating than solo mode, whereas no significant difference was found between collaborative and competitive mode. Mean accuracies of 71.3 and 73.9% were found for solo and collaborative mode, respectively.

Taken together these results show that asynchronous gaming MI-BCIs appear to be more common than asynchronous rehabilitation BCIs, possibly in part due to the lower cost associated with misclassifications. There is a much wider range of methods used in comparison to gaming SSVEP-BCIs, however, they also tend to use a small number of commands.

3.4   SSVEP Normalisation

A notable characteristic of EEG is that the EEG frequency components from low frequencies tend to have higher power than those from high frequencies, making them easier to detect, and leaving a signal naturally skewed in favour of low frequency RVS. One way to minimise this bias is to only use stimulus frequencies from the same range. However, it would be preferable to adjust our feature extraction methods in a way that gives a balanced result. Having access to more stimulus frequencies means more unique commands can be sent and thus with a higher information transfer rate. It is noted in [73] that uneven distribution between classification accuracy of classes leads to a skewed performance - the ideal BCI will have an equal chance of selecting any command. This skewness can be alleviated by normalisation, also known as feature scaling, which standardises features based on some relationship within or between groups of features for reducing the impact of extreme values and/or the difference between features of different classes.

A number of studies have used methods of normalising EEG signals for SSVEP detection. Nakashini and colleagues [62] took CCA features from their target frequencies and normalised them against CCA features from neighbouring frequency bands, to help compensate for poorer classification with higher frequency RVS. They found that these features could perform as well as (and sometimes outperform) the standard CCA, and performance improved as the number of neighbours increased. Castillo et al. [57] applied a similar method of normalising features against neighbouring frequencies using PSDA, where they would normalise against a single value to find the largest ratio. This led to a more accurate BCI and had less variance than using PSDA alone. Despite a relatively low SNR of the high-frequency visual input, Sakurada et al. [111] created a high frequency PSD SSVEP-BCI with good three-class classification accuracy, normalising all the RVS frequencies against the inter-trial average of spectral power across the fixation period, and also against competing frequencies. In effect each normalised SSVEP amplitude was the baseline corrected amplitude with the mean amplitude of the (baseline-corrected) competitors subtracted from it. Diez et al. [112] had participants operate a BCI-controlled navigation robot using SSVEP features from high-frequency ($f > 35$ Hz) RVS. PSD features were normalised against the periodogram of baseline data collected prior to the study. There was no direct comparison with other normalisation methods as this was a navigation

study. However, all participants were able to successfully operate the BCI using the baseline-corrected features.

The previous literature illustrates that there are a variety of different ways to improve SSVEP performance using normalisation methods. However, the majority of studies focus on PSDA-based techniques, whereas the current state-of-the-art SSVEP-BCI algorithms use CCA and CCA-based methods. Previous research has indicated that it is possible to improve CCA performance using normalisation methods, and also that data from the pre-fixation period can be used to normalise the SSVEP response across frequencies, albeit with PSDA. Therefore, we hypothesise SSVEP-BCI performance can be improved by using CCA data from the pre-fixation period.

3.5 Stimulus Colour

While a number of studies have investigated the effects of colour on SSVEP response, it is a relatively under-explored area of BCI research. Yan et al. [113] tested the effect with RVS that moves on an LCD (liquid crystal display) screen, and found that users were more accurate when using red/green alternating RVS checkerboards instead of black/white RVS. Another study investigating moving RVS stimuli [114] reported that green/red alternating RVS can elicit brain responses with a higher amplitude at the target frequencies than black/white stimuli. This suggests that red/green stimuli may perform better, although classification was not performed in this study. Nezamfar et al [115] compared three sets of RVS containing colour combinations based on the opponent-process theory of colour vision [116]: black and white, red and green, and blue and yellow. The theory posits that each of the three aforementioned pairs contain colours that cannot be perceived together; for example, while a colour may be seen as a mix of black and blue, a colour cannot be perceived as a mix of black and white. Flashing stimuli that alternates between opponent colours could be expected to have maximal contrast. Comparison of stimuli containing the opponent colours revealed that red/green outperformed black/white and blue/yellow checkerboard stimuli in terms of classification accuracy. Wei et al.'s [117] experiment to determine the optimal parameters for SSVEP stimuli reported that white stimuli outperformed red, green, blue, and yellow in terms of classification accuracy. A number of studies have used LED (light-emitting diode) RVS rather than on-screen stimuli, for

Authors	Method	Colours*	Best*	Metrics	Frequencies (Hz)
[113]	PSDA or CCA	R/G, W/Bk	R/G	Amplitude and classification accuracy	11, 16, 18, or 8, 9, 10, or 10.5, 11.5, 12.5
[114]	PSDA	W/Bk, R/G	R/G	Amplitude spectrum	7.5
[117]	CCA	R, G, B, Y, W	W	Classification accuracy	Unknown
[118]	PSDA	R, G, B, Y, W	R or G	SNR	10, 20, 30, 40
[115]	Template matching	W/Bk	R/G, B/Y	R/G	-
[119]	MSI	R, G, B, Y	R	Classification accuracy	8, 11, 13, 15
Chapter 5	CCA	W, R, B, Y	POC	Game completion speed	6.5, 7, 7.5, 8

TABLE 3.2: Average game experience during real-time BCI control
Bk = black, W = white, R = red, B = blue, G = green, Y = yellow, MSI = multivariate synchronization index

example, Jukiewicz et al. [118] found that green or red LED stimuli had the best trade-off between eliciting high amplitude brain responses and providing visual comfort. Tello et al. [119] found similar results when testing LEDs: red produced the highest classification accuracy; however, green had the best trade-off between accuracy and visual comfort. The results of these studies are summarised in Table 3.2.

Taken together, these results indicate that red RVS elicits the strongest and most consistent SSVEP response, while it is unclear which colour is the most comfortable visually for users.

3.6 BCI Use and Fatigue

Research into fatigue and BCI generally focuses on neurophysiological or psychological changes caused by BCI induced fatigue, or the effects of fatigue on classification accuracy. Cao et al. [120] tested the former with their offline-BCI study, reporting: a significant negative relationship between fatigue and both the amplitude and signal-to-noise ratio (SNR) of the SSVEP response; increased noise

in the delta, theta, and alpha frequency bands; and a significant increase in self-reported fatigue after viewing the RVS for an extended period. Another study [33] validated the increase in fatigue, whilst Xie et al. [121] also confirmed BCI-induced physiological changes finding an increase in both the alpha, and alpha plus theta band. Tang et al. [122] found no significant decrease in SSVEP amplitude as fatigue increased during their SSVEP-speller task, although they did find a significant positive relationship between sleepiness and BCI use. It has been noted that fatigue can also reduce the amplitude of the P300-response [123], presumably decreasing the P300-BCI's effectiveness. Regarding the effect of fatigue on BCI accuracy, Chen et al. [124] saw no drop in classification accuracy after a one and a half hour experiment, whilst Sprague et al. [125] found no significant correlation between fatigue and BCI accuracy, although they did find a significant correlation between mood and accuracy.

3.7 BCI Use and Mood

Across all BCI types, the effect of mood is highly under-researched. Subramaniam and Vinogradov [126] found that positive mood can affect underlying neural processes in a number of ways, including: helping broaden one's scope of attention, and helping processes involved in task switching, both of which could potentially impact positively on BCI performance. While this was not a BCI study, it does highlight the motivation behind researching mood and BCI. Paul et al [127] looked at the impact of mood on ErrPs during a BCI task. They found that a positive mood can decrease the Pe component of the ErrP, and speculate that this may be because it makes errors less salient. Interestingly, this effect would likely lead to the ErrP-BCI being less effective. Nijboer et al. [128] found a positive relationship between mood and performance while testing their auditory-BCI using a group of healthy subjects. However, in later work [129] using seven tetraplegic ALS (amyotrophic lateral sclerosis) patients operating a P300- or SMR-BCI, it was concluded that mood did not affect BCI performance in any of the participants.

BCI-induced fatigue causes detectable changes in brain activity, and fatigue levels increase whilst viewing SSVEP stimulus offline, however, this does not lead to any appreciable reduction in classification accuracy. Positive mood can affect most different types of BCI, either in a positive or negative manner. Due to a lack of research in the area it is unclear what effect BCI use has on mood.

3.8 Conclusions

3.8.1 BCIs and Rehabilitation

Numerous studies have been conducted into rehabilitation BCI. BCIs can be used as assistive devices in two main ways: motor recovery or motor substitution. The most popular method for motor recovery was to implement BCIs that work in conjunction with FES. Non-invasive motor substitution BCIs generally used more reliable methods for control such as gaze-dependent BCIs. Invasive motor substitution BCIs are currently much more effective than their non-invasive counterparts, and allow for high classification accuracy, high degrees of control, and grant the user the ability to complete complex tasks. As with all invasive BCIs the disadvantage is that they come with the risks associated with surgery. In the work described in Chapter 6, we created a non-invasive motor imagery BCI for motor substitution that can be used by disabled users.

3.8.2 BCIs and Gaming

There are a number of consistencies across SSVEP-BCI games: they generally use a small number of classes (< 5); goal selection strategies are used a lot more frequently than kinematic control; while older games were more likely to use synchronous control, as advances are being made in BCI research asynchronous control is becoming more popular; and studies were generally technologically centred, with fewer studies focused on user-experience. Regarding the technological state of the art, SSVEP-BCI games are generally accurate and responsive, with a large number of different available approaches for achieving asynchronous control. The studies have also shown that regarding user-experience, the BCI increases the level of immersion. Previous research has shown that SSVEP-BCI games increase immersion and can make gaming more enjoyable. There are a number of ways to implement the games, including more complex control strategies such as kinematic control and asynchronous control. Based on the previous research, we designed a three-dimensional SSVEP-BCI game using state-of-the-art methods, which is described in Chapter 5.

3.8.3 SSVEP-BCIs and Normalisation

The majority of research into SSVEP-BCI normalisation has approached this topic indirectly, applying normalisation methods to PSD- and CCA-based BCIs while investigating a different topic.What can be deduced is that although the SSVEP response is generally weaker at higher frequencies, effective SSVEP-BCIs can be operated using low, medium, or high frequency RVS. However, studies tend to either use frequencies within a relatively narrow band, or test the methods without a control condition, meaning the full scope of this problem is not understood. Additionally, the majority of work has been conducted using PSD-based BCIs, whilst CCA is currently the more effective method. Therefore, as described in Chapter 4 we conduct a structured comparison of normalisation methods for SSVEP-BCI.

3.8.4 SSVEP-BCIs and RVS Colour, Fatigue, and Mood

Research suggests that red is the most effective RVS colour for BCI operation. Experiments have focused primarily on the effect different colour RVS have on the SSVEP response and classification accuracy; therefore, no definitive colour has been identified as preferable for users, and there have been no attempts to exploit these colour properties in an user-specific manner. The current evidence suggests that BCI use increases fatigue and can make detectable changes to brain activity during use. However, the evidence also suggests that despite this it does not usually lead to an appreciable decrease in classification accuracy, meaning this can be viewed an anthropocentric issue. Similarly, differences in mood have been shown to impact on brain activity in a way that could impact on BCI performance, but with no major negative impact on performance found. As a result, the work described in Chapter 5 includes proposing and evaluate a method for improving SSVEP performance using RVS colour properties, and evaluating aspects of user experience related to fatigue and mood.

Chapter 4

Improving the SSVEP BCI using Normalisation

4.1 Introduction

SSVEP-BCIs are one of the fastest non-invasive BCIs; however, frequency selection is still an issue, as seen in Section 3.4, and due to the mismatch in power the BCI is biased towards certain frequencies. As discussed in chapter 3, to the authors' knowledge there is currently very little research into SSVEP normalisation methods, however, they have been demonstrated to be effective at increasing SSVEP detection accuracy with PSD-based methods. Currently there is no work investigating the effects of normalisation on SSVEP-BCIs that use CCA-based methods, which are currently the preferred detection method. The current chapter assesses two normalisation methods which are aimed at improving the quality of SSVEP features extracted using EEG: Baseline-Corrected CCA (BC-CCA), and Scaled CCA. Both methods were found to be able to improve classification accuracy in conditions using frequencies with a large range, whilst BC-CCA was found to be the superior of the two, improving SSVEP detection accuracy by as much as 9.22% [130].
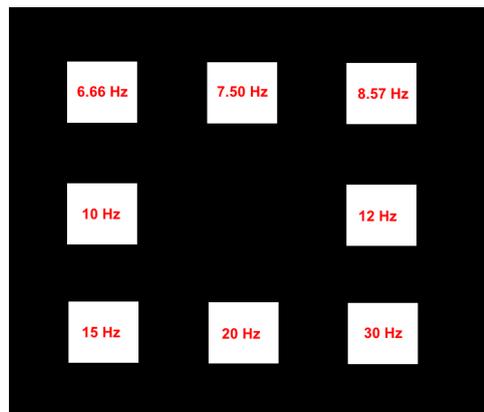
FIGURE 4.1: SSVEP stimulus screen layout

4.2 Methodology

4.2.1 Participants

Participants were 17 students recruited using the university mailing system (4 female, 13 male) with a mean age of 26.5 years old.

4.2.2 SSVEP Stimulus

An RVS was created and displayed on a separate computer, using code written on MATLAB (MathWorks Inc.) plugin Psychtoolbox ([131], [132], [133]. Eight SSVEP stimulus frequencies: 6.66, 7.5, 8.57, 10, 12, 15, 20, and 30 Hz, were produced using the method outlined by Cecotti et al. [134], and displayed on a 60 Hz screen in a 3×3 layout, as shown in Fig. 4.1.

4.2.3 Data Collection

Each participant's EEG activity was recorded as they gazed at the on-screen stimulus, using a Neuroelectrics[1] Enobio 20-channel EEG system with AgCl electrodes, referenced to the right mastoid. In a single group of eight trials, the participant was instructed (via the fixation cross) to gaze at subsequent stimulus squares in a *left-to-right, top-to-bottom* fashion, meaning the frequency values increased for

---

[1]www.neuroelectrics.com
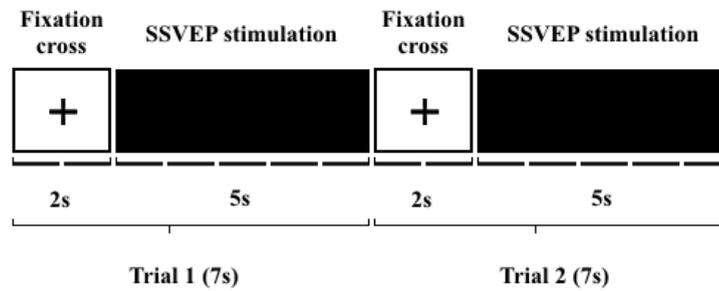
FIGURE 4.2: Trial outline

each of the eight trials. This pattern was repeated for all 30 groups of trials, giving a total of 240 trials, which took 30 minutes per participant. Each individual trial lasted seven seconds: a two-second fixation period, followed by five seconds of SSVEP stimulation (Fig. 4.2). Participants were given a one-minute break every nine minutes. During recording, participants were seated 60 cm away from the screen, in a room with reduced natural light.

This study used CCA both for feature extraction and classification.

4.2.4 Normalisation

One of the main advantages of using CCA in SSVEP-BCIs is that it can be used without any training data. In order to retain these benefits, this study is focused on normalisation methods that can classify commands without the use of training data. The first step of normalisation requires data from the pre-trial fixation period, during which no RVS is displayed on-screen (Fig. 4.2). A baseline correlation score is calculated across the pre-fixation period by calculating the maximum canonical correlation for each class multiple times using an overlapping window. Taking the mean of these scores gives a single value for each class, which will be termed the "baseline ρ" for convenience. Later in the trial, the baseline ρ is used to perform normalisation against the standard CCA correlation scores.

Three CCA methods are compared: *Standard CCA*, which uses no normalisation (Fig. 4.3); *Baseline-Corrected CCA* (BC-CCA), which subtracts the baseline ρ values from the maximum correlation coefficient values at the target time (Fig. 4.4); and *Scaled CCA*, which divides the maximum correlation coefficient values at the target time by the baseline ρ values (Fig. 4.5).
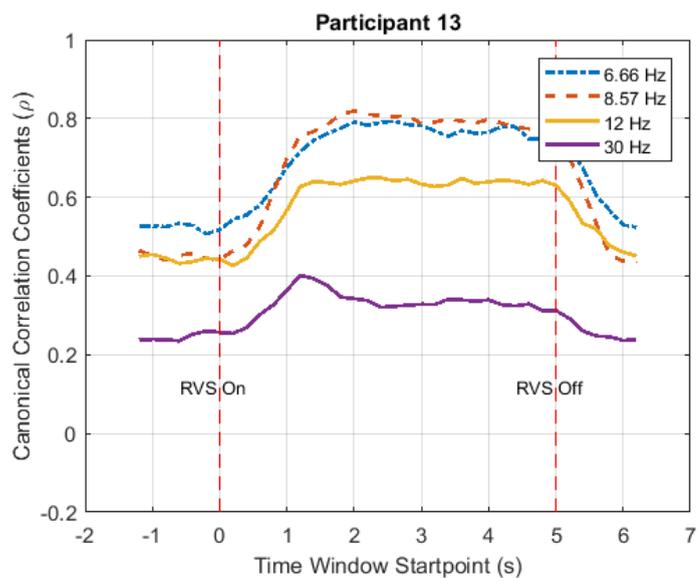
FIGURE 4.3: Standard canonical correlation coefficients
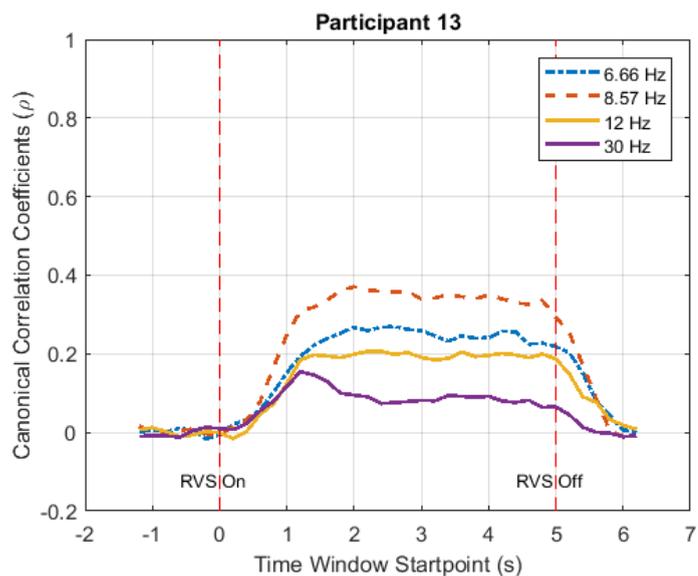
FIGURE 4.4: Baseline-corrected canonical correlation coefficients

TABLE 4.1: Frequency combination groups

Condition	Freq. 1	Freq. 2	Freq. 3	Freq. 4	Range
Low	6.66 Hz	7.5 Hz	8.57 Hz	12 Hz	5.34 Hz
Medium	8.57 Hz	12 Hz	15 Hz	20 Hz	11.43 Hz
Wide Range	6.66 Hz	8.57 Hz	12 Hz	30 Hz	23.43 Hz
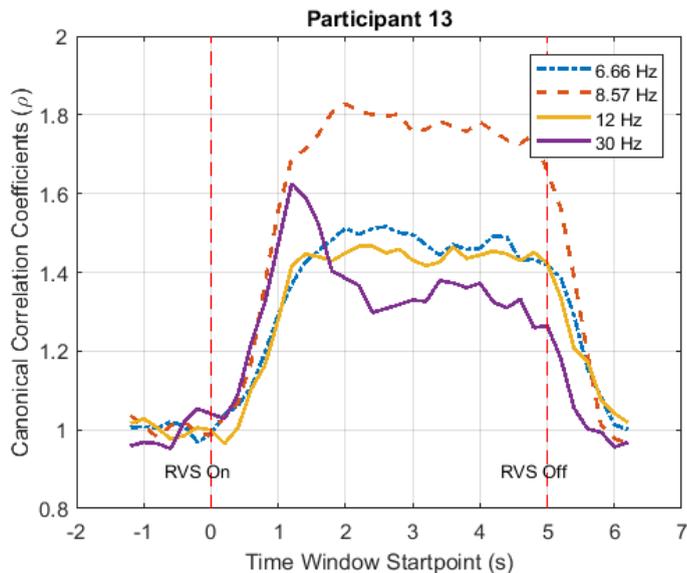
FIGURE 4.5: Scaled canonical correlation coefficients

4.2.5 Analysis

Normalisation requires calculating the correlation coefficients for each class several times during a single trial. To achieve this, the EEG data was downsampled to 250 Hz and separated into analysis windows using MATLAB plugin Field-Trip [135]. Each analysis window contained one second of data, filtered from 1-49 Hz using a zero-phase Butterworth band-pass filter with two seconds of data padding on either side. The ρ values of each class were calculated for every analysis window. The start points of the analysis windows, that is, the left corners, were positioned as follows: the windows for calculating baseline ρ were offset to $t\Delta = [-2, -1.8, -1.6, -1.4, -1.2]$ seconds, relative to $t0$ (stimulus onset). These overlapping one-second windows effectively covered most of the two-second period between the previous trial and stimulus onset of the current trial. The analysis windows for calculating Standard CCA was offset to $t\Delta = 1$ second relative to $t0$, in order to avoid the "dead time" [136], the period occurring after RVS onset but before the SSVEP response reaches maximum effectiveness.

Condition	Standard CCA (%)	BC-CCA (%)	Scaled CCA (%)
Low	**73.48**	72.99	71.13
Medium	64.46	**71.72**	70.20
Wide Range	57.84	**67.06**	64.41

TABLE 4.2: Mean Accuracy Across Conditions

Offline analysis tests were conducted using four different frequencies, which would provide enough degrees of freedom to control many simple games or assistive devices. The stimulation frequencies were separated into three conditions: Low Frequency, Medium Frequency, and Wide Range condition (Table 4.1). These three conditions allowed for combinations of RVS frequencies that had no inter-frequency interference within the first three harmonics. Analysis included all 30 trials for each class, giving a total of 120 trials per condition. Each trial had Standard CCA, Scaled CCA, and BC-CCA applied to it.

4.3 Results

Each participant had their data (120 trials per condition, three conditions) analysed using the Standard CCA, Scaled CCA, and BC-CCA methods (Fig. 4.6). The highest accuracies were found in the Low Frequency condition (mean = 72.53%), followed by the Medium Frequency condition (mean = 68.79%), with the lowest accuracies found in the Wide Range condition (mean = 63.11%). Standard CCA has a very slightly improved performance in the Low Frequency condition (+0.49%); however, both Scaled CCA and BC-CCA outperformed it in the other conditions (Table 4.2), with BC-CCA outperforming it by 7.26% in the Medium Frequency condition, and by 9.22% in the Wide Range condition. A closer look at the Wide Range condition (Table 4.3) shows that this effect is fairly consistent across participants, with only one user performing better using Standard CCA. Separating participants into performance-based groups using Tan et al.'s [137] threshold for acceptable BCI control accuracy (>70% accuracy) produces 11 higher accuracy participants versus 6 lower accuracy participants. The performance of these groups in the Wide Range condition suggests that the majority of improvements are made by the more accurate participants (Fig. 4.7, +11.81%), with less change attributed to the less accurate participants (Fig. 4.8, +4.45%).
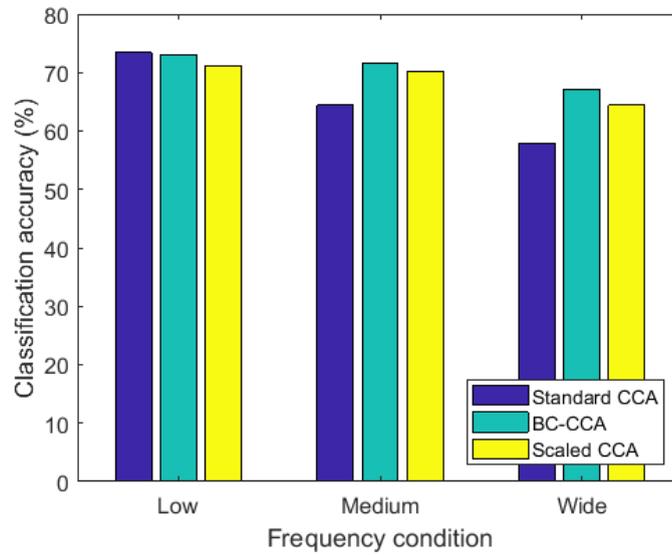
FIGURE 4.6: Mean classification accuracy

TABLE 4.3: Classification accuracy (Wide Range condition)

Participant	Standard CCA (%)	BC-CCA (%)	Scaled-CCA (%)
1	33.33	**34.17**	33.33
2	75.83	87.50	**89.17**
3	50	**50.83**	49.17
4	75	**87.50**	83.33
5	35	40	**44.17**
6	61.67	**70.83**	**70.83**
7	76.67	**96.67**	90
8	50.83	**57.50**	51.67
9	55.83	64.17	**66.67**
10	35.83	41.67	**42.50**
11	26.67	**34.17**	30.83
12	61.67	**74.17**	**74.17**
13	72.50	85.83	**86.67**
14	70	**87.50**	80.83
15	74.17	**94.17**	85
16	70	**80**	70
17	**58.33**	53.33	46.67
Mean	57.84	67.06	64.41
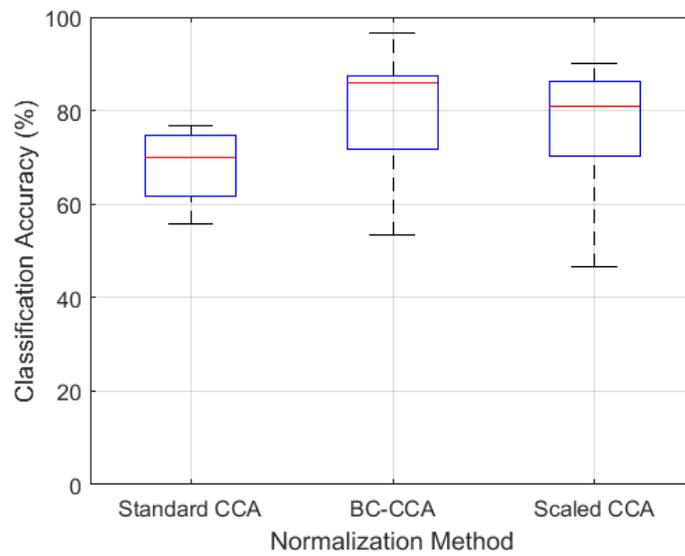
FIGURE 4.7: Higher accuracy participants (wide condition)
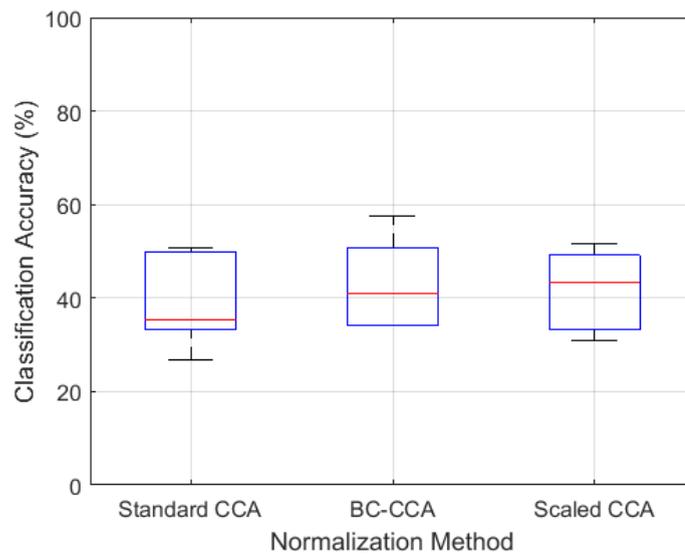
FIGURE 4.8: Lower accuracy participants (wide condition)

4.4 Discussion

This study has investigated the problem of whether it is possible to further improve CCA performance without the use of training data. The results show that it is indeed possible, and its effectiveness is dependent upon the RVS frequencies selected for use. Both Scaled CCA and BC-CCA were found to be effective,

60

with BC-CCA in particular found to improve performance for certain frequency combinations, with no appreciable loss of performance for other combinations.

As shown by the plots of each method's canonical coefficient values across time (Figs. 4.3, 4.4, and 4.5), BC-CCA and Scaled CCA appear to minimize the difference between the CCA coefficients, thereby making it more likely that weaker SSVEP responses such as at 20 and 30 Hz can be correctly detected. However, it is unclear why BC-CCA appears to perform better than Scaled CCA on a fairly consistent basis. As it is a baseline correction method, BC-CCA preserves the changes of each frequencies correlation score over time, relative to itself; it simply equalizes their value at t0. Whereas, Scaled CCA effectively applies a penalty to frequencies with a high baseline ρ, and applies that to their correlation score at every time point which should theoretically allow weaker frequencies a stronger response. This should give some insight into why the methods perform differently, although further work is required to determine which situations are preferable for each method.

Future work should look at whether training data can be used to further improve the results of BC-CCA and Scaled CCA, and test their effectiveness with a larger number of frequencies. A more structured approach to selecting the pre-trial fixation period may reduce the computations required for real-time control.

4.5   Conclusion

BC-CCA and Scaled CCA were both found to be effective normalisation methods, mitigating the decrease in BCI performance seen as the distance between frequencies increases, thus allowing a greater range of visual stimulus frequencies to be selected. Of all the methods investigated, BC-CCA was found to be the most effective.

Chapter 5

Improving the SSVEP-BCI by Exploiting Stimulus Colour Properties

5.1 Introduction

As discussed in Section 3.5, research into stimulus colour has shown that it can have a significant impact on user performance, with correct stimulus colour selection leading to higher classification accuracy or higher SSVEP response amplitudes; however, there is a lack of applied research. In this chapter an SSVEP-BCI game is created that exploits RVS colour properties to improve performance, as well as an automatic method for stimulus colour selection. We investigate whether it is possible to improve BCI performance and user-experience by predicting each individual user's optimal combination of stimulus colours, as well as investigating the effect of operating a gaming BCI on mood and fatigue. Twenty-three participants took part in the study, which involved: measuring brain responses to different coloured visual stimuli in an online experiment; predicting individual participants' optimal colour combination using a correlation based approach; and then comparing its performance against white stimuli using an online BCI game. It is found that using predicted optimal colours can lead to significantly faster game completion times, and a significantly higher overall mood. Operating a BCI game is found to lead to a significant decrease in fatigue.

5.1.1 Hypothesis

Based on previous research several hypotheses are proposed. We hypothesise that: red RVS will lead to the highest offline classification accuracies; a BCI with pre-selected RVS colours will outperform a BCI using white RVS; and finally that fatigue levels will increase after playing a BCI game in real-time.

5.2 Methodology

Participants completed an offline and online BCI experiment. Game completion times, as well as different metrics about their user experience were collected during the study, including: questions regarding stimulus colour preference, and questionnaires measuring various aspects of mood and fatigue.

5.2.1 Participants

23 healthy participants (4 females, 19 males; aged 23-53 years, mean = 29.78) with normal or corrected-to-normal vision participated in this study. Participants were recruited via the university's mailing system, were given an information sheet outlining the experimental procedure, and signed a consent form before taking part. All participants were informed of their right to withdraw at any time. One additional participant (Participant 21) began the experiment, but withdrew due to time constraints, and therefore their data has been excluded from analysis. This study was approved by the University of Sheffield Ethics Committee.

5.2.2 Questionnaires and Assessments

- **Colour Blindness Test**[1]: An online test assessed whether participant's colour vision was Normal (no colour deficiency), Deutanopia (green cone deficiency), Protanopia (red cone deficiency), or Tritanopia (poor yellow/blue discrimination), using the 'Ishihara Test for Colour Blindness'. This involved discriminating a number against a different coloured background (Fig. 5.1).

---

[1]http://enchroma.com/test/
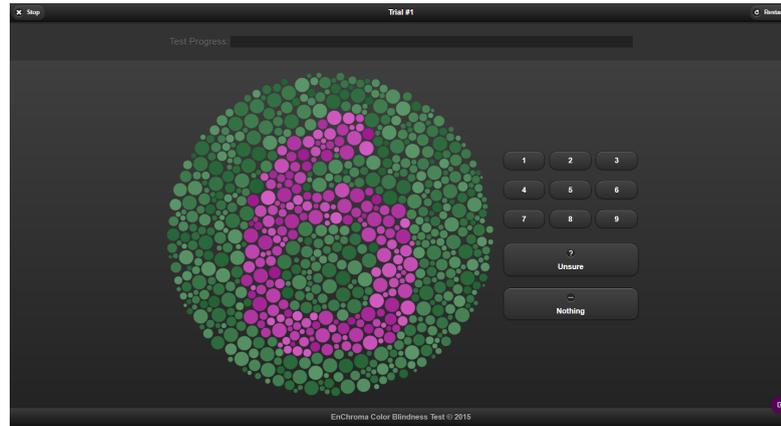
FIGURE 5.1: Colour blindness test showing a purple number "6" on a green background (or nothing, if you are viewing this in black-and-white!)

This test served as an exclusion criteria, colour blind participants would not be included in the study.

- **Mood/Fatigue Questionnaire**: This was a combination of two validated questionnaires: the Brief Mood Introspection Scale [138] (BMIS), and the Fatigue Scale [139]. Duplicate, overlapping, or task-irrelevant questions were removed.

- **Task Preference Questionnaire**: A custom-made questionnaire which asked participants to rate their visual comfort levels during the offline BCI experiment.

- **Game Preference Questionnaire**: A custom-made questionnaire which asked task-relevant questions about their comfort during game control in the online BCI experiment.

- **Game Experience Questionnaire**: A condensed 20-question version of IJsselsteijn et al.'s [140] Game Experience Questionnaire. Duplicate or task-irrelevant questions were removed.

All questionnaires were displayed using Google Forms[2], and are available in Appendix A.

---

[2]https://www.google.co.uk/forms/about/
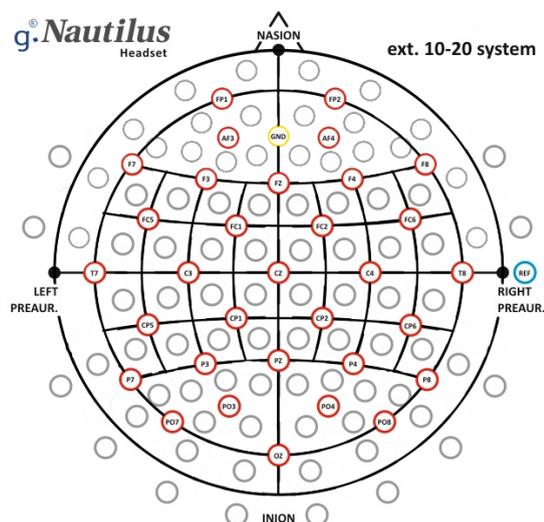
FIGURE 5.2: Electrode Layout

5.2.3 Data Collection

Participants were seated on a comfortable chair in front of a computer screen in a well lit computer laboratory for the duration of the experiment. Each participant's EEG data was acquired using a g.Nautilus[3] 32-channel EEG device (Guger Technologies) with gold-plated dry electrodes, arranged using the 10-20 system (Fig. 5.2) and referenced to the right mastoid. Data from the electrodes located above the parietal and occipital brain lobes (P7, P3, Pz, P4, P8, PO7, PO3, PO4, PO8, and Oz), was used for further analysis. In the online experiment, a Simulink model was used both for data streaming and online SSVEP detection. In the offline experiment, data analysis was conducted using a MATLAB script.

5.2.4 SSVEP Stimulus

An RVS displaying four unique frequencies (6.5, 7, 7.5, and 8 Hz) onscreen was created and displayed on Windows Forms using code written in C# (Fig. 5.3). The flickering RVS squares were made using a slightly modified version of Manyakov's 'sampled sinusoidal stimulation method' [141], which calculates an RVS's intensity at any given time point, as a value between 0 and 1, using:

---

[3]http://www.gtec.at/Products/Hardware-and-Accessories/g.Nautilus-Specs-Features
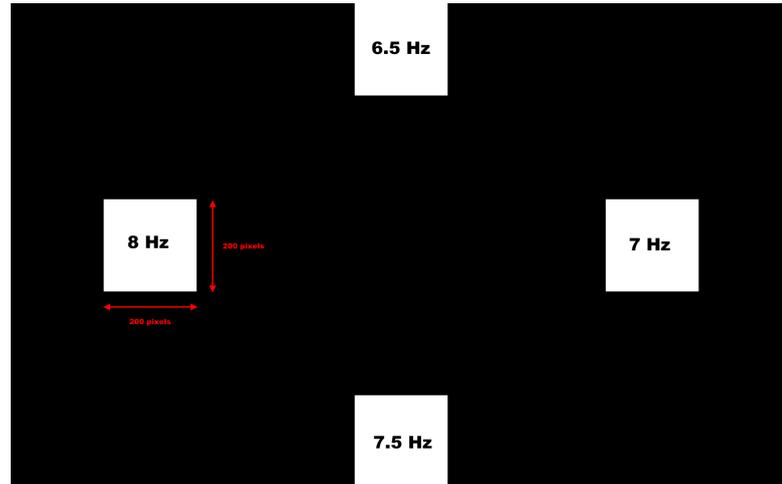
FIGURE 5.3: SSVEP stimulus layout

$$\alpha_f(t) = \frac{1}{2}(1 + \sin(2\pi f t + \Delta\phi)) \tag{5.1}$$

where f is the target stimulus frequency, $\alpha_f[0,1]$ is the stimulus intensity value of frequency f, and $\Delta\phi$ is the phase shift. During this study $\Delta\phi = 0$.

This method was slightly modified in order to display the stimulus intensity as a three-element RGB vector $\tilde{\alpha}_f$, by multiplying the RVS intensity values by the desired colour's maximal RGB values

$$\tilde{\alpha}_f(t) = \alpha_f(t) \times \boldsymbol{v} \tag{5.2}$$

where $\boldsymbol{v} \in \mathbb{R}^{1\times 3}$ is a three-element vector containing the desired colour's maximal RGB values. As an example, for a blue RVS, $\boldsymbol{v} = [0, 0, 255]$.

Figure 5.4 gives examples of the brain's response whilst the user is gazing at the RVS. Typically, peaks can be seen either at the target frequency or at its 'harmonics', which are multiples of the target frequency.

The frequencies used in the current study were selected because: 1. They are located away from the noisy occipital mu band (8-13 Hz), 2. Low frequency flickering can be annoying, which is actually beneficial to the aims of this study in terms of not underestimating fatigue levels, 3. They also fall outside of the 15-25 Hz range, which was reported to be the most provocative for epileptic seizures [32].

67

(a) 6.5 Hz response

(b) 7 Hz response

(c) 7.5 Hz response

(d) 8 Hz response
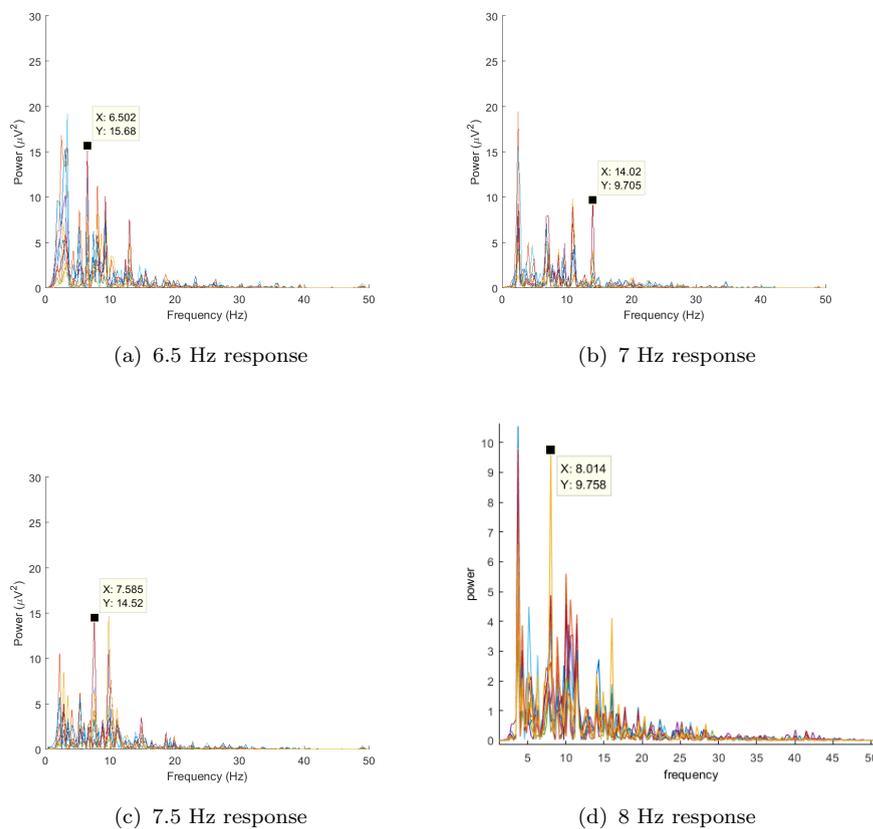
FIGURE 5.4: Sample power spectral density plots of the neural response to RVS at different frequencies

5.2.5 SSVEP Classification

This study uses canonical correlation analysis (CCA) for SSVEP detection and classification.

5.2.6 Predicted Optimal Colour (POC) Combination

The 'Predicted Optimal Colour' (POC) combination was the collection of colours that were chosen for use in the online experiment. This is a correlation-based method where POCs are selected based on the canonical coefficient values determined from calibration data collected in the offline experiment, with the highest correlation value at each frequency selected. This was implemented by evaluating all 40 trials from the calibration data against the same sine wave templates that are used in real-time control. Taking the mean correlation value in the 'true' condition allows us to compare identical frequencies with different colour stimuli.

	Red	Blue	Yellow	White
6.5 Hz	**0.67**	0.56	0.59	0.57
7 Hz	**0.66**	0.57	0.59	0.59
7.5 Hz	**0.61**	0.6	0.61	0.59
8 Hz	**0.68**	0.55	0.64	0.57

TABLE 5.1: Average correlation scores (Participant 1)

	Up	Right	Down	Left
P1	R	R	R	R
P2	Y	Y	B	R
P3	R	R	R	R
P4	Y	R	Y	Y
P5	R	R	Y	R
P6	R	R	Y	R
P7	Y	Y	R	Y
P8	R	R	R	R
P9	Y	R	R	R
P10	B	B	B	Y
P11	R	R	R	R
P12	R	R	R	R
P13	Y	R	R	Y
P14	R	R	Y	R
P15	Y	Y	R	Y
P16	R	R	R	R
P17	R	Y	Y	R
P18	R	R	R	R
P19	R	B	B	R
P20	Y	R	Y	Y
P21	-	-	-	-
P22	Y	Y	Y	Y
P23	Y	R	B	R
P24	Y	Y	Y	R

TABLE 5.2: Participant's predicted optimal colour for each direction

This is demonstrated in Table 5.1 for Participant 1, whose POC was red for each frequency (note: the coefficients for red were slightly higher than yellow at the 7.5 Hz frequency, values have been rounded to two decimal places). This method of colour selection was chosen instead of classification accuracy, as it allowed colours of the same frequency to be compared. A full list of the colours selected for each participant per frequency can be found in Table 5.2, while Fig. 5.5 displays the total number of selections for each colour across all frequencies.
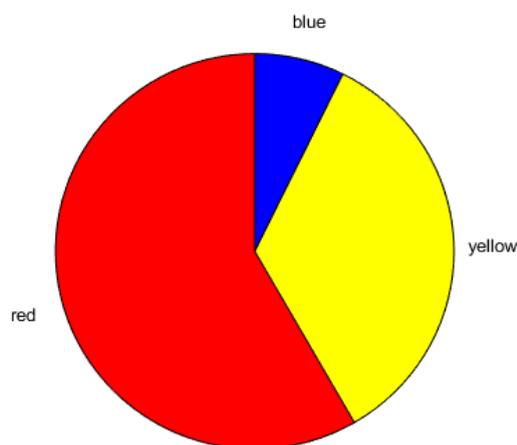
FIGURE 5.5: Total number of times each colour was selected by the correlation-based stimulus selection

5.2.7 BCI Game Design

The BCI game *SnookerMaze* was created using Unity Game Engine[4] (Fig. 5.6). Participants steered the ball by gazing at the RVS in the direction they wish to travel. The game's objective was to collect all 16 pink objects by rolling over them, with the game ending either when all objects were collected or when users exceeded the two-minute time limit.The maze was designed to resemble a snooker table, with a brown outer border, green floor representing the felt table surface, dark green obstacles as the cushions, and a white cue ball as the avatar. The game had several realistic features to increase immersion, including: shadows and a light source, a 'heavy' ball that accelerates and decelerates slowly, and slightly bouncy cushions. Incorrectly steering the ball into a cushion provided feedback even when the avatar's initial position was against the cushion, as it bounced against it slightly, indicating that an incorrect command had been made. The avatar was controlled using a synchronous BCI, meaning commands were sent at a pre-determined pace. The BCI would detect the user's intent every four seconds (based on the previous two seconds of data), then update the user's position. These time lengths were chosen in order to give the user enough time to identify whether the command was detected successfully, pick their next direction, and adjust their gaze.

---

[4]https://unity3d.com/
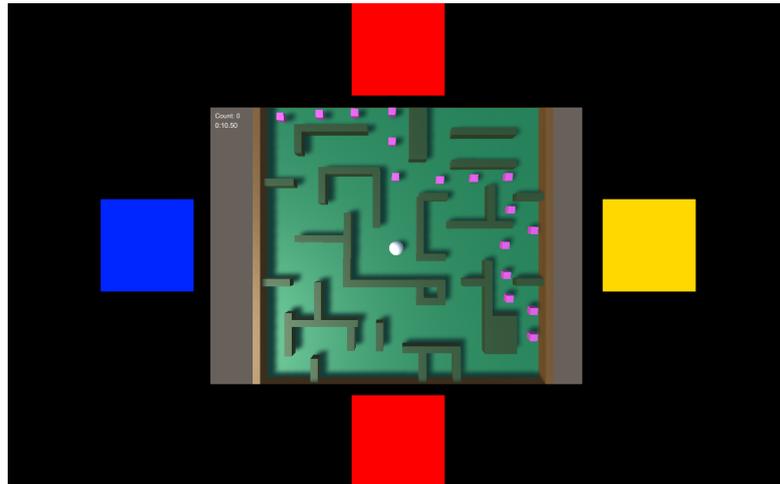
FIGURE 5.6: Example layout from SSVEP game *SnookerMaze*, with coloured RVS optimally selected for a single participant. *Clockwise from top: red, yellow, red, blue*
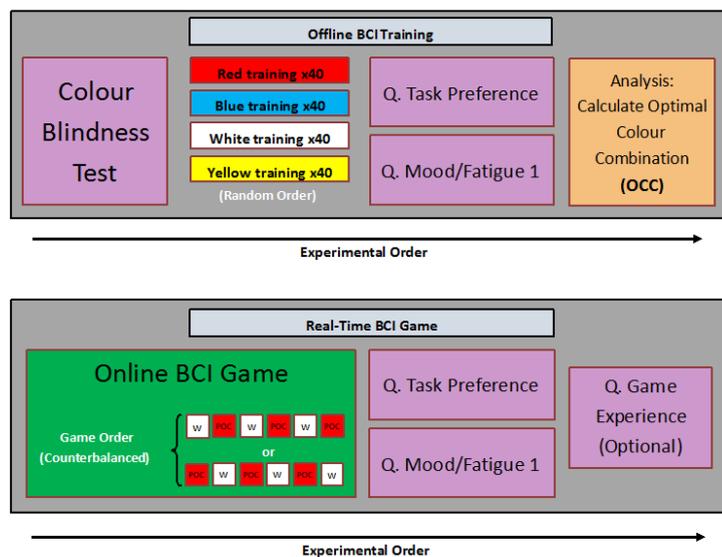
FIGURE 5.7: Experimental outline

5.2.8 Experiment One - Offline BCI

This study contained two parts: and online and an offline BCI section, which are outlined below. A visual display of both experimental outlines can be seen in Fig. 5.7. Experiment one was an offline BCI experiment which aimed to determine which colour stimuli produced the largest neural response.

The experiment began with a colour blindness test. Next, participants had the

71
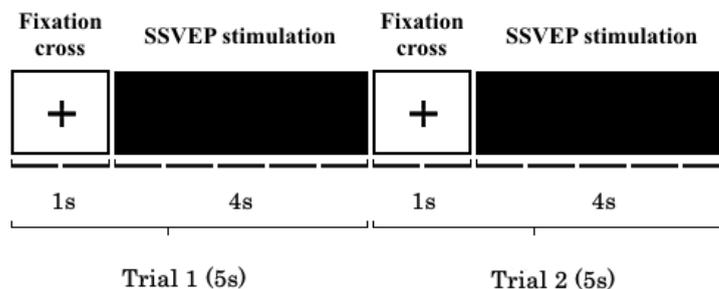
Figure 5.8: Trial outline

EEG cap fitted and were seated 60 cm away from the screen. The visual stimulus shown in Fig. 5.3 appeared on screen, preceded by a fixation cross indicating which stimulus the participant should gaze at. The fixation cross appeared on-screen for one second, followed by four seconds of RVS (Fig. 5.8). Participants gazed at each of the four RVS squares ten times each, and repeated this for each of the four colour conditions, giving a total of 160 trials (4 RVS × 10 repetitions × 4 conditions). The four colours selected were the primary colours (red, blue, yellow), plus white. Total recording time was 13.33 minutes (160 trials × 5 seconds). Colour order was randomised between participants, who were offered a break every 40 trials to reduce eye strain and fatigue levels between colours.

Next, participants completed the Task Preference Questionnaire, and a Mood/-Fatigue Questionnaire. From the collected EEG data, each trial was analysed to determine which four colours formed the POC, as described in 5.2.6.

5.2.9   Experiment Two - Online BCI

Experiment two was an online BCI experiment which aimed to determine whether it was better to control a BCI using white stimuli or POC stimuli. This would be determined based on game completion speed and participant experience.

Participants had six turns playing the game, steering by gazing at the RVS in the direction that they wished to travel (Fig. 5.9). The stimuli alternated between white and POC on subsequent game attempts, with this task order being counterbalanced between participants. Participants had a maximum of two minutes

FIGURE 5.9: BCI game control

per turn, giving a maximum play time of around 12 minutes. After playing, participants were given the Game Preference Questionnaire, another Mood/Fatigue Questionnaire, and the Game Experience Questionnaire.

5.3 Results

Offline Experiment

Participants reported their perceived levels of eye strain during experiment one, and offline classification of their EEG data was performed. Statistical analysis was performed using the Wilcoxon Signed Rank Test and the Friedman Test.

On a 10-point scale (1 = very uncomfortable, 10 = very comfortable), blue (6.74) was visually the most comfortable, followed by yellow (6.35), red (6), and white (5.87), as shown in Fig. 5.10. Offline SSVEP detection across all participants was found to be significantly more accurate with red RVS (77.28 %) than the second best performer yellow (69.13 %) ($\chi^2(2) = 22.04, p < 0.05$). White (66.2%) and blue (52.17 %) were the worst performing RVS colours during the offline experiment, as shown in Fig. 5.11, taken from the Task Preference Questionnaire. The lower quartile of classification results from red RVS reaches approximately to the upper

	Red	Blue	Yellow	White
P1	**100**	**100**	97.5	**100**
P2	**70**	42.5	62.5	40
P3	**100**	90	97.5	90
P4	75	37.5	**90**	82.5
P5	**100**	50	97.5	95
P6	**100**	47.5	87.5	92.5
P7	**100**	75	**100**	**100**
P8	**95**	**95**	92.5	85
P9	**75**	40	37.5	47.5
P10	**100**	**100**	87.5	82.5
P11	**82.5**	70	52.5	55
P12	**45**	**45**	30	25
P13	**65**	40	62.5	47.5
P14	**65**	32.5	45	35
P15	72.5	45	65	**77.5**
P16	**100**	52.5	67.5	75
P17	92.5	37.5	95	**100**
P18	**87.5**	30	72.5	45
P19	**60**	47.5	55	50
P20	40	37.5	45	**70**
P21	-	-	-	-
P22	32.5	17.5	30	**35**
P23	**35**	**35**	27.5	27.5
P24	85	32.5	**92.5**	65
Mean	**77.28**	52.17	69.13	66.2

TABLE 5.3: Offline classification accuracies (%)

quartile of blue, and the median of the yellow and white RVS, as seen in Fig. 5.12. Individual classification accuracies are shown in Table 5.3.

Online Experiment

Participants were assessed based on their mean game completion times for each stimulus type, and self-reported various aspects to the game experience.

Fig. 5.13(a) shows that participants generally completed the game faster using POC than white RVS (mean = 90.14 and 94.80s, respectively) Fig. 5.13(b), shows that while POC stimuli worked better for more participants, the difference in overall speed was balanced heavily by one participant, Participant 17. Participants were significantly faster in completing the game when using the POC SSVEP-BCI
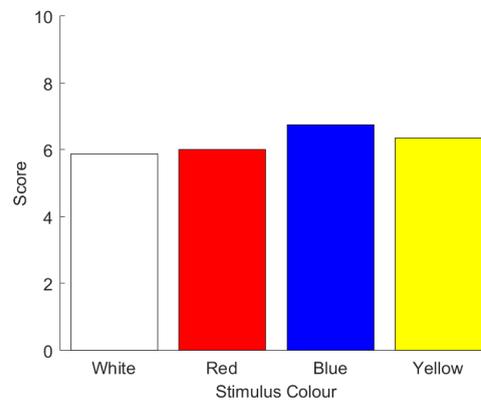
FIGURE 5.10: Mean stimulus eye comfort level (offline) across all participants
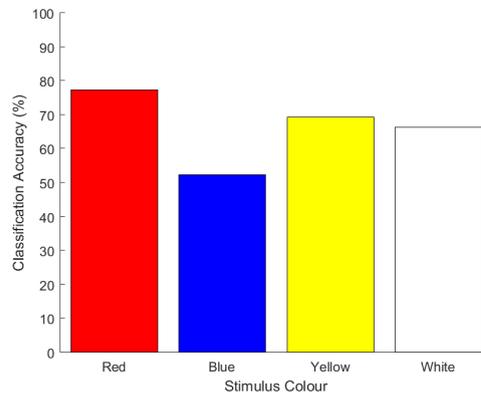
FIGURE 5.11: Average classification accuracy (offline)
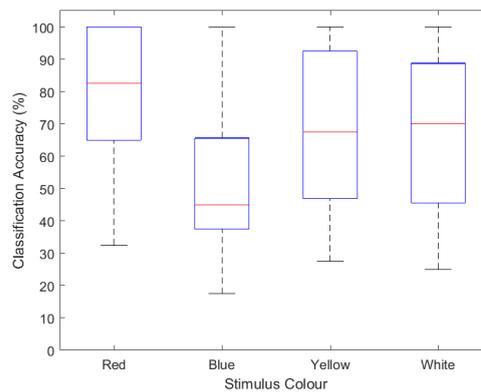
FIGURE 5.12: Classification accuracy (offline)

	Race 1 *	Race 2	Race 3**	Mean
White	98.26	97.43	98.38	98.02
POC	**90.9**	**96.15**	**91.44**	**92.83**

TABLE 5.4: Average race speeds across participants (in seconds), ($* = p > 0.1, ** = p > 0.05$)

	White	Colour
Eye Strain	**5.783**	6.174
Feeling of Control	6	**6.348**
Overall Fatigue	**5.217**	5.609
Overall Mood*	6.261	**7**

TABLE 5.5: Average game experience during real-time BCI control ($* = p > 0.1, ** = p > 0.05$)

in race 1 ($\chi^2(1) = 3.77, p < 0.1$) and race 3 ($\chi^2(1) = 5.333, p < 0.05$), with a small non-significant improvement over the white RVS also seen in race, as shown in Table 5.4. Participants reported a preference for the POC stimulus (13, 56.52%) over the white stimulus (9, 39.13%), with only one participant reporting no preference (4.35%) (Fig. 5.14, taken from the Game Preference Questionnaire). Self-reported results from the Game Preference Questionnaire regarding user game experience during real-time control are displayed in Fig. 5.15 and Table 5.5, and show that white stimuli were deemed to cause the least eye strain and fatigue during real-time control, while POC stimuli produced the highest feeling of control and the best mood, which was a significant increase ($Z = -1.732, p < 0.1$).

The net changes in mood and fatigue across participants after playing the BCI game, measured using the Mood/Fatigue Questionnaire, are shown in Figs. 5.16 and 5.17. Fatigue levels were found to decrease along every measured metric, except for 'problems thinking clearly', which showed a small increase. Of these decreases in fatigue, three were significant: 'sleepy or drowsy' ($Z = -1.934, p < 0.1$); 'lacking energy' ($Z = -1.998, p < 0.05$); and 'less muscle strength' ($Z = -1.732, p < 0.1$). Regarding mood levels, most of the positive mood changes were related to fatigue: tiredness (-13), liveliness (+5), and peppiness (+5). Generally the majority of mood changes were negative: happiness (-2), sadness (+1), caring (-4), contentment (-2), grouchiness (+2), nervousness (+4), and calmness (-1). Only two metrics did not fit this pattern: loving (+2), and fed up (-1).
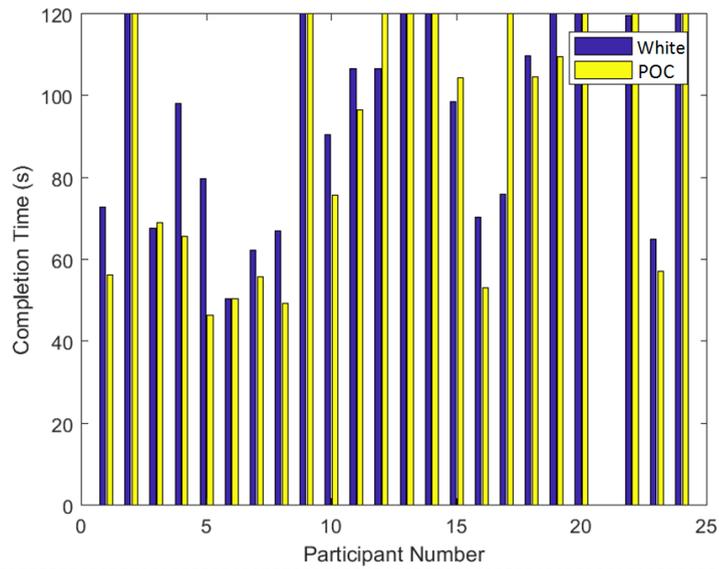
(a) Game completion times
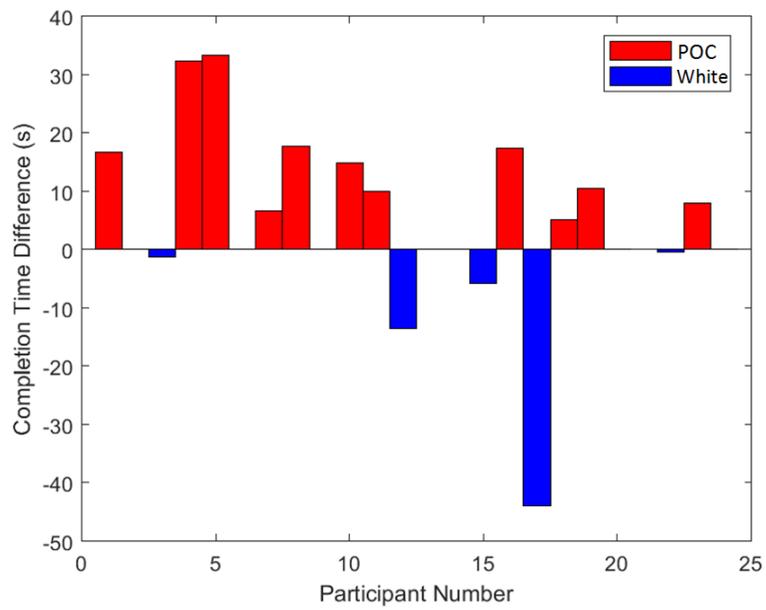
(b) Difference between RVS

FIGURE 5.13: Mean game completion times
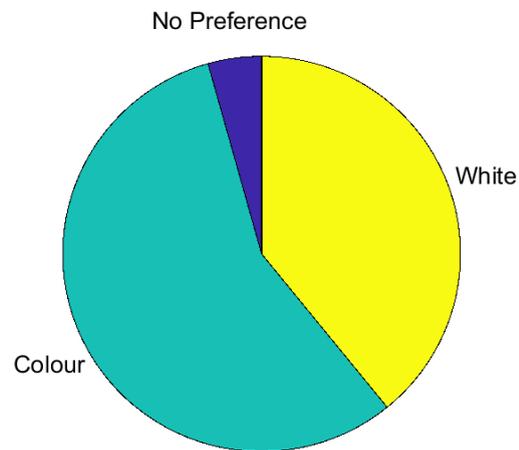
FIGURE 5.14: Stimulus type preference (online)
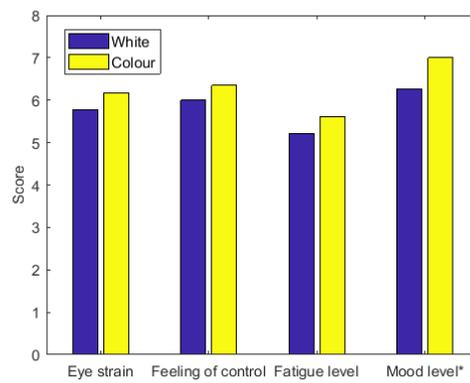
FIGURE 5.15: Participant experience during game control
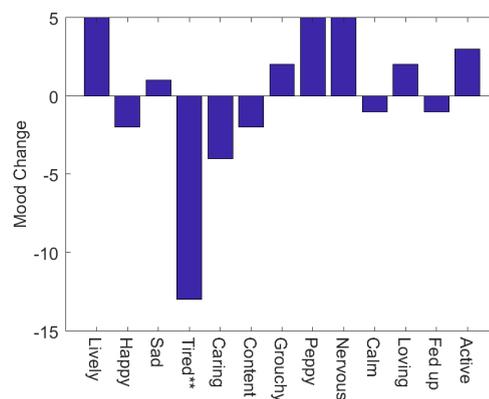
FIGURE 5.16: Change in mood level
$(* = p > 0.1, ** = p > 0.05)$
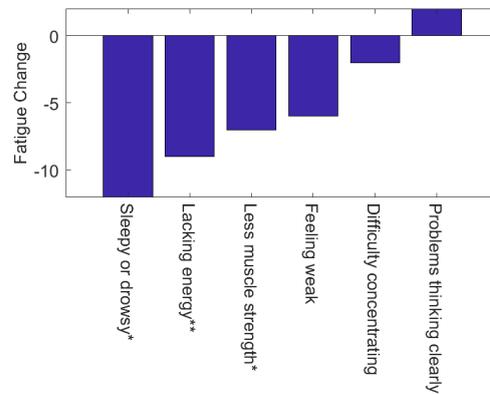
FIGURE 5.17: Change in fatigue
$(* = p > 0.1, ** = p > 0.05)$

5.4 Discussion

Results from the online experiment showed that on average, participants were able to complete an SSVEP-BCI game faster using a specially selected combination of coloured visual stimuli, the 'POC' combination (90.14s), than using white visual stimuli (94.80s). More participants cited an overall preference for POC stimuli than white, and reported that it produced a slightly higher feeling of control and and a significantly better overall mood when compared to white stimuli. The white stimuli were found to produce slightly less fatigue and eye strain during real-time control. Participant's fatigue levels were found to decrease on almost all available metrics after controlling the BCI game, which was unexpected, as studies using offline SSVEP-BCI reporting an increase in fatigue. Mood changed negatively, albeit non-significantly, on several individual metrics after playing the BCI game aside from mood aspects related to fatigue. The offline experiment showed that the best RVS colour for SSVEP classification is red, which improved performance significantly over all other RVS, which supports the majority of previous colour SSVEP research. This was followed by yellow, white, and then blue. In terms of visual comfort during the offline experiment, the colours were ranked as blue (6.74), yellow (6.35), red (6), and then white (5.87).

One of this study's interesting results was that overall participants found the white RVS caused more fatiguing than uniform colour stimulus during the offline training, but the POC SSVEP-BCI caused more fatigue during online control. There could be a few possible reasons for this. Training against a black background

means that a white flickering stimulus has the maximum possible contrast, which could be quite tiring. However, during online control there is a colourful game to navigate on the screen. It is possible that having a bright clear stimulus has some benefits in this situation. Another interesting result is that participants were less tired after playing the BCI game. This could imply that the enjoyment aspect of operating a BCI compensates for the fatiguing effects, despite being arguably more labour-intensive than passively watching a screen during training.

5.4.1 Critique

To the authors' knowledge, this was the first experiment to determine individual participant's best stimulus colours for operating a real-time BCI. It also appears to be the first paper to use canonical correlation coefficients for stimulus selection. Additionally, no previous literature was found that measured the effect of SSVEP-BCI usage on mood, using a validated questionnaire.

The online experiment could have been improved by increasing the amount of feedback received from the game, accomplished by reducing the time between player avatar moves, as well as the distance it moved. This would give participants more opportunities to reflect on their control techniques, and adjust them if necessary. Additionally, the game itself could have been improved by implementing kinematic control using an overlapping time window, however, due to time constraints on the availability of the EEG equipment, this was not possible. Locking the stimulus position to the player avatar (and overlaying the game map), would reduce the amount of eye movements required by the player, and could potentially improve completion times, albeit at the cost of partial map blocking. In the offline experiment, having participants complete RVS training blocks one colour at a time may have introduced some bias into the offline classification results; however, this was unavoidable in order to properly assess participant's visual comfort for each stimulus colour. Attempts were made to reduce this bias by having each participant complete this training in a unique order. Additionally, whilst using the canonical correlation coefficients for stimulus colour selection allows colours of the same frequency to be compared fairly, it is still somewhat naïve.

5.4.2 Future Developments

Future research could look at the impact of including useful features such as baseline coefficient values or coefficient variance, which could potentially lead to a more accurate colour selection method. The current correlation-based selection method, which selects stimulus colour based upon the highest mean correlation between calibration data trials and sine wave templates, could be improved by selecting colours with a similar chance of being selected. This could be achieved by taking into account the variance in the correlation coefficients, or selecting RVS with similar mean correlation values instead of simply taking the highest. Another way that future research can build on these results is by comparing POC SSVEP-BCI performance to the participants' best individual set of colours instead of white, which can also be determined by training data. Future developments for SnookerMaze include: implementing kinematic control, as mentioned previously, and using the customisable game to investigate control strategies and user experience in SSVEP-BCIs. Also, as mentioned in 5.4.1 an alternative method for displaying the RVS (locked to avatar position) has been proposed.

5.5 Conclusion

The results of this study show that it is possible to exploit the colour properties of SSVEP visual stimulus in order to improve performance. Stimulus colour selection using the average canonical correlation coefficient values from training data has produced a set of visual stimuli that improved BCI accuracy, and given participants an increased feeling of control, and a significantly better overall mood.

Chapter 6

Gaming Using a Motor Imagery-Based BCI

6.1 Introduction

The research reviewed in Chapter 3 demonstrated the potential that rehabilitation BCIs have for improving disabled users' quality of life as part of an assistive device, either by restoring motor function, or by replacing the missing function. This chapter focuses on motor substitution; specifically, the process of training a user to play a computer game using a novel SMR-BCI. Additionally, this work forms a feasibility study for testing neural predictors of BCI performance using a longitudinal study.

6.1.1 Cybathlon 2016

Cybathlon 2016[1] was a robotics competition that was billed as the "Worlds first bionic Olympics"[142], and took place in Zurich, Switzerland in October 2016. Each race involved disabled athletes with bionic enhancements competing against each other. Along with a group of several other researchers, I joined a team to help an athlete enter the BCI race. *Team Gray Matter* was comprised of: Ivan Nixon (Team Leader); Peter Gray (BCI Pilot); Dr James Law (Resource Manager); Dr Alexander Zaitcev, Dr Mahnaz Arvaneh, Dr Liat Levita, and James

---

[1]http://www.cybathlon.ethz.ch/en
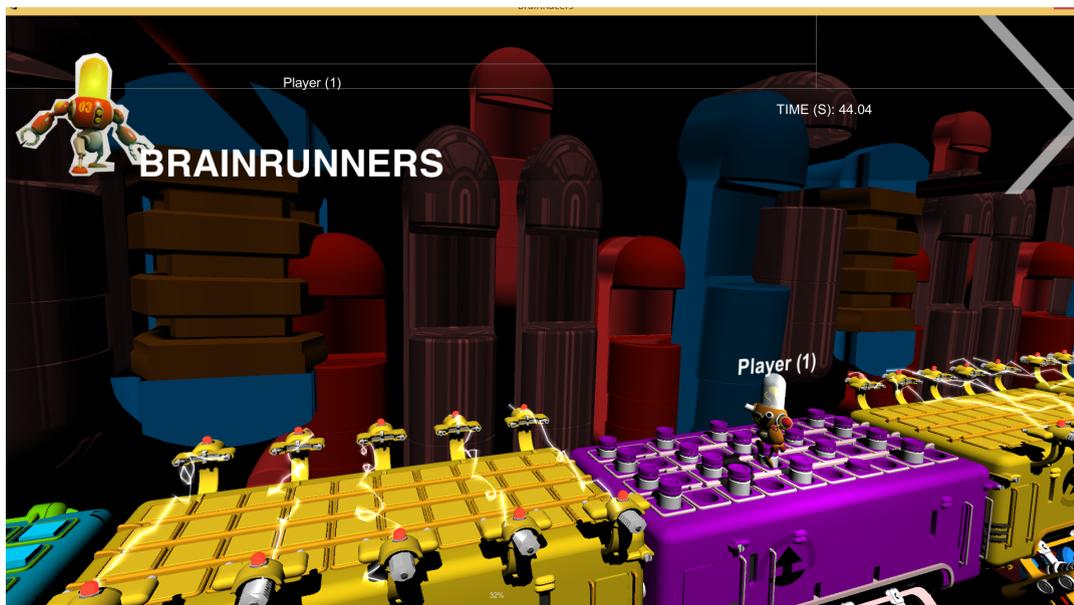
FIGURE 6.1: Brainrunners

Henshaw (Researchers - University of Sheffield); and Dr Rolando Grave de Peralta (Researcher - Electrical Neuroimaging Group, Switzerland). Unfortunately, due to health complications the BCI pilot had to withdraw from training around six weeks prior to the competition, and eventually the competition itself. Dr Zaitcev and I decided later to continue the work, following the competition restrictions mentioned above, the results of which are described in this chapter.

6.1.2 Competition Rules

The BCI race involved groups of four competitors controlling an avatar using their brainwaves, on a game called BrainRunners (Fig. 6.1). Each participant had to be either paraplegic or tetraplegic, and had to control the avatar asynchronously, using active BCI control. To clarify, the sending of movement commands had to be self-paced, and not rely on brain signals elicited using external stimuli, such as the SSVEP or P300 response.

6.1.3 BrainRunners

BrainRunners is a BCI game designed by Swiss Realtime Solutions[2]. The player must steer their avatar across a virtual course, using their brain signals to avoid obstacles. Over the course of a single run, the player's avatar runs across different coloured blocks. The blocks would be randomly ordered, and one of three colours: blue, purple, or yellow. Within each block was an obstacle corresponding to the block's colour.

- Blue blocks had moving tiles that the player must be sprint over

- Purple blocks had rising and descending objects that the player must jump over

- Yellow blocks had electrical traps that the player must slide under

6.1.4 Work Allocation

Dr Zaitcev and I wrote and tested code to stream and record data from the gtec EEG headset using MATLAB and Simulink. The feature selection algorithm used in the post-Cybathlon online experiments used source localisation, and was implemented by Dr Zaitcev, while I conducted the real-time recording sessions. Finally, we each conducted our offline analysis separately, as Dr Zaitcev's research investigated source localisation, while the current chapter investigates EEG predictors of performance.

6.1.5 Predictors of BCI Performance

In their study into neurophysiological predictors of SMR-BCI performance with eighty participants, Blankertz et al. [143] demonstrated that information extracted during restful idling with eyes open can be sufficient to predict performance, by estimating the strength of the SMR over the sensorimotor cortex. Ahn et al. [144] found that data extracted from periods where users rested with eyes open produced additional information about performance; BCI-deficient users showed high theta and low alpha activity when compared to non-deficient users, which

---

[2]http://www.swissrealtimesolutions.com/project/BrainRunners/

the authors suggested represented the low contribution levels of the alpha band to the ERD response, whilst the theta waves may have played a role in attention. Maeder et al [145] examined data from participants operating an SMR-BCI during the one-second period prior to trial onset, and reported a higher amplitude in the SMR bands (alpha and beta), finding a strong negative correlation ($r = -0.61$) between pre-trial bandpower, and eventual classifier output.

Taken together, these results indicate that the idling rhythms and resting state periods while operating an SMR-BCI are extremely informative with respect to user performance, particularly in the alpha, beta, and theta bands.

6.1.6 Hypothesis

Based on previous research, it was hypothesised that resting alpha activity would correlate positively with classification activity, while pre-trial alpha and beta activity was hypothesised to correlate positively with trial outcome. We also hypothesise that the correlation between pre-trial bandpower and classification outcome will strengthen as the number of training sessions our participant completes increases.

6.2 Methodology

6.2.1 Participants

This study used one participant, a 29 year-old, healthy, right-handed male, recruited through the university.

6.2.2 BCI Training

The BCI training was comprised of three parts: preliminary offline training; feedback training with PSD features; feedback training with source localisation-selected CSP features (described in 6.2.2). EEG data was recorded using the g.Nautilus device (Fig. 6.2) 500 Hz, 32 channel system, which is described in more detail in Chapter 5.
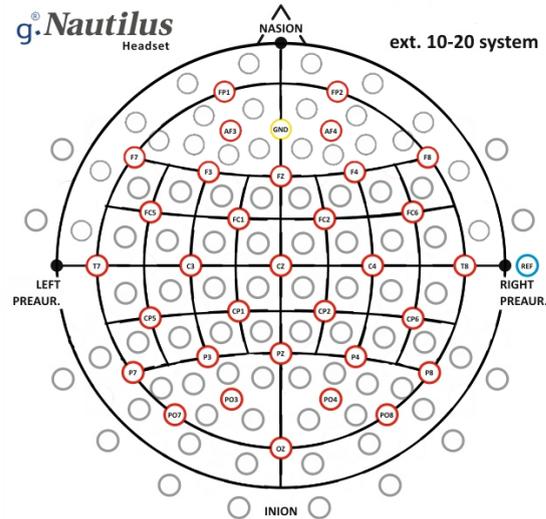
FIGURE 6.2: Electrode layout

Source CSP Features

This study used a novel real-time feature extraction approach, using features we have termed 'source CSP' features for convenience. Source CSP features are CSP features extracted from EEG data that has undergone an additional preprocessing step, where source localisation is used to remove data that is estimated to have occurred outside of a region of expected ERD/ERS activity. Source CSP is a multi-step process, which can be summarised thusly: raw EEG data is transported into source space to remove data outside of the region of expected ERD/ERS activity, then back into sensor space. Next the EEG is filtered into a relevant sub-band, and CSP spatial filters are trained and used to extract useful features from the EEG data. Finally, the number of features are ranked and reduced using entropy-based feature selection and forward selection.

- **Source reconstruction:** EEG data was transformed into source space using source localisation. A headmodel was constructed using forward modeling, based upon the ICBM 152 head atlas, which was created using non-linear averaging of 152 MRI scans of adult participants [146, 147]. A linear inverse operator G was created using weighted minimum norm estimates (WNME [17]), in order to move the data between sensor and source space. In sensor space, everything outside of the pre-selected region of interest (an area spanning 1201 locations where ERD/ERS activity was predicted to occur) was removed, and the data transported back to sensor space.

87

- **Band-pass Filtering:** Initial filter bandwidth was decided based upon visual inspection of time-frequency representation (TFR) outputs from EEG data collected during trials. These TFRs were averaged across each condition in order to determine which band contained the most ERD/ERS activity. For participant One this was the 10-15 Hz band.

- **CSP feature extraction and selection:** CSP feature extraction was performed using CSP to train spatial filters. After spatial filtering the trials from the calibration data, log-variance features were extracted for all classes. These features were ranked initially using Kullback-Liebler (KL) divergence (also known as relative entropy [65]), a technique which measures the divergence between two probability distributions. Using KL divergence in a one-versus-rest manner allowed us to compare similar predictors between classes, with the aim of maximising the KL distance. After performing feature ranking based on KL distance, feature selection was completed using forward selection with SVM classifiers.

More details on source CSP features can be found in Dr Zaitcev's doctoral thesis [148].

Preliminary Offline Training

Preliminary training consisted of the participant performing imagined movements in the absence of visual feedback, in order to collect enough neural data to train the initial SVM classifier. A single trial lasted approximately nine seconds; 0-2s fixation, 2-3s blank screen, 3-4.5s visual cue, 4.25-8s motor imagery, 8-9s rest. Sessions were grouped in sets of 3 to 5 runs of approximately 45 trials each.

Feedback Training with PSD or Source CSP Features

Feedback training involved completing multiple runs of the BrainRunners game within a session, recording the EEG data between sets of runs, and updating the classifier. Each run used seven randomly ordered trials from each of the three classes, giving twenty-one in total. The mental tasks our participant performed were: right hand punch to run (class one), left hand grab to jump (class two), and dorsiflexion of both feet to slide (class three, Fig. 6.3).

FIGURE 6.3: Avatar Control

In total, twenty sessions were recorded. Each session contained around 56 trials per class (two sets of four runs, with each class having seven trials in a single run), although due to fatigue levels some sessions were a little shorter. The classifier was retrained after every set of runs using the last five sets.

The online classification process can be seen in Fig. 6.4. PSD online feature extraction used a 3 Hz highpass filter to remove low frequency artifacts, removed the latest one-second time segment and applied a Hamming window to reduce the effects of spectral leakage. PSD features were extracted using the FFT, which extracted the PSD coefficients for all $Fs/2$ frequency points, where Fs is the sampling rate 500 Hz. The number of features were reduced from 8000 predictors, giving 65-110 features per class after using entropy-based feature selection, which were then classified using three OVR SVM classifiers. Source CSP online classification worked similarly, except that data was bandpass filtered between 10-15 Hz to focus on the participant's mu activity. Source CSP feature extraction for each class was applied using six CSP filters that were pre-selected using KL entropy-based feature selection. Classification was performed using three OVR (one-versus-rest) SVM multiclass classifiers, a set of classifiers where for each class a single classifier is trained to detect one class against the rest.

Sessions 1-9 used PSD feature extraction, while sessions 10-20 used source CSP feature extraction. Additionally, one minute of idle eyes open EEG data was recorded at the beginning of each of the source CSP sessions.

6.2.3 EEG Datasets

One of the two datasets (longitudinal dataset) used for offline analysis was from EEG recordings of our participant while they played BrainRunners during feedback training. Due to this being feedback training trial lengths vary, as a successful
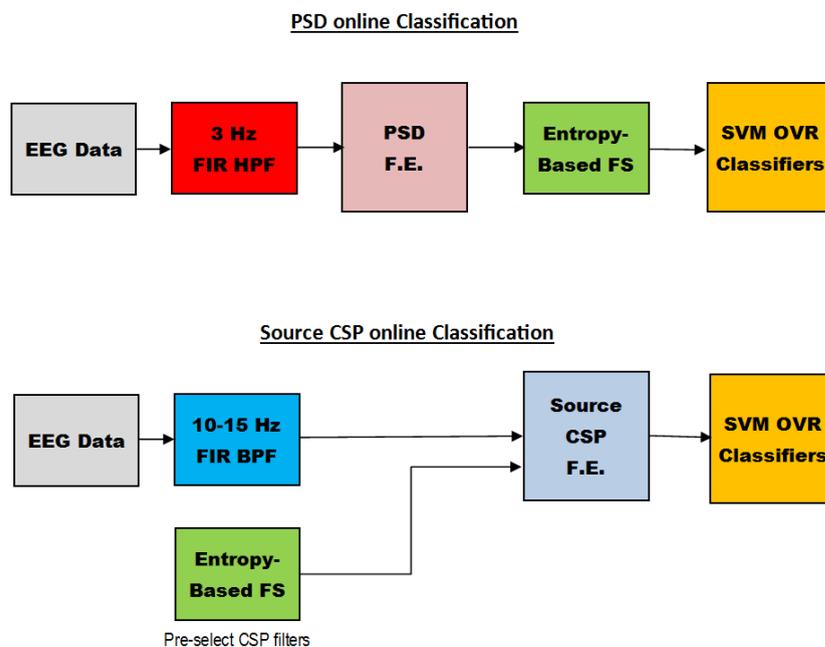
FIGURE 6.4: BrainRunners online classification

classification causes the avatar to progress through the game quicker. However, each trial is at least 2500ms long, in order to provide enough time for analysis.

Additional offline analysis was conducted using EEG data from BCI competition (BRIC) IV, dataset 2 [149], provided by Gray BCI laboratory researchers Runner, Lee, Roller-skate, Cheerfuller, and Sch.ölg In this dataset, EEG activity was recorded from nine participants as they performed various motor imagery tasks. Data was recorded using Ag Cl Electrodes positioned at twenty-two scalp locations, including Z, 3, Z, 4, and Z (Fig. 6.5). Data was referenced to the left mastoid, sampled at 250 Hz, and bandpass filtered between 0.5-100 Hz. Additionally, three EGO sensors were placed along the forehead to detect eye movement-related artefacts

A single trial lasted approximately 7.5 seconds and was broken down into: an auditory beep signalling the beginning of the trial; two seconds of a fixation cross appearing; a cue appearing on-screen for 1.25s which instructed the participant which imagined movement task to perform next; three seconds of imagined movements from the participant; and finally, a 1.5s break before the next trial, as shown in Fig. 6.6. Each participant performed two sessions, with 288 trials per session, which was broken down into: 12 trials per class for each run, with six runs per
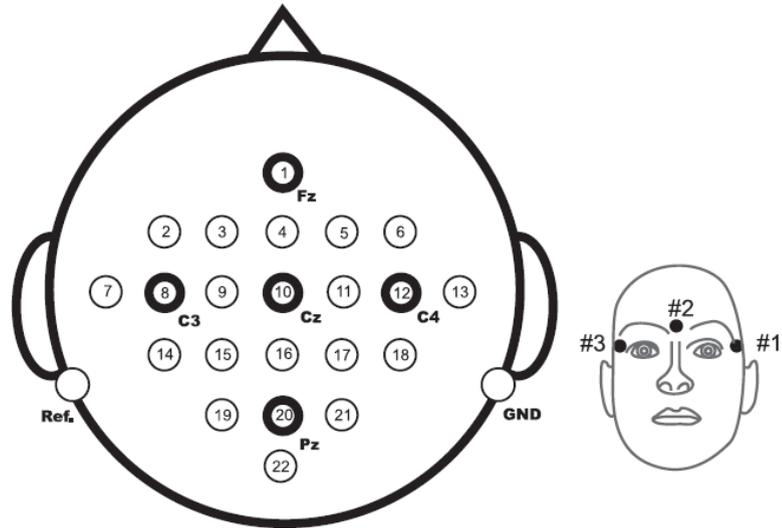
FIGURE 6.5: Electrode Montage - BCIC IV dataset 2a
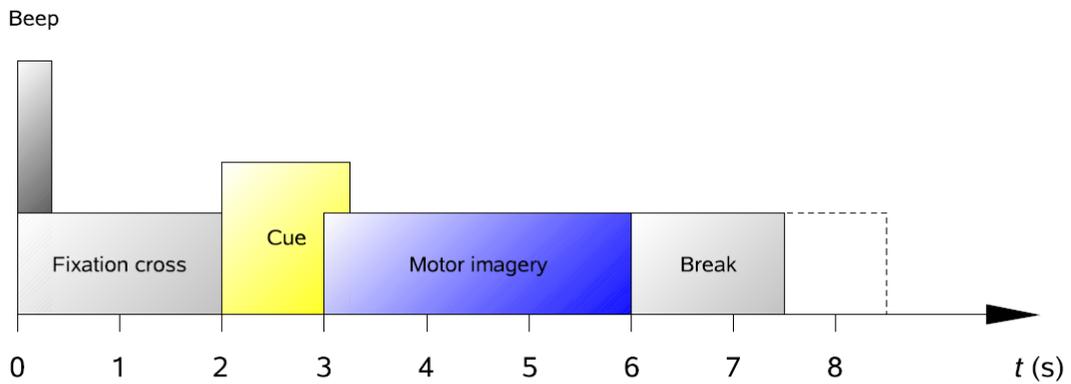
FIGURE 6.6: Timing scheme for a single trial - BCIC IV dataset 2a

session. each of the two sessions began with: a two minute block of the participant resting with eyes open, one minute with eyes closed, and one minute performing eye movements, before moving onto the trial runs (Fig. 6.7).

To keep as much consistency as possible between the two datasets, two-second long trials were extracted from both data sets.

6.2.4 Artifact Detection

Analysis of the BCIC data and offline longitudinal SMR data both utilised the automatic variance-based trial rejection method described in [145]; the raw EEG
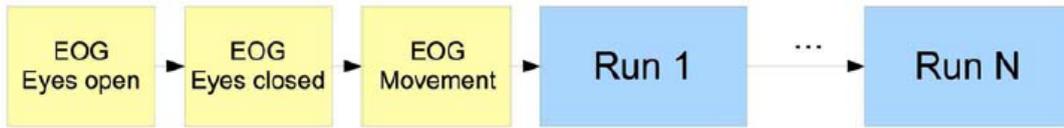
FIGURE 6.7: Trial block order - BCIC IV dataset 2a

Data was low-pass filtered at 45 Hz and downsampled to 100 Hz. Trials were then rejected based on their post-stimulus variance during the motor imagery phase; trials whose standard deviation was two times greater than the mean standard deviation across all trials were removed. Standard deviations were then re-calculated, and this process was repeated until no more trials were rejected.

6.2.5   Offline Data Analysis: Correlation

Offline analyses were performed on both the BCIC dataset and the participant's longitudinally recorded data, making it possible to investigate both interparticipant and intraparticipant effects.

The relationship between resting alpha wave activity and BCI performance was tested using both the BCIC dataset and the participant's longitudinal EEG data. For both datasets the evaluation data was classified, with the classification accuracy compared to the participant's resting EEG levels on that day, and the bandpower calculated over a 60-second interval. Each participant's resting EEG was split into four bands (theta, alpha, beta, and gamma), and the Pearson product-moment correlation coefficient between the two was calculated using:

$$\rho_{X,Y} = \frac{\text{cov}(X,Y)}{\sigma_X \sigma_Y},$$ (6.1)

where $\text{cov}(X,Y)$ represents the covariance of X and Y, and σ_X and σ_Y represent the standard deviations of X and Y.

The relationship between pre-trial neural activity and classification outcome was classified using the data occurring two seconds prior to motor imagery onset. This data was also split into four bands (theta, alpha, beta, and gamma), and compared to the eventual classification outcome of the trial. As a continuous
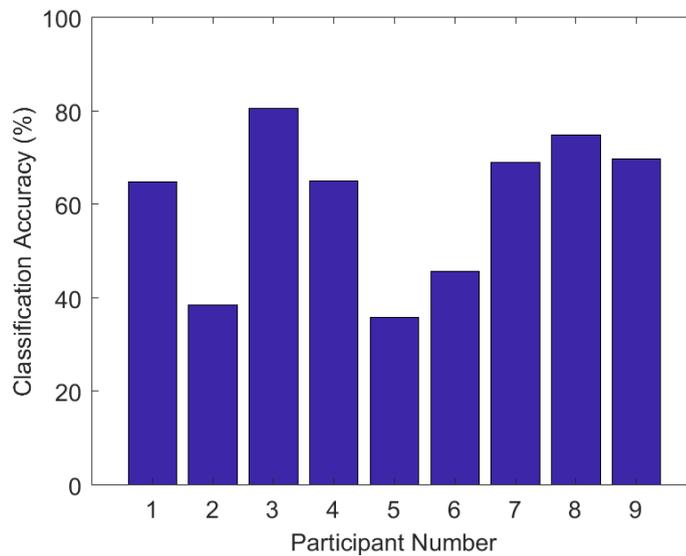
FIGURE 6.8: BCIC data classification accuracy

variable (bandpower) was being compared to a dichotomous variable (classification outcome), the point biserial correlation coefficient was found, using:

$$r_{pb} = \frac{M_1 - M_0}{s_n} \sqrt{\frac{n_1 n_0}{n^2}}, \tag{6.2}$$

where n_1 and n_0 are the number of data points in each class (correct class versus incorrect class), n is the total number of data points, M_1 and M_0 are the mean bandpower values across the corresponding classes, and s_n is the standard deviation across the whole population. As an approximate guide of effect size, Cohen [150] defines 0.1 as a small effect, 0.3 as a medium effect, and 0.5 as a strong effect.

6.3 Results

6.3.1 Offline Evaluation

Offline analysis shows that both the BCIC and longitudinal data was able to be classified fairly well using CSP and an SVM classifier (Figs. 6.8 and 6.9).

Evaluation of the BCIC dataset showed there to be a strong positive correlation between each participant's resting alpha waves and classification accuracy ($\rho =$
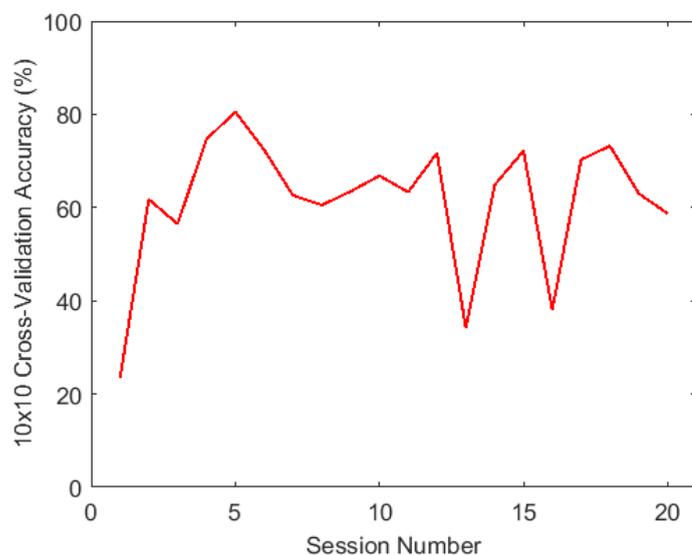
FIGURE 6.9: Session-to-session 10×10 cross-validation accuracy using CSP features

0.78, Fig. 6.10b), while resting gamma activity was found to have a strong negative correlation ($\rho = -0.60$, Fig. 6.10d). Theta and beta were also found to have strong correlations ($\rho = 0.50$ and $\rho = 0.49$, respectively, Figs. 6.10a and 6.10c).

Evaluation of our participant's longitudinal data found there to be weaker correlations intra-participant bandpower and accuracy, although in similar proportions to the BCIC data. Positive alpha and negative gamma correlations provided the strongest effects ($\rho = 0.19$ and $\rho = -0.19$, respectively, Figs. 6.11b and 6.11d), with a small-to-medium correlation. The beta band provided a small positive correlation ($\rho = 0.12$, Fig. 6.11c), while theta activity provided no correlation ($\rho = 0.07$, Fig. 6.11a).

The relationship between pre-trial bandpower in several bands and classification outcome was tested using the biserial correlation coefficient, however, no effect was found (Table 6.1). Additionally, the pre-trial correlations with trial outcome were plotted across sessions to determine whether any strong correlations developed as the participant's training progressed, but no noticeable increases in correlation were detected (Fig. 6.12).
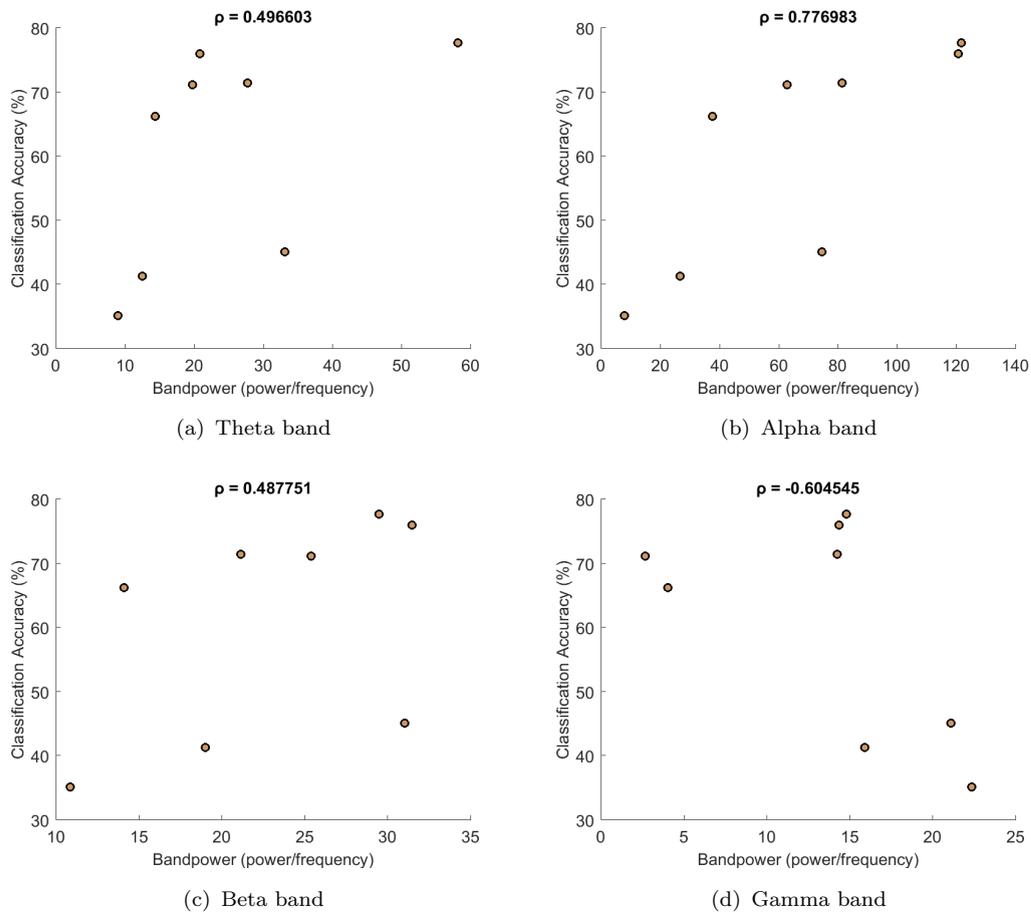
FIGURE 6.10: BCIC resting neural activity versus classification accuracy

	Theta	Alpha	Beta	Gamma
BCIC ρ	0.01397	-0.0225	-0.0236	-0.04294
Longitudinal ρ	-0.0441	-0.0106	-0.0112	0.0069

TABLE 6.1: Point biserial correlation between pre-trial bandpower and trial outcome

6.3.2 Race Performance Over Time

The participant's online performance over time using classifiers trained using the previous five runs of data can be seen in Fig. 6.13 which shows the race completion speeds for each run performed. Initial training with PSD features produced mixed results, as rather than improving results with increased number of training sessions, the participant's speed vary greatly from run to run and actually show a gradual negative trend despite the participant reporting that the task seemed to become easier over time. After switching to source CSP features, which occurs at run

(a) Theta band

(b) Alpha band

(c) Beta band

(d) Gamma band
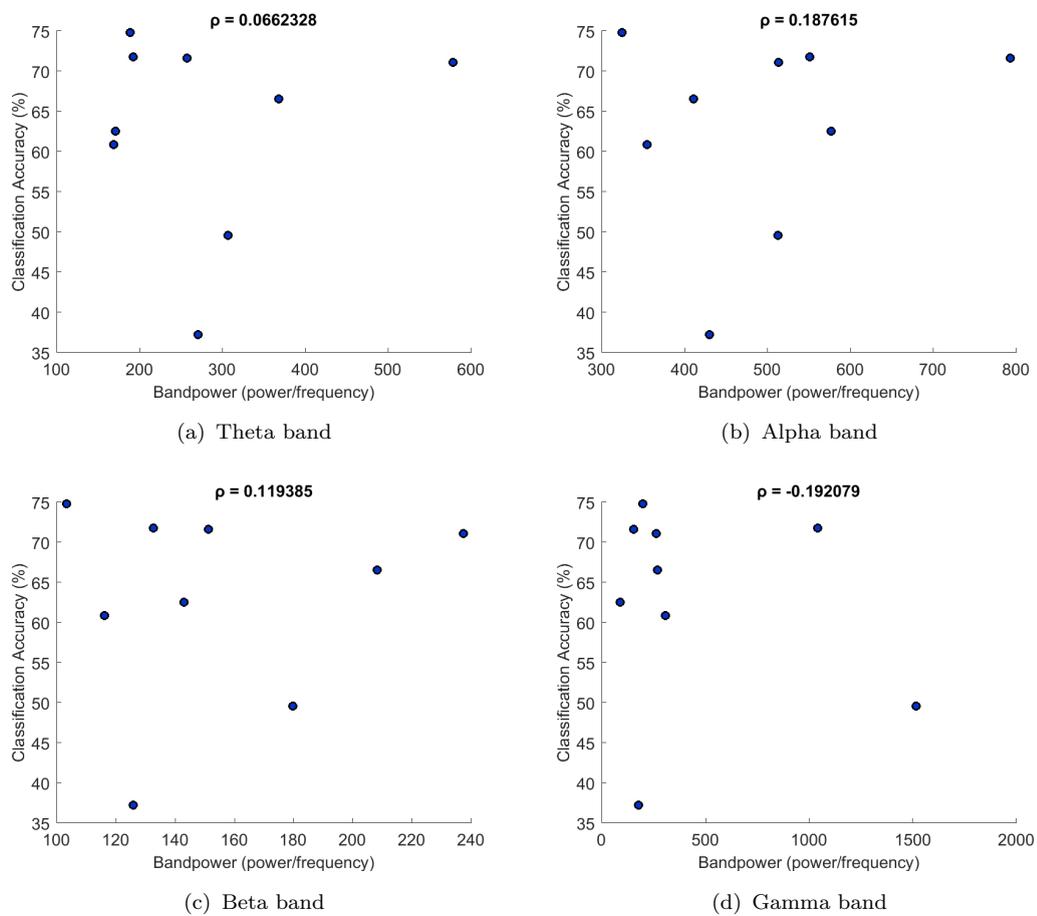
FIGURE 6.11: Our participant's resting neural activity versus 10×10 cross-validation accuracy
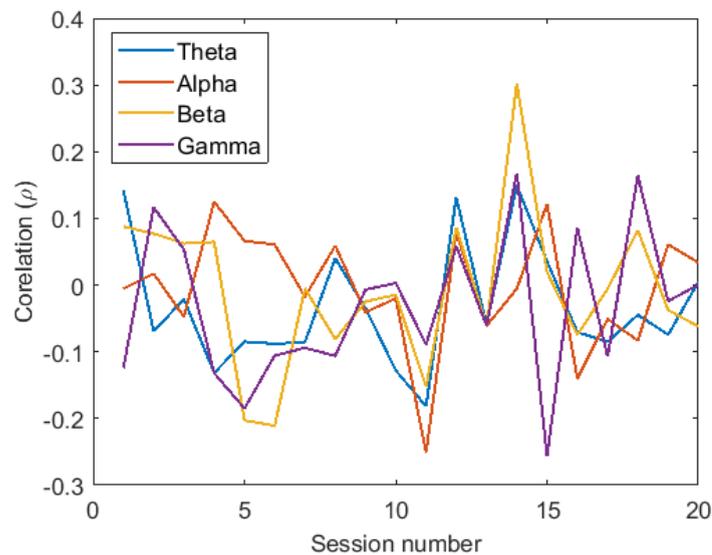
FIGURE 6.12: Participant point biserial correlation between pre-trial band-power and trial outcome

96
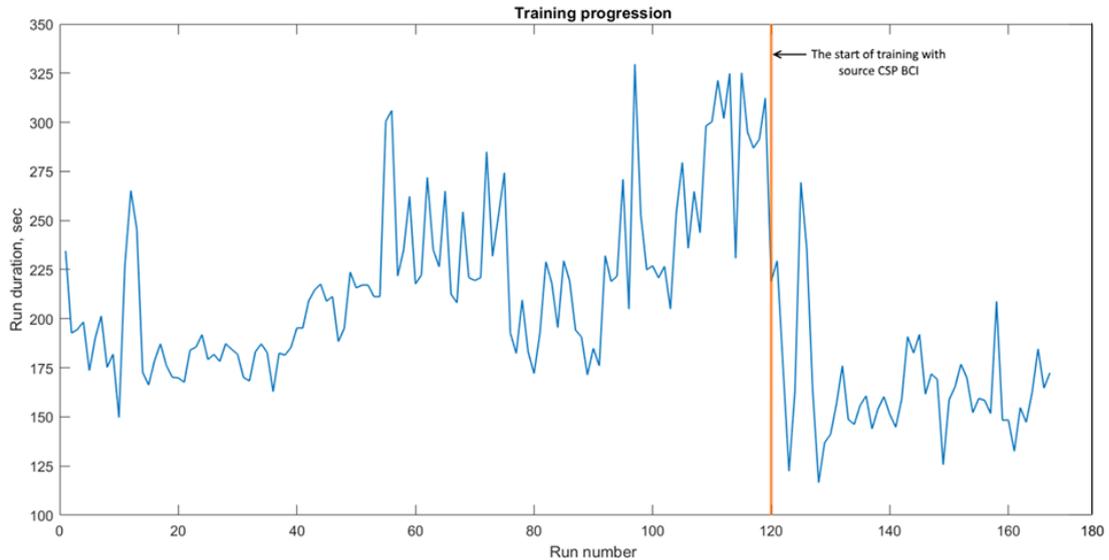
FIGURE 6.13: BrainRunners race completion speeds. Figure edited from [148]

120 and is denoted by the orange line, the participant's performance improves, as demonstrated by the shorter run times, which peak with a 116.6 second trial.

6.4 Discussion

The current chapter details the successful efforts towards creating a synchronous three-command gaming BCI operated using motor imagery commands. The online assessment of our participant's performance suggests that the source CSP features led to some benefits for this participant in terms of BCI accuracy; performance was faster and more consistent after the introduction of source CSP features. This may reflect improved class separability, although more work will be required before establishing whether this effect is at all significant. The effects of brain activity outside of the motor imagery period is also investigated, and it is found that classification accuracy had a strong positive inter-participant correlation with resting alpha activity ($\rho = 0.78$) which supports our hypothesis, as well as a strong negative correlation with resting gamma activity ($\rho = -0.60$). Theta ($\rho = 0.50$) and beta ($\rho = 0.49$), were found to have weaker, but strong positive correlations. Weaker correlations of similar proportions were seen with the longitudinal intraparticipant study, with the strongest correlations being seen with a positive alpha ($\rho = 0.19$) and negative gamma correlation ($\rho = -0.19$). No correlation was found between pre-trial bandpower and classification outcome,

97

meaning we were unable to reject our null hypothesis. There was also no evidence of increasing correlation between pre-trial bandpower and classification outcome as our participant's number of training sessions increased.

6.4.1 Critique

Due to differences in the data collection methods between the BCIC study and the longitudinal study, such as numbers of classes, trials per session, and tasks chosen, comparisons between the two are difficult. The BCIC study used two large sessions per participant, whilst the longitudinal motor imagery experiments used a larger number of sessions with less trials. As a result 10×10 cross-validation was used as the evaluation metric for this study. While it can be noted that some of our hypotheses were not accepted, namely that no evidence was found to support the existence of a correlation between pre-trial alpha and beta activity, this was a feasibility study with one participant, so this should not detract from the overall objectives of the study.

6.5 Conclusion

The results of this study have showed that there is a strong correlation between classification accuracy and resting alpha activity. A new approach for designing a motor imagery BCI using source CSP training was tested, and saw some success, although due to the extremely limited sample size it is impossible to make generalisations without further work.

Chapter 7

Conclusion

7.1 Thesis Summary and Contributions

This thesis has covered several aspects of the gaming BCI, with the aim of improving them. Each of the main studies approached BCI gaming in a different manner: designing methods using offline BCI data, designing a BCI that can operate and existing game using neural data, and building a game from scratch for BCI use and implementing algorithms to control it. A number of approaches were used throughout, including: taking both a technocentric and anthropocentric approach to BCI research, in order to improve two aspects simultaneously, and developing automatic methods for improving BCI function. These methods have been applied across two of the main modalities in BCI research, SSVEP-BCI and MI-BCI.

Chapter 2 reviewed the underlying neural processes that make human operation of a BCI possible, as well as the neuroimaging methods and algorithms that allow a BCI to be implemented. Chapter 3 defined the state of the art across several BCI areas: rehabilitation, SSVEP and motor-imagery BCI gaming, and SSVEP-BCI normalisation. Additionally, this chapter reviewed research into RVS stimulus colour, mood, and fatigue.

In Chapter 4 two normalisation methods which preserve the unsupervised classification abilities of CCA, have been tested. We addressed a problem relating to stimulus selection, in that high and low RVS frequencies often perform badly together, thus limiting the options for RVS selection in SSVEP-BCIs. BC-CCA and Scaled CCA were both found to improve standard CCA, by reducing the

performance mismatch between distant RVS frequencies. These methods are not only for gaming, and can be used for CCA SSVEP detection outside of this area. Whilst the results were positive, it is possible that such perfect conditions such as a perfectly quiet, darkened room with only one source of electrical interference, may have produced overly positive classification accuracies, although this would be across all conditions, so may not affect the overall outcome.

The work in Chapter 5 is in response to questions regarding how the effect of stimulus colour can influence SSVEP performance. We succeeded in improving the SSVEP-BCI by exploiting the RVS colour information, as shown in in Chapter 5. A three-dimensional SSVEP-BCI game, *SnookerMaze*, was developed, as well as the POC-SSVEP-BCI, which uses a novel method for stimulus colour selection was introduced, and found to significantly improve game performance and increase mood positively. A number of issues were found while conducting the study: we only focused on four colours (red, blue, yellow, and white) as we wished to investigate the primary colours, due to their opposite positions on the colour wheel. However, in doing this we neglected green, which has shown some promising results in other experiments. Additionally, whilst several benefits were found to using the POC-SSVEP-BCI, it comes at the sacrifice of the ability to use CCA without calibration data. Regarding the game itself, we believe that the layout of the game, with the RVS set at fixed positions at the edges of the screen may make it difficult for participants to elicit a strong SSVEP response and navigate the map at the same time, although we have made suggestions on how to improve this in future work (see 7.2).

Finally, the work in Chapter 6 demonstrated a novel approach to training users to operate a BCI using motor imagery commands. Additionally, we were able to create a training method that can be used by users to enjoy playing video games with a BCI, using features extracted after preprocessing the data with an additional source localisation step, referred to as 'source CSP' features. Additional work conducted involved us contributing to the development of automatic BCI methods by investigating predictors of BCI performance. Whilst making a critical appraisal of our work, we believe the online control aspect study could be designed in a more fair way, by using a between-participants design. The current method tests one method after the other, giving an advantage to the BCI operated using source CSP features. The study itself was somewhat hamstrung by a small number of participants, although as a feasibility study it does highlight some promising

areas for further research, and we were able to set up the experiment in a way which tested several predictors simultaneously, whilst also testing the effectiveness of source CSP features.

7.2   Future Work

Future research into the normalisation methods (Scaled CCA and BC-CCA) should include application to CCA variants such as filter bank CCA [48] (FBCCA), another method which requires no training data, but has higher dimensionality. The normalisation methods can be further developed by investigating automatic methods of selecting the baseline period for improved performance.

Areas for building on the POC SSVEP-BCI were identified, including developing an intelligent RVS colour selection method, such as one that takes the variance of correlation coefficients, similarity of mean correlation coefficients, or even baseline coefficient values into account in order to select colours with a more even likelihood of selection. Various approaches for improving the functionality on the POC-SSVEP-BCI game have been identified, including: adding kinematic control and giving the option for different RVS layouts, such as one that is locked to the avatar's position instead of fixed positions on the screen, which would reduce the amount of eye movements required by the player. Another way that future research can build on these results is by comparing POC RVS performance to the participant's best individual set of colours instead of white. What we are proposing is to compare two RVS groups: a group of identically-coloured RVS selected by classification accuracy, and a group of individually-coloured RVS selected based on their correlation coefficients, as done in Chapter 5. This would be another effective way of testing the effectiveness of the POC-SSVEP BCI. This would effectively compare the commonly used stimulus selection method with our new method. The normalisation methods from Chapter 4 were not applied, however this could be a promising avenue of research.

The approaches applied to motor imagery BCI were found to be successful for developing a user-centred BCI, although this was severely limited due to the sample size. For the next step, more participants are required in order to test the source CSP features, which will allow us to take a look at group-level statistics regarding the impact of source-CSP. Some areas of interest would include: and an in-depth

look can be taken at group-level neural changes over time. No user experience data was collected during this experiment, as this was primarily a technical challenge, however it would be interesting to monitor levels of engagement as well as participant feedback on the source CSP approach, as compared to others. One major technological challenge to address in future work will be detecting the 'idle state' in order to make this a truly asynchronous BCI. A number of approaches were discussed in Chapter 3, such as setting confidence thresholds for each class and setting the BCI output to idle if these thresholds are not met. Successfully implementing this would allow the user much greater control over how they operate the game. In the current BCI, we limited ourselves to movement commands based on three of the most popular commands (right hand, left hand, and feet), although it would be appropriate to test source how our proposed training methods perform using other approaches for generating movement commands, such a cube rotation and number subtraction. Additionally, more disabled users should be recruited to test the BCI; the majority of research includes healthy participants as they are easy to recruit, however disabled users have complex needs that cannot be accounted for without including them in this process.

Bibliography

[1] Jonathan R Wolpaw, Niels Birbaumer, Dennis J McFarland, Gert Pfurtscheller, and Theresa M Vaughan. Brain-computer interfaces for communication and control. Clinical neurophysiology : official journal of the International Federation of Clinical Neurophysiology, 113(6):767–91, jun 2002. ISSN 1388-2457. URL http://www.ncbi.nlm.nih.gov/pubmed/12048038.

[2] Emilie Loup-Escande, Fabien Lotte, Guillaume Loup, and Anatole Lecuyer. User-Centred BCI Videogame Design. In Ryohei Nakatsu, Matthias Rauterberg, and Paolo Ciancarini, editors, Handbook of Digital Games and Entertainment Technologies, pages 225–250. Springer, 2015. ISBN 9789814560528.

[3] David Steyrl, Reinmar J Kobler, and Gernot R Müller-Putz. On Similarities and Differences of Invasive and Non-Invasive Electrical Brain Signals in Brain-Computer Interfacing. J. Biomedical Science and Engineering, 9(9):393–398, 2016. ISSN 1937-6871. doi: 10.4236/jbise.2016.98034. URL http://www.scirp.org/journal/jbise{%}5Cnhttp://dx.doi.org/10.4236/jbise.2016.98034{%}5Cnhttp://creativecommons.org/licenses/by/4.0/.

[4] Frederico A.C. Azevedo, Ludmila R.B. Carvalho, Lea T. Grinberg, José Marcelo Farfel, Renata E.L. Ferretti, Renata E.P. Leite, Wilson Jacob Filho, Roberto Lent, and Suzana Herculano-Houzel. Equal numbers of neuronal and nonneuronal cells make the human brain an isometrically scaled-up primate brain. Journal of Comparative Neurology, 513(5):532–541, 2009. ISSN 00219967. doi: 10.1002/cne.21974.

[5] P C Fletcher and R N Henson. Frontal lobes and human memory: insights from functional neuroimaging. Brain: a journal of neurology, 124(Pt 5): 849–881, 2001. ISSN 0006-8950. doi: 10.1093/brain/124.5.849.

[6] Richard P Dum and Peter L Strick. Motor areas in the frontal lobe of the primate. Physiology & Behavior, 77:677–682, 2002.

[7] Anthony D. Wagner, Benjamin J. Shannon, Itamar Kahn, and Randy L. Buckner. Parietal lobe contributions to episodic memory retrieval. Trends in Cognitive Sciences, 9(9):445–453, 2005. ISSN 13646613. doi: 10.1016/j. tics.2005.07.001.

[8] J C Lynch, V B Mountcastle, W H Talbot, and T C Yin. Parietal lobe mechanisms for directed visual attention. Journal of neurophysiology, 40(2): 362–389, 1977. ISSN 0022-3077.

[9] Hans-Otto Karnath, Susanne Ferber, and Marc Himmelbach. Spatial awareness is a function of the temporal not the posterior parietal lobe. Cortex, 411 (6840):950–953, 2001. ISSN 00109452. doi: 10.1016/S0010-9452(08)70654-3.

[10] Kalanit Grill-Spector, Tammar Kushnir, Talma Hendler, Shimon Edelman, Yacov Itzchak, and Rafael Malach. A sequence of object-processing stages revealed by fMRI in the human occipital lobe. Human Brain Mapping, 6 (4):316–328, 1998. ISSN 10659471. doi: 10.1002/(SICI)1097-0193(1998)6: 4⟨316::AID-HBM9⟩3.0.CO;2-6.

[11] Jennifer L Collinger, Brian Wodlinger, John E Downey, Wei Wang, Elizabeth C Tyler-Kabara, Douglas J Weber, Angus J C McMorland, Meel Velliste, Michael L Boninger, and Andrew B Schwartz. High-performance neuroprosthetic control by an individual with tetraplegia. Lancet, 381(9866): 557–564, feb 2013. ISSN 1474-547X. doi: 10.1016/S0140-6736(12)61816-9. URL http://www.ncbi.nlm.nih.gov/pubmed/23253623.

[12] Leigh R Hochberg, Daniel Bacher, Beata Jarosiewicz, Nicolas Y Masse, D John, Joern Vogel, Sami Haddadin, Jie Liu, Sydney S Cash, John P Donoghue, Development Service, and General Hospital. Reach and grasp by people with tetraplegia using a neurally controlled robotic arm. Nature, 485 (7398):372–375, 2013. doi: 10.1038/nature11076.Reach. URL http://www. nature.com/nature/journal/v485/n7398/abs/nature11076.html.

[13] Vadim S. Polikov, Patrick A. Tresco, and William M. Reichert. Response of brain tissue to chronically implanted neural electrodes. Journal of Neuroscience Methods, 148(1):1–18, 2005. ISSN 01650270. doi: 10.1016/j.jneumeth.2005.08.015.

[14] G. Pfurtscheller and F. H. Lopes Da Silva. Event-related EEG/MEG synchronization and desynchronization: Basic principles. Clinical Neurophysiology, 110(11):1842–1857, 1999. ISSN 13882457. doi: 10.1016/S1388-2457(99)00141-8.

[15] G Klem, H Luders, H Jasper, and C Elger. The ten-twenty electrode system of the International Federation. Electroencephalography and Clinical Neurophysiology, 10(2):371–375, 1958. ISSN 00134694. doi: 10.1016/0013-4694(58)90053-1. URL http://www.ncbi.nlm.nih.gov/pubmed/10590970.

[16] Kyle E. Mathewson, Tyler J.L. Harrison, and Sayeed A.D. Kizuk. High and dry? Comparing active dry EEG electrodes to active and passive wet electrodes. Psychophysiology, 54(1):74–82, 2017. ISSN 14698986. doi: 10.1111/psyp.12536.

[17] Matti Hämäläinen, Riitta Hari, Risto J. Ilmoniemi, Jukka Knuutila, and Olli V. Lounasmaa. Magnetoencephalography theory, instrumentation, and applications to noninvasive studies of the working human brain. Reviews of Modern Physics, 65(2):413–497, 1993. ISSN 00346861. doi: 10.1103/RevModPhys.65.413.

[18] Janet S. Soul and Adré J. du Plessis. Near-infrared spectroscopy. Seminars in Pediatric Neurology, 6(2):101–110, 1999. ISSN 10719091. doi: 10.1016/S1071-9091(99)80036-9. URL http://www.sciencedirect.com/science/article/pii/S1071909199800369.

[19] Byoung-Kyong Min, Matthew J Marzelli, and Seung-Schik Yoo. Neuroimaging-based approaches in the brain-computer interface. Trends in biotechnology, 28(11):552–60, nov 2010. ISSN 1879-3096. doi: 10.1016/j.tibtech.2010.08.002. URL http://www.ncbi.nlm.nih.gov/pubmed/20810180.

[20] David A. Boas, Anders M. Dale, and Maria Angela Franceschini. Diffuse optical imaging of brain activation: Approaches to optimizing image sensitivity, resolution, and accuracy. NeuroImage, 23(1):S275–S288, 2004. ISSN 10538119. doi: 10.1016/j.neuroimage.2004.07.011.

[21] C. S. Herrmann. Human EEG responses to 1-100 Hz flicker: Resonance phenomena in visual cortex and their potential correlation to cognitive phenomena. Experimental Brain Research, 137(3-4):346–353, 2001. ISSN 00144819. doi: 10.1007/s002210100682.

[22] Hovagim Bakardjian, Toshihisa Tanaka, and Andrzej Cichocki. Optimization of SSVEP brain responses with application to eight-command Brain-Computer Interface. Neuroscience letters, 469(1):34–38, jan 2010. ISSN 1872-7972. doi: 10.1016/j.neulet.2009.11.039. URL http://www.ncbi.nlm.nih.gov/pubmed/19931592.

[23] G R Burkitt, R B Silberstein, P J Cadusch, and a W Wood. Steady-state visual evoked potentials and travelling waves. Clinical neurophysiology : official journal of the International Federation of Clinical Neurophysiology, 111(2):246–258, 2000. ISSN 1388-2457. doi: 10.1016/S1388-2457(99)00194-7.

[24] Samuel Garrett Thorpe, Paul L Nunez, and Ramesh Srinivasan. Identification of wave-like spatial structure in the SSVEP: Comparison of simultaneous EEG and MEG. Statistics in Medicine, 26(August):3911–3926, 2007. doi: 10.1002/sim.

[25] Jian Ding, George Sperling, and Ramesh Srinivasan. Attentional modulation of SSVEP power depends on the network tagged by the flicker frequency. Cerebral Cortex, 16(7):1016–29, jul 2006. ISSN 1047-3211. doi: 10.1093/cercor/bhj044. URL http://www.pubmedcentral.nih.gov/articlerender.fcgi?artid=1880883{&}tool=pmcentrez{&}rendertype=abstract.

[26] B Graimann, B Allison, and G Pfurtscheller. Brain-computer interfaces: Revolutionizing human-computer interaction. Springer Science & Business Media, 2010. ISBN 9783642020902.

[27] Andrew J. McDaid, Song Xing, and Sheng Q. Xie. Brain controlled robotic exoskeleton for neurorehabilitation. 2013 IEEE/ASME International

Conference on Advanced Intelligent Mechatronics: Mechatronics for Human Wellbeing, AIM 2013, pages 1039–1044, 2013. ISSN 2159-6255. doi: 10.1109/AIM.2013.6584231.

[28] Takeshi Sakurada, Toshihiro Kawase, Kouji Takano, Tomoaki Komatsu, and Kenji Kansaku. A BMI-based occupational therapy assist suit: Asynchronous control by SSVEP. Frontiers in Neuroscience, 7(7 SEP):1–10, 2013. ISSN 1662453X. doi: 10.3389/fnins.2013.00172.

[29] Sandra Mara Torres Müller and Teodiano Freire Bastos-filho. Brain-computer Interface Based on Visual Evoked Potentials to Command Autonomous Robotic Wheelchair. Journal of Medical and Biological Engineering, 30(6):407–416, 2010. doi: 10.5405/jmbe.765.

[30] Gerolf Vanacker, José Del R. Millán, Eileen Lew, Pierre W. Ferrez, Ferran Galán Moles, Johan Philips, Hendrik Van Brussel, and Marnix Nuttin. Context-based filtering for assisted brain-actuated wheelchair driving. Computational Intelligence and Neuroscience, 2007:1–12, 2007. ISSN 16875265. doi: 10.1155/2007/25130.

[31] Christian J Bell, Pradeep Shenoy, Rawichote Chalodhorn, and Rajesh P N Rao. Control of a humanoid robot by a noninvasive brain-computer interface in humans. Journal of neural engineering, 5(2):214–20, jun 2008. ISSN 1741-2560. doi: 10.1088/1741-2560/5/2/012. URL http://www.ncbi.nlm.nih.gov/pubmed/18483450.

[32] Robert S. Fisher, Graham Harding, Giuseppe Erba, Gregory L. Barkley, and Arnold Wilkins. Photic- and pattern-induced seizures: A review for the epilepsy foundation of america working group. Epilepsia, 46(9):1426–1441, 2005. ISSN 00139580. doi: 10.1111/j.1528-1167.2005.31405.x.

[33] Dimitra Makri, Christina Farmaki, and Vangelis Sakkalis. Visual fatigue effects on Steady State Visual Evoked Potential-based Brain Computer Interfaces. International IEEE/EMBS Conference on Neural Engineering, NER, 2015-July:70–73, 2015. ISSN 19483554. doi: 10.1109/NER.2015.7146562.

[34] H Yuan and B He. Brain-Computer Interfaces Using Sensorimotor Rhythms: Current State and Future Perspectives. IEEE Transactions on Biomedical Engineering, PP(99):1, 2014. doi: 10.1109/TBME.2014.2312397.

[35] Christoph Guger, Günter Edlinger, and Gunther Krausz. Hardware/Software Components and Applications of BCIs. In Reza Fazel-Rezai, editor, Recent Advances in Brain-Computer Interface Systems, pages 1–24. InTech, 2011.

[36] Steven J Luck. An Introduction to the Event-Related Potential Technique. MIT press, 2014. ISBN 0262122774. doi: 10.1118/1.4736938. URL http://mitpress.mit.edu/sites/default/files/titles/content/9780262621960{_}sch{_}0001.pdf{%}5Cnhttp://cognet.mit.edu/library/books/view?isbn=0262122774{%}5Cnhttp://www.amazon.com/Introduction-Event-Related-Potential-Technique-Neuroscience/dp/0262621967http://doi.

[37] S. Sutton, M. Braten, J. Zubin, and E.R. John. Evoked-potentials correlates of stimulus uncertainty. Science, 150(3700):1187–1188, 1965. ISSN 0036-8075. doi: 10.1126/science.150.3700.1187.

[38] Nikolay V. Manyakov, Nikolay Chumerin, Adrien Combaz, and Marc M. Van Hulle. Comparison of classification methods for P300 brain-computer interface on disabled subjects. Computational Intelligence and Neuroscience, 2011:1–12, 2011. ISSN 16875265. doi: 10.1155/2011/519868.

[39] E. Fabiani, M., Gratton G., Karis, D., Donchin. Definition, identification and reliability of the P300 component of the event related brain potential. Advances in Psychophysiology, 2(1):1–78, 1987.

[40] Christoph Guger, Shahab Daban, Eric Sellers, Clemens Holzner, Gunther Krausz, Roberta Carabalona, Furio Gramatica, and Guenter Edlinger. How many people are able to control a P300-based brain-computer interface (BCI)? Neuroscience Letters, 462(1):94–98, 2009. ISSN 03043940. doi: 10.1016/j.neulet.2009.06.045.

[41] Martin Spüler, Michael Bensch, Sonja Kleih, Wolfgang Rosenstiel, Martin Bogdan, and Andrea Kübler. Online use of error-related potentials in healthy users and people with severe motor impairment increases performance of a P300-BCI. Clinical neurophysiology : official journal of the International Federation of Clinical Neurophysiology, 123(7):1328–37, jul 2012. ISSN 1872-8952. doi: 10.1016/j.clinph.2011.11.082. URL http://www.ncbi.nlm.nih.gov/pubmed/22244309.

[42] Saeid Sanei and Jonathon. A. Chambers. EEG Signal Processing, volume 1. John Wiley and Sons, Chichester, 2007. ISBN 9780470025819. doi: 10.1002/9780470511923. URL http://books.google.com/books?hl=en{&}lr={&}id=vIuCV2IKwasC{&}oi=fnd{&}pg=PR5{&}dq=EEG+signal+Processing{&}ots=vgIh2fC4mB{&}sig=nigFhniJIEdj6sZekh5zu1taauc.

[43] Rajesh P N Rao. Brain-Computer Interfacing: An Introduction. Cambridge University Press, 2013. ISBN 9781139032803.

[44] Hao-Teng Hsu, I-Hui Lee, Han-Ting Tsai, Hsiang-Chih Chang, Kuo-Kai Shyu, Chuan-Chih Hsu, Hsiao-Huang Chang, Ting-Kuang Yeh, Chun-Yen Chang, and Po-Lei Lee. Evaluate the Feasibility of Using Frontal SSVEP to Implement an SSVEP-Based BCI in Young, Elderly and ALS Groups. IEEE Transactions on Neural Systems and Rehabilitation Engineering, 24(5):603–615, 2016. ISSN 1534-4320. doi: 10.1109/TNSRE.2015.2496184. URL http://ieeexplore.ieee.org/lpdocs/epic03/wrapper.htm?arnumber=7335644.

[45] Sandra Mara Torres Müller, Teodiano Freire Bastos-Filho, and Mário Sarcinelli-Filho. Monopolar and bipolar electrode settings for SSVEP-based brain-computer interface. Journal of Medical and Biological Engineering, 35(4):482–491, 2015. ISSN 21994757. doi: 10.1007/s40846-015-0056-1.

[46] Luisa Suarez, Eleri Cardozo, Romis Attux, and Diogo Soriano. An implementation of SSVEP-BCI system based on a cluster measure for feature selection. In ISSNIP Biosignals and Biorobotics Conference, BRC, pages 1–6, 2014. ISBN 9781479956890. doi: 10.1109/BRC.2014.6880994.

[47] Abdullah Akce, James J S Norton, and Timothy Bretl. An SSVEP-based brain-computer interface for text spelling with adaptive queries that maximize information gain rates. IEEE Transactions on Neural Systems and Rehabilitation Engineering, 23(5):857–866, 2015. ISSN 15344320. doi: 10.1109/TNSRE.2014.2373338.

[48] Xiaogang Chen, Yijun Wang, Shangkai Gao, Tzyy-Ping Jung, and Xiaorong Gao. Filter bank canonical correlation analysis for implementing a high-speed SSVEP-based braincomputer interface. Journal of Neural Engineering, 12(4):46008, 2015. ISSN 1741-2552. doi: 10.1088/1741-2560/12/4/046008. URL http://stacks.iop.org/1741-2552/12/i=4/a=046008.

Bibliography

[49] No-Sang Kwak, Klaus-Robert Müller, and Seong-Whan Lee. A lower limb exoskeleton control system based on steady state visual evoked potentials. Journal of Neural Engineering, 12(5):056009, 2015. ISSN 1741-2560. doi: 10. 1088/1741-2560/12/5/056009. URL http://stacks.iop.org/1741-2552/12/i=5/a=056009?key=crossref.d574e38494295e53b491abb83540a57c.

[50] Laura Acqualagna, Loic Botrel, Carmen Vidaurre, Andrea Kübler, and Benjamin Blankertz. Large-scale assessment of a fully automatic co-adaptive motor imagery-based brain computer interface. PLoS ONE, 11(2):1–19, 2016. ISSN 19326203. doi: 10.1371/journal.pone.0148886.

[51] Jürgen Kayser and Craig E. Tenke. Issues and considerations for using the scalp surface Laplacian in EEG/ERP research: A tutorial review. International Journal of Psychophysiology, 97(3):189–209, 2015. ISSN 18727697. doi: 10.1016/j.ijpsycho.2015.04.012. URL http://dx.doi.org/10.1016/j.ijpsycho.2015.04.012.

[52] Herbert Ramoser, Johannes Müller-Gerking, and Gert Pfurtscheller. Optimal spatial filtering of single trial EEG during imagined hand movement. IEEE Transactions on Rehabilitation Engineering, 8(4):441–446, 2000. ISSN 10636528. doi: 10.1109/86.895946.

[53] Kai Keng Ang, Zheng Yang Zhang Yang Chin, Haihong Zhang, and Cuntai Guan. Filter Bank Common Spatial Pattern (FBCSP) in Brain-Computer Interface. In International Joint Conference on Neural Networks (IJCNN), pages 2390–2397, 2008. ISBN 978-1-4244-1820-6. doi: 10.1109/IJCNN.2008.4634130. URL http://ieeexplore.ieee.org/xpls/abs{_}all.jsp?arnumber=4634130{%}5Cnhttp://ieeexplore.ieee.org/lpdocs/epic03/wrapper.htm?arnumber=4634130.

[54] Kai Keng Ang, Zheng Yang Chin, Chuanchu Wang, Cuntai Guan, and Haihong Zhang. Filter bank common spatial pattern algorithm on BCI competition IV datasets 2a and 2b. Frontiers in Neuroscience, 6(MAR):1–9, 2012. ISSN 16624548. doi: 10.3389/fnins.2012.00039.

[55] Aleksandr Zaitcev, Greg Cook, Wei Liu, and Elizabeth Milne. Application of Compressive Sensing for EEG Source Localization in Brain Computer Interfaces. In Antennas and Propagation Conference (LAPC), pages 272–276, 2014. ISBN 9781479936625. doi: 10.1109/LAPC.2014.6996374.

[56] G Pfurtscheller and C Neuper. Motor imagery and direct brain- computer communication. Proceedings of the IEEE, 89(7):1123–1134, 2001. ISSN 00189219. doi: 10.1109/5.939829.

[57] Javier Castillo, Sandra Muller, Eduardo Caicedo, and Teodiano Bastos. Feature extraction techniques based on power spectrum for a SSVEP-BCI. In 2014 IEEE 23rd International Symposium on Industrial Electronics (ISIE), pages 1051–1055, 2014. ISBN 978-1-4799-2399-1. doi: 10.1109/ISIE.2014. 6864758. URL http://ieeexplore.ieee.org/lpdocs/epic03/wrapper. htm?arnumber=6864758.

[58] Ola Friman, Ivan Volosyak, and Axel Gräser. Multiple channel detection of steady-state visual evoked potentials for brain-computer interfaces. IEEE transactions on bio-medical engineering, 54(4):742–50, 2007. ISSN 0018- 9294. doi: 10.1109/TBME.2006.889160. URL http://www.ncbi.nlm.nih. gov/pubmed/17405382.

[59] Sn Resalat and Sk Setarehdan. An Improved SSVEP Based BCI System Using Frequency Domain Feature Classification. American Journal of Biomedical . . . , 3(1):1–8, 2013. doi: 10.5923/j.ajbe.20130301.01. URL http://article.sapub.org/10.5923.j.ajbe.20130301.01.html.

[60] Zhonglin Lin, Changshui Zhang, Wei Wu, and Xiaorong Gao. Frequency Recognition Based on Canonical Correlation Analysis for SSVEP-Based BCIs. IEEE Transactions on Biomedical Engineering, 53(12):315–323, 2006. doi: 10.1007/978-3-319-25393-0_35. URL http://link.springer.com/10. 1007/978-3-319-12436-0.

[61] Guangyu Bin, Xiaorong Gao, Zheng Yan, Bo Hong, and Shangkai Gao. An online multi-channel SSVEP-based brain-computer interface using a canonical correlation analysis method. Journal of neural engineering, 6(4):046002, 2009. ISSN 1741-2560. doi: 10.1088/1741-2560/6/4/046002.

[62] Masaki Nakanishi, Yijun Wang, Yu-te Wang, Yasue Mitsukura, and Tzyy Jung. Enhancing Unsupervised Canonical Correlation Analysis-Based Frequency Detection of SSVEPs by Incorporating Background EEG. In 36th Annual International Conference of the IEEE Engineering in Medicince and Biology Society, pages 3053–3056, 2014. ISBN 9781424479290. doi: 10.1109/EMBC.2014.6944267.

[63] Yu Zhang, Guoxu Zhou, Jing Jin, Xingyu Wang, and Andrzej Cichocki. FREQUENCY RECOGNITION IN SSVEP-BASED BCI USING MULTI-SET CANONICAL CORRELATION ANALYSIS. International Journal of Neural Systems, 24(4):1450013, 2014. doi: 10.1142/S0129065714500130.

[64] Sarah N. Carvalho, Thiago B.S. Costa, Luisa F.S. Uribe, Diogo C. Soriano, Glauco F.G. Yared, Luis C. Coradine, and Romis Attux. Comparative analysis of strategies for feature extraction and classification in SSVEP BCIs. Biomedical Signal Processing and Control, 21:34–42, 2015. ISSN 17468094. doi: 10.1016/j.bspc.2015.05.008. URL http://linkinghub.elsevier.com/retrieve/pii/S1746809415000877.

[65] CM Bishop. Pattern recognition and machine learning. Springer Science+Business Media, New York, 2006. ISBN 9780387310732. URL http://www.library.wisc.edu/selectedtocs/bg0137.pdf.

[66] Isabelle Guyon and André Elisseeff. An Introduction to Variable and Feature Selection Isabelle. Journal of machine learning research, 3(Mar):1157–1182, 2003. ISSN 00032670. doi: 10.1016/j.aca.2011.07.027.

[67] George H. John, Ron Kohavi, and Karl Pfleger. Irrelevant Features and the Subset Selection Problem. In Machine Learning Proceedings 1994, pages 121–129, 1994. ISBN 1558603352. doi: 10.1016/B978-1-55860-335-6.50023-4. URL http://linkinghub.elsevier.com/retrieve/pii/B9781558603356500234.

[68] Sebastian Mika, Gunnar Ratsch, Jason Weston, Bernhard Schölkopf, and Klaus-Robert Muller. Fisher discriminant analysis with kernels. In Neural Networks for Signal Processing IX, 1999. Proceedings of the 1999 IEEE Signal Processing Society Workshop, pages 41–48, 1999. ISBN 0-7803-5673-X. doi: 10.1109/NNSP.1999.788121.

[69] M A Hearst, S T Dumais, E Osman, J Platt, and B Scholkopf. Support vector machines. IEEE Intelligent Systems, 13(4):18–28, 1998. ISSN 1094-7167. doi: 10.1109/5254.708428.

[70] Thomas Hofmann, Bernhard Schölkopf, and Alexander J. Smola. Kernel methods in machine learning. Annals of Statistics, 36(3):1171–1220, 2008. ISSN 00905364. doi: 10.1214/009053607000000677.

[71] Ron Kohavi. A Study of Cross-Validation and Bootstrap for Accuracy Estimation and Model Selection. International Joint Conference on Artificial Intelligence (IJCAI), 14(2):1137–1145, 1995. ISSN 10450823. doi: 10.1067/mod.2000.109031. URL http://robotics.stanford.edu/{~}ronnyk.

[72] Bernhard Obermaier, Christa Neuper, Christoph Guger, and Gert Pfurtscheller. Information transfer rate in a five-classes brain-computer interface. IEEE Transactions on Neural Systems and Rehabilitation Engineering, 9(3):283–288, 2001. ISSN 15344320. doi: 10.1109/7333.948456.

[73] Peng Yuan, Xiaorong Gao, Brendan Allison, Yijun Wang, Guangyu Bin, and Shangkai Gao. A study of the existing problems of estimating the information transfer rate in online brain-computer interfaces. Journal of neural engineering, 10(2):026014, 2013. ISSN 1741-2552. doi: 10.1088/1741-2560/10/2/026014. URL http://www.ncbi.nlm.nih.gov/pubmed/23448963.

[74] Jacob Cohen. A coefficient of agreement for nominal scales. Educational and psychological measurement, 20(1):37–46, 1960.

[75] Brendan Z. Allison, Jing Jin, Yu Zhang, and Xingyu Wang. A four-choice hybrid P300/SSVEP BCI for improved accuracy. Brain-Computer Interfaces, 1(1):17–26, jan 2014. ISSN 2326-263X. doi: 10.1080/2326263X.2013.869003. URL http://www.tandfonline.com/doi/abs/10.1080/2326263X.2013.869003.

[76] Petar Horki, Teodoro Solis-Escalante, Christa Neuper, and Gernot Müller-Putz. Combined motor imagery and SSVEP based BCI control of a 2 DoF artificial upper limb. Medical & biological engineering & computing, 49(5):567–77, may 2011. ISSN 1741-0444. doi: 10.1007/s11517-011-0750-2. URL http://www.ncbi.nlm.nih.gov/pubmed/21394652.

[77] Jinyi Long, Yuanqing Li, Tianyou Yu, and Zhenghui Gu. Target selection with hybrid feature for BCI-based 2-D cursor control. IEEE transactions on bio-medical engineering, 59(1):132–40, jan 2012. ISSN 1558-2531. doi: 10.1109/TBME.2011.2167718. URL http://www.ncbi.nlm.nih.gov/pubmed/21926016.

[78] Erwei Yin, Zongtan Zhou, Jun Jiang, Fanglin Chen, Yadong Liu, and Dewen Hu. A speedy hybrid BCI spelling approach combining P300 and SSVEP. IEEE transactions on bio-medical engineering, 61(2):473–83, feb 2014. ISSN

1558-2531. doi: 10.1109/TBME.2013.2281976. URL http://www.ncbi.nlm.nih.gov/pubmed/24058009.

[79] Bongjae Choi and Sungho Jo. A low-cost EEG system-based hybrid brain-computer interface for humanoid robot navigation and recognition. PloS one, 8(9):e74583, jan 2013. ISSN 1932-6203. doi: 10.1371/journal.pone.0074583. URL http://www.pubmedcentral.nih.gov/articlerender.fcgi?artid=3762758{&}tool=pmcentrez{&}rendertype=abstract.

[80] Brendan Z Allison, Clemens Brunner, Christof Altstätter, Isabella C Wagner, Sebastian Grissmann, and Christa Neuper. A hybrid ERD/SSVEP BCI for continuous simultaneous two dimensional cursor control. Journal of neuroscience methods, 209(2):299–307, aug 2012. ISSN 1872-678X. doi: 10.1016/j.jneumeth.2012.06.022. URL http://www.ncbi.nlm.nih.gov/pubmed/22771715.

[81] Carla J. Shatz. The developing brain., 1992. ISSN 0036-8733. URL http://www.ncbi.nlm.nih.gov/pubmed/1502524.

[82] Gert Pfurtscheller, Gernot R Müller, Jörg Pfurtscheller, Hans Jürgen Gerner, and Rüdiger Rupp. Thought' control of functional electrical stimulation to restore hand grasp in a patient with tetraplegia. Neuroscience Letters, 351(1):33–36, nov 2003. ISSN 03043940. doi: 10.1016/S0304-3940(03)00947-9. URL http://linkinghub.elsevier.com/retrieve/pii/S0304394003009479.

[83] Henrik Gollee, Ivan Volosyak, Angus J McLachlan, Kenneth J Hunt, and Axel Gräser. An SSVEP-based brain-computer interface for the control of functional electrical stimulation. IEEE transactions on bio-medical engineering, 57(8):1847–55, aug 2010. ISSN 1558-2531. doi: 10.1109/TBME.2010.2043432. URL http://www.ncbi.nlm.nih.gov/pubmed/20176528.

[84] An H Do, Po T Wang, Christine E King, Ahmad Abiri, and Zoran Nenadic. Brain-computer interface controlled functional electrical stimulation system for ankle movement. Journal of neuroengineering and rehabilitation, 8:49, jan 2011. ISSN 1743-0003. doi: 10.1186/1743-0003-8-49. URL http://www.pubmedcentral.nih.gov/articlerender.fcgi?artid=3247850{&}tool=pmcentrez{&}rendertype=abstract.

[85] Keiichiro Shindo, Kimiko Kawashima, Junichi Ushiba, Naoki Ota, Mari Ito, Tetsuo Ota, Akio Kimura, and Meigen Liu. Effects of neurofeedback training with an electroencephalogram-based brain-computer interface for hand paralysis in patients with chronic stroke: a preliminary case series study. Journal of rehabilitation medicine : official journal of the UEMS European Board of Physical and Rehabilitation Medicine, 43(10): 951–7, oct 2011. ISSN 1651-2081. doi: 10.2340/16501977-0859. URL http://www.ncbi.nlm.nih.gov/pubmed/21947184.

[86] Janis J Daly, Roger Cheng, Jean Rogers, Krisanne Litinas, Kenneth Hrovat, and Mark Dohring. Feasibility of a new application of noninvasive Brain Computer Interface (BCI): a case study of training for recovery of volitional motor control after stroke. Journal of neurologic physical therapy : JNPT, 33 (4):203–11, dec 2009. ISSN 1557-0584. doi: 10.1097/NPT.0b013e3181c1fc0b. URL http://www.ncbi.nlm.nih.gov/pubmed/20208465.

[87] J del R Millán, F Renkens, J Mourino, and W Gerstner. Noninvasive Brain-Actuated Control of a Mobile Robot by Human EEG. IEEE Transactions on Biomedical Engineering, 51(6)(6):1026–1033, 2004. ISSN 0018-9294. doi: 10.1109/TBME.2004.827086.

[88] Brice Rebsamen, Cuntai Guan, Haihong Zhang, Chuanchu Wang, Cheeleong Teo, Marcelo H Ang, and Etienne Burdet. A brain controlled wheelchair to navigate in familiar environments. IEEE transactions on neural systems and rehabilitation engineering : a publication of the IEEE Engineering in Medicine and Biology Society, 18(6):590–8, dec 2010. ISSN 1558-0210. doi: 10.1109/TNSRE.2010.2049862. URL http://www.ncbi.nlm.nih.gov/pubmed/20460212.

[89] Gernot R. Müller-Putz and Gert Pfurtscheller. Control of an electrical prosthesis with an SSVEP-based BCI. IEEE Transactions on Biomedical Engineering, 55(1):361–364, 2008. ISSN 00189294. doi: 10.1109/TBME.2007.897815.

[90] Leigh R Hochberg, Mijail D Serruya, Gerhard M Friehs, Jon a Mukand, Maryam Saleh, Abraham H Caplan, Almut Branner, David Chen, Richard D Penn, and John P Donoghue. Neuronal ensemble control of prosthetic devices by a human with tetraplegia. Nature, 442(7099):164–71, jul 2006. ISSN

1476-4687. doi: 10.1038/nature04970. URL http://www.ncbi.nlm.nih.gov/pubmed/16838014.

[91] Danny Plass-oude Bos, Boris Reuderink, Bram Van De Laar, Hayrettin Gürkök, Christian Mühl, Mannes Poel, Anton Nijholt, and Dirk Heylen. Brain-Computer Interfaces. In Brain-Computer Interfaces: Applying our Minds to Human-Computer Interaction, chapter Brain-Comp, pages 149–178. Springer London, London, 2010. ISBN 978-3-642-02090-2. doi: 10.1007/978-3-642-02091-9. URL http://link.springer.com/10.1007/978-3-642-02091-9.

[92] Bojan Kerous, Filip Skola, and Fotis Liarokapis. EEG-based BCI and video games: a progress report. Virtual Reality, pages 1–17, 2017. ISSN 1359-4338. doi: 10.1007/s10055-017-0328-x. URL http://link.springer.com/10.1007/s10055-017-0328-x.

[93] Alessandro Luiz Stamatto Ferreira, Juvane Nunes Marciano, Leonardo Cunha de Miranda, and Erica Esteves Cunha de Miranda. Understanding and Proposing a Design Rationale of Digital Games based on Brain-Computer Interface: Results of the AdmiralMind Battleship Study. SBC Journal on Interactive Systems, 5(1):3–15, 2014. ISSN 2236-3297. URL http://seer.ufrgs.br/index.php/jis/article/view/42950{%}5Cnhttp://seer.ufrgs.br/index.php/jis/article/download/42950/30095.

[94] Bonkon Koo, Hwan Gon Lee, Yunjun Nam, and Seungjin Choi. Immersive BCI with SSVEP in VR head-mounted display. Proceedings of the Annual International Conference of the IEEE Engineering in Medicine and Biology Society, EMBS, 2015-Novem:1103–1106, 2015. ISSN 1557170X. doi: 10.1109/EMBC.2015.7318558.

[95] Abdulla Ali and Sadasivan Puthusserypady. A 3D learning playground for potential attention training in ADHD: A brain computer interface approach. Proceedings of the Annual International Conference of the IEEE Engineering in Medicine and Biology Society, EMBS, 2015-Novem:67–70, 2015. ISSN 1557170X. doi: 10.1109/EMBC.2015.7318302.

[96] Chi Man Wong, Qi Tang, Janir Nuno Da Cruz, and Feng Wan. A multi-channel SSVEP-based BCI for computer games with analogue control. 2015

IEEE International Conference on Computational Intelligence and Virtual Environments for Measurement Systems and Applications, CIVEMSA 2015, 2015. doi: 10.1109/CIVEMSA.2015.7158612.

[97] Nikolay Chumerin, Nikolay V. Manyakov, Marijn Van Vliet, Arne Robben, Adrien Combaz, and Marc M. Van Hulle. Steady-state visual evoked potential-based computer gaming on a consumer-grade EEG device. IEEE Transactions on Computational Intelligence and AI in Games, 5(2):100–110, 2013. ISSN 1943068X. doi: 10.1109/TCIAIG.2012.2225623.

[98] Jozef Legény, Raquel Viciana-Abad, and Anatole Lécuyer. Toward contextual SSVEP-based BCI controller: Smart activation of stimuli and control weighting. IEEE Transactions on Computational Intelligence and AI in Games, 5(2):111–116, 2013. ISSN 1943068X. doi: 10.1109/TCIAIG.2013. 2252348.

[99] Ricardo Parafita, Gabriel Pires, Urbano Nunes, and Miguel Castelo-Branco. A spacecraft game controlled with a brain-computer interface using SSVEP with phase tagging. SeGAH 2013 - IEEE 2nd International Conference on Serious Games and Applications for Health, Book of Proceedings, 2013. doi: 10.1109/SeGAH.2013.6665309.

[100] Marijn Van Vliet, Arne Robben, Nikolay Chumerin, Nikolay V. Manyakov, Adrien Combaz, and Marc M. Van Hulle. Designing a brain-computer interface controlled video-game using consumer grade EEG hardware. In Biosignals and Biorobotics Conference (BRC), 2012 ISSNIP, pages 1–6, 2012. ISBN 9781467324762. doi: 10.1109/BRC.2012.6222186.

[101] Gido Hakvoort, Hayrettin Gürkök, Danny Plass-Oude Bos, Michel Obbink, and Mannes Poel. Measuring immersion and affect in a brain-computer interface game. Lecture Notes in Computer Science (including subseries Lecture Notes in Artificial Intelligence and Lecture Notes in Bioinformatics), 6946 LNCS(PART 1):115–128, 2011. ISSN 03029743. doi: 10.1007/978-3-642-23774-4_12.

[102] Nishant a. Mehta, Sadhir Hussain S. Hameed, and Melody Moore Jackson. Optimal Control Strategies for an SSVEP-Based Brain-Computer Interface. International Journal of Human-Computer Interaction, 27(1):85–101, 2010. ISSN 1044-7318. doi: 10.1080/10447318.2011.535755.

[103] C. Mühl, H. Gürkök, D. Plass-Oude Bos, M.E. ME Thurlings, L. Scherffig, M. Duvinage, A.A. AA Elbakyan, S. Kang, M. Poel, and DKJ D.K.J. Heylen. Bacteria Hunt: A multimodal, multiparadigm BCI game. In Proceedings of the Fifth International Summer Workshop on Multimodal Interfaces, eNTERFACE'09, pages 41–62, 2010. doi: 10.1007/s12193-010-0046-0. URL http://doc.utwente.nl/69553/.

[104] E. C. Lalor, S. P. Kelly, C. Finucane, R. Burke, R. Smith, R. B. Reilly, and G. McDarby. Steady-state VEP-based brain-computer interface control in an immersive 3D gaming environment. Eurasip Journal on Applied Signal Processing, 2005(19):3156–3164, 2005. ISSN 11108657. doi: 10.1155/ASP. 2005.3156.

[105] Bashar Awwad Shiekh Hasan and John Q Gan. Hangman BCI : An unsupervised adaptive self-paced Brain Computer Interface for playing games. Computers in Biology and Medicine, 42(5):598–606, 2012. ISSN 0010-4825. doi: 10.1016/j.compbiomed.2012.02.004. URL http://dx.doi.org/10.1016/j.compbiomed.2012.02.004.

[106] Javier Asensio-Cubero, John Q. Gan, and Ramaswamy Palaniappan. Multiresolution analysis over graphs for a motor imagery based online BCI game. Computers in Biology and Medicine, 68:21–26, 2016. ISSN 18790534. doi: 10.1016/j.compbiomed.2015.10.016. URL http://dx.doi.org/10.1016/j.compbiomed.2015.10.016.

[107] Qi Bin Zhao, Li Qing Zhang, and Andrzej Cichocki. EEG-based asynchronous BCI control of a car in 3D virtual reality environments. Chinese Science Bulletin, 54(1):78–87, 2009. ISSN 10016538. doi: 10.1007/s11434-008-0547-3.

[108] Robert Leeb, Marcel Lancelle, and Vera Kaiser. Thinking Penguin:Multimodal Brain-Computer Interface Control of a VR Game. Computational . . . , 5(c):1–12, 2013. ISSN 1943-068X. doi: 10.1109/TCIAIG.2013.2242072. URL http://www.marcel-lancelle.de/research/publications/.

[109] M. Pregenzer. Distinction Sensitive Learning Vector Quantization (DSLVQ) - application as a classifier based feature selection method for a brain computer interface. In 4th International Conference on Artificial Neural Networks, pages 433–436, 1995. ISBN 0 85296 641 5. doi: 10.

1049/cp:19950595. URL http://digital-library.theiet.org/content/conferences/10.1049/cp{_}19950595.

[110] Laurent Bonnet, Fabien Lotte, L Anatole, Inria Rennes, and Inria Bordeaux. Two Brains , One Game : Design and Evaluation of a Multi-User BCI Video Game Based on Motor Imagery To cite this version : Two Brains , One Game : Design and Evaluation of a Multi-User BCI Video Game Based on Motor Imagery. IEEE Transactions on Computational Intelligence and AI in games, IEEE Computational Intelligence Society, 5(2):185–198, 2013. ISSN 1943-068X. doi: 10.1109/TCIAIG.2012.2237173.

[111] Takeshi Sakurada, Toshihiro Kawase, Tomoaki Komatsu, and Kenji Kansaku. Use of high-frequency visual stimuli above the critical flicker frequency in a SSVEP-based BMI. Clinical Neurophysiology, 126(10):1972–1978, 2015. ISSN 18728952. doi: 10.1016/j.clinph.2014.12.010. URL http://dx.doi.org/10.1016/j.clinph.2014.12.010.

[112] Pablo F. Diez, Vicente A. Mut, Eric Laciar, and Enrique M. Avila Perona. Mobile robot navigation with a self-paced brain-computer interface based on high- frequency SSVEP. Robotica, 32(November 2013): 695–709, 2014. ISSN 0263-5747. doi: 10.1017/S0263574713001021. URL http://www.scopus.com/inward/record.url?eid=2-s2.0-84888194023{&}partnerID=tZOtx3y1.

[113] Wenqiang Yan, Guanghua Xu, Min Li, Jun Xie, Chengcheng Han, Sicong Zhang, Ailing Luo, and Chaoyang Chen. Steady-State Motion Visual Evoked Potential (SSMVEP) based on equal luminance colored enhancement. PLoS ONE, 12(1):1–18, 2017. ISSN 19326203. doi: 10.1371/journal.pone.0169642.

[114] Jing Chen, Matteo Valsecchi, and Karl R Gegenfurtner. Enhanced brain responses to color during smooth pursuit eye movements. Journal of Neurophysiology, 49(0):jn.00208.2017, 2017. ISSN 0022-3077. doi: 10.1152/jn.00208.2017. URL http://jn.physiology.org/lookup/doi/10.1152/jn.00208.2017.

[115] Hooman Nezamfar, Seyed Sadegh Mohseni Salehi, and Deniz Erdogmus. Stimuli with opponent colors and higher bit rate enable higher accuracy for C-VEP BCI. 2015 IEEE Signal Processing in Medicine and Biology Symposium - Proceedings, 2016. doi: 10.1109/SPMB.2015.7405476.

[116] Leo M. Hurvich and Dorothea Jameson. An opponent-process theory of color vision. Psychological Review, 64(6, Pt.1):384–404, 1957. ISSN 0033-295X. doi: 10.1037/h0041403. URL http://doi.apa.org/getdoi.cfm?doi=10.1037/h0041403.

[117] Qingguo Wei, Siwei Feng, and Zongwu Lu. Stimulus specificity of brain-computer interfaces based on code modulation visual evoked potentials. PLoS ONE, 11(5):1–17, 2016. ISSN 19326203. doi: 10.1371/journal.pone.0156416.

[118] Marcin Jukiewicz and Anna Cysewska-Sobusiak. Stimuli design for SSVEP-based brain computer-interface. International Journal of Electronics and Telecommunications, 62(2):109–113, 2016. ISSN 20818491. doi: 10.1515/eletel-2016-0014.

[119] Richard Junior Manuel Godinez Tello, Sandra Mara Torres Müller, André Ferreira, and Teodiano Freire Bastos. Comparison of the influence of stimuli color on steady-state visual evoked potentials. Revista Brasileira de Engenharia Biomedica, 31(3):218–231, 2015. ISSN 19847742. doi: 10.1590/2446-4740.0739.

[120] Teng Cao, Feng Wan, Chi Man Wong, Janir Nuno da Cruz, and Yong Hu. Objective evaluation of fatigue by EEG spectral analysis in steady-state visual evoked potential-based brain-computer interfaces. Biomedical engineering online, 13(1):28, 2014. ISSN 1475-925X. doi: 10.1186/1475-925X-13-28. URL http://www.pubmedcentral.nih.gov/articlerender.fcgi?artid=3995691{&}tool=pmcentrez{&}rendertype=abstract.

[121] Jun Xie, Guanghua Xu, Jing Wang, Min Li, Chengcheng Han, and Yaguang Jia. Effects of mental load and fatigue on steady-state evoked potential based brain computer interface tasks: A comparison of periodic flickering and motion-reversal based visual attention. PLoS ONE, 11(9):1–15, 2016. ISSN 19326203. doi: 10.1371/journal.pone.0163426.

[122] Zhihua Tang, Yijun Wang, Guoya Dong, and Weihua Pei. Learning to Control an SSVEP-Based BCI Speller in Naïve Subjects. In Engineering in Medicine and Biology Society (EMBC), 2017 39th Annual International Conference of the IEEE, pages 1934–1937, 2017. ISBN 9781509028092.

[123] Ivo Käthner, Selina C. Wriessnegger, Gernot R. Müller-Putz, Andrea Kübler, and Sebastian Halder. Effects of mental workload and fatigue on the P300, alpha and theta band power during operation of an ERP (P300) brain-computer interface. Biological Psychology, 102(1):118–129, 2014. ISSN 18736246. doi: 10.1016/j.biopsycho.2014.07.014. URL http://dx.doi.org/10.1016/j.biopsycho.2014.07.014.

[124] Jingjing Chen, Dan Zhang, Andreas K. Engel, Qin Gong, and Alexander Maye. Application of a single-flicker online SSVEP BCI for spatial navigation. PLoS ONE, 12(5):1–13, 2017. ISSN 19326203. doi: 10.1371/journal.pone.0178385.

[125] Samantha A. Sprague, Matthew T. McBee, and Eric W. Sellers. The effects of working memory on brain-computer interface performance. Clinical Neurophysiology, 127(2):1331–1341, 2016. ISSN 18728952. doi: 10.1016/j.clinph.2015.10.038. URL http://dx.doi.org/10.1016/j.clinph.2015.10.038.

[126] Karuna Subramaniam and Sophia Vinogradov. Improving the neural mechanisms of cognition through the pursuit of happiness. Frontiers in Human Neuroscience, 7(August):1–11, 2013. ISSN 1662-5161. doi: 10.3389/fnhum.2013.00452.

[127] Katharina Paul, Wioleta Walentowska, Jasmina Bakic, Thibaut Dondaine, and Gilles Pourtois. Modulatory effects of happy mood on performance monitoring: Insights from error-related brain potentials. Cognitive, Affective, & Behavioral Neuroscience, 17(1):106–123, 2017. ISSN 1530-7026. doi: 10.3758/s13415-016-0466-8. URL http://link.springer.com/10.3758/s13415-016-0466-8.

[128] Femke Nijboer, Adrian Furdea, Ingo Gunst, Jürgen Mellinger, Dennis J. McFarland, Niels Birbaumer, and Andrea Kübler. An auditory brain-computer interface (BCI). Journal of Neuroscience Methods, 167(1):43–50, 2008. ISSN 01650270. doi: 10.1016/j.jneumeth.2007.02.009.

[129] Femke Nijboer, Niels Birbaumer, and Andrea Kübler. The influence of psychological state and motivation on brain-computer interface performance in patients with amyotrophic lateral sclerosis - a longitudinal study. Frontiers in Neuroscience, 4(JUL):1–13, 2010. ISSN 16624548. doi: 10.3389/fnins.2010.00055.

Bibliography

[130] James Henshaw, Wei Liu, and Daniela Romano. Problem Solving Using Hybrid Brain-Computer Interface Methods : a Review. In Cognitive Infocommunications (CogInfoCom), 2014 5th IEEE Conference on, pages 215–219, 2014.

[131] D H Brainard. The Psychophysics Toolbox. Spatial vision, 10(4):433–436, 1997. ISSN 0169-1015. doi: 10.1163/156856897X00357.

[132] D G Pelli. The VideoToolbox software for visual psychophysics: transforming numbers into movies., 1997. ISSN 0169-1015.

[133] Mario Kleiner, David Brainard, Denis Pelli, Allen Ingling, Richard Murray, and Christopher Broussard. What ' s new in Psychtoolbox-3 ? Foreword ; -). Perception, 36(14):1–89, 2007.

[134] Hubert Cecotti, Ivan Volosyak, and Axel Gräser. RELIABLE VISUAL STIMULI ON LCD SCREENS FOR SSVEP BASED BCI. In The 2010 European Signal Processing Conference (EUSIPCO-2010), pages 919–923, 2010.

[135] Robert Oostenveld, Pascal Fries, Eric Maris, and Jan Mathijs Schoffelen. FieldTrip: Open source software for advanced analysis of MEG, EEG, and invasive electrophysiological data. Computational Intelligence and Neuroscience, 2011, 2011. ISSN 16875265. doi: 10.1155/2011/156869.

[136] Malte Sengelmann, Andreas K. Engel, and Alexander Maye. Maximizing information transfer in SSVEP-based brain computer interfaces. IEEE Transactions on Biomedical Engineering, 9294(c):1–1, 2016. ISSN 0018-9294. doi: 10.1109/TBME.2016.2559527. URL http://ieeexplore.ieee.org/lpdocs/epic03/wrapper.htm?arnumber=7460915.

[137] Desney Tan and Anton Nijholt. Human-computer Interaction. 2010. ISBN 9781849962711.

[138] John D Mayer and Y N Gaschke. Brief Mood Introspection Scale (BMIS). Psychology, 19(3):1995–1995, 2001. ISSN 0022-3514.

[139] Trudie Chalder, G Berelowitz, Teresa Pawlikowska, Louise Watts, S Wessely, D Wright, and E P Wallace. Development of a Fatigue Scale. Journal of Psychsomatic Research, 37 (2):147–153, 1993. URL http://ac.els-cdn.com.acces.bibl.

ulaval.ca/002239999390081P/1-s2.0-002239999390081P-main.
pdf?{_}tid=feda7a26-7879-11e7-a2f4-00000aacb35f{&}acdnat=
1501785283{_}ac70ec437dd00596ec6bfdf7529db68b.

[140] Wijnand IJsselsteijn, Karolien Poels, and Yvonne A. de Kort. The Game
Experience Questionnaire: Development of a self-report measure to assess
player experiences of digital games. Technical report, TU Eindhoven, Eind-
hoven, The Netherlands, 2008.

[141] Nikolay V Manyakov, Nikolay Chumerin, Arne Robben, Adrien Combaz,
Marijn van Vliet, and Marc M Van Hulle. Sampled sinusoidal stimulation
profile and multichannel fuzzy logic classification for monitor-based phase-
coded SSVEP brain-computer interfacing. Journal of neural engineering, 10
(3):036011, 2013. ISSN 1741-2552. doi: 10.1088/1741-2560/10/3/036011.
URL http://www.ncbi.nlm.nih.gov/pubmed/23594762.

[142] Cybathlon: World's first 'bionic Olympics' gears up, 2016. URL http:
//www.bbc.co.uk/news/technology-37196860.

[143] Benjamin Blankertz, Claudia Sannelli, Sebastian Halder, Eva M. Ham-
mer, Andrea K??bler, Klaus Robert M??ller, Gabriel Curio, and Thorsten
Dickhaus. Neurophysiological predictor of SMR-based BCI perfor-
mance. NeuroImage, 51(4):1303–1309, 2010. ISSN 10538119. doi:
10.1016/j.neuroimage.2010.03.022. URL http://dx.doi.org/10.1016/j.
neuroimage.2010.03.022.

[144] Minkyu Ahn, Hohyun Cho, Sangtae Ahn, and Sung Chan Jun. High theta
and low alpha powers may be indicative of BCI-illiteracy in motor imagery.
PLoS ONE, 8(11), 2013. ISSN 19326203. doi: 10.1371/journal.pone.0080886.

[145] Cecilia L. Maeder, Claudia Sannelli, Stefan Haufe, and Benjamin Blankertz.
Pre-stimulus sensorimotor rhythms influence brain-computer interface clas-
sification performance. IEEE Transactions on Neural Systems and
Rehabilitation Engineering, 20(5):653–662, 2012. ISSN 15344320. doi:
10.1109/TNSRE.2012.2205707.

[146] D Louis Collins, Alex P Zijdenbos, W F C Baaré, and Alan C
Evans. ANIMAL+INSECT: Improved cortical structure seg-
mentation. In Information Processing In Medical Imaging,
Proceedings, pages 210–223, 1999. ISBN 978-3-540-66167-2. doi:

10.1007/3-540-48714-X. URL `http://apps.webofknowledge.com/InboundService.do?SID=V1Mh6doOHnf4594ppeI{&}product=WOS{&}UT=000170515200016{&}SrcApp=Papers{&}DestFail=http://www.webofknowledge.com{&}Init=Yes{&}action=retrieve{&}Func=Frame{&}customersID=mekentosj{&}SrcAuth=mekentosj{&}IsProductC{%}5Cnhttp://a`.

[147] Vladimir Fonov, Alan C. Evans, Kelly Botteron, C. Robert Almli, Robert C. McKinstry, and D. Louis Collins. Unbiased average age-appropriate atlases for pediatric studies. NeuroImage, 54(1):313–327, 2011. ISSN 10538119. doi: 10.1016/j.neuroimage.2010.07.033. URL `http://dx.doi.org/10.1016/j.neuroimage.2010.07.033`.

[148] Aleksandr Zaitcev. EEG source imaging for improved control BCI performance. PhD thesis, 2016.

[149] Michael Tangermann, Klaus Robert Müller, Ad Aertsen, Niels Birbaumer, Christoph Braun, Clemens Brunner, Robert Leeb, Carsten Mehring, Kai J. Miller, Gernot R. Müller-Putz, Guido Nolte, Gert Pfurtscheller, Hubert Preissl, Gerwin Schalk, Alois Schlögl, Carmen Vidaurre, Stephan Waldert, and Benjamin Blankertz. Review of the BCI competition IV. Frontiers in Neuroscience, 6(JULY):1–31, 2012. ISSN 16624548. doi: 10.3389/fnins.2012.00055.

[150] Jacob Cohen. A power primer. Psychological Bulletin, 112(1):155–159, 1992. ISSN 1939-1455. doi: 10.1037/0033-2909.112.1.155. URL `http://doi.apa.org/getdoi.cfm?doi=10.1037/0033-2909.112.1.155`.

Appendix A

Appendix A - Questionnaires Used

Colour 1: Participant Information

*Required

Participant Number *

Your answer

Sex

○ Female

○ Male

○ Prefer not to say

○ Other:

Age

Your answer

Handedness

○ Right

○ Left

○ Ambidextrous

Colour Perception (Completed By Researcher)

○ Normal Colour Vision

○ Mild Deutan

○ Moderate Deutan

○

○ Strong Deutan

○ Mild Protan

○ Moderate Protan

○ Strong Protan

○ Tritan

SUBMIT

Never submit passwords through Google Forms.

This form was created inside University of Sheffield. Report Abuse - Terms of Service - Additional Terms

Google Forms

QUESTIONS   RESPONSES   21

Colour 2: Task Preference Questionnaire

Please rate the level of visual comfort of each stimulus colour

Participant Number *

Short-answer text

White

	1	2	3	4	5	6	7	8	9	10	
Very uncomfortable	○	○	○	○	○	○	○	○	○	○	Very Comfortable

Red

	1	2	3	4	5	6	7	8	9	10	
Very uncomfortable	○	○	○	○	○	○	○	○	○	○	Very Comfortable

Blue

	1	2	3	4	5	6	7	8	9	10	
Very uncomfortable	○	○	○	○	○	○	○	○	○	○	Very Comfortable

Yellow

	1	2	3	4	5	6	7	8	9	10

Colour 3: Mood/fatigue Questionnaire 1

This questionnaire assesses your current mood and fatigue levels

*Required

1. **Participant Number** *

   _____

2. **I feel lively** *
   Mark only one oval.

   ( ) Strongly disagree

   ( ) Disagree

   ( ) Neither agree or disagree

   ( ) Agree

   ( ) Strongly Agree

3. **I feel happy** *
   Mark only one oval.

   ( ) Strongly disagree

   ( ) Disagree

   ( ) Neither agree or disagree

   ( ) Agree

   ( ) Strongly Agree

4. **I feel sad** *
   Mark only one oval.

   ( ) Strongly disagree

   ( ) Disagree

   ( ) Neither agree or disagree

   ( ) Agree

   ( ) Strongly Agree

5. **I feel tired** *
   Mark only one oval.

   ( ) Strongly disagree

   ( ) Disagree

   ( ) Neither agree or disagree

   ( ) Agree

   ( ) Strongly Agree

6. **I feel caring** *
Mark only one oval.

- ( ) Strongly disagree
- ( ) Disagree
- ( ) Neither agree or disagree
- ( ) Agree
- ( ) Strongly Agree

7. **I feel content (satisfied)** *
Mark only one oval.

- ( ) Strongly disagree
- ( ) Disagree
- ( ) Neither agree or disagree
- ( ) Agree
- ( ) Strongly Agree

8. **I feel grouchy (grumpy, moody)** *
Mark only one oval.

- ( ) Strongly disagree
- ( ) Disagree
- ( ) Neither agree or disagree
- ( ) Agree
- ( ) Strongly Agree

9. **I feel peppy (alert, active)** *
Mark only one oval.

- ( ) Strongly disagree
- ( ) Disagree
- ( ) Neither agree or disagree
- ( ) Agree
- ( ) Strongly Agree

10. **I feel nervous** *
Mark only one oval.

- ( ) Strongly disagree
- ( ) Disagree
- ( ) Neither agree or disagree
- ( ) Agree
- ( ) Strongly Agree

11. **I feel calm** *

Mark only one oval.

- ( ) Strongly disagree
- ( ) Disagree
- ( ) Neither agree or disagree
- ( ) Agree
- ( ) Strongly Agree

12. **I feel loving** *

Mark only one oval.

- ( ) Strongly disagree
- ( ) Disagree
- ( ) Neither agree or disagree
- ( ) Agree
- ( ) Strongly Agree

13. **I feel fed up** *

Mark only one oval.

- ( ) Strongly disagree
- ( ) Disagree
- ( ) Neither agree or disagree
- ( ) Agree
- ( ) Strongly Agree

14. **I feel active** *

Mark only one oval.

- ( ) Strongly disagree
- ( ) Disagree
- ( ) Neither agree or disagree
- ( ) Agree
- ( ) Strongly Agree

15. **Do you feel sleepy or drowsy?** *

Mark only one oval.

- ( ) Strongly disagree
- ( ) Disagree
- ( ) Neither agree or disagree
- ( ) Agree
- ( ) Strongly Agree

16. **Are you lacking in energy?** *
   Mark only one oval.

   ( ) Strongly disagree

   ( ) Disagree

   ( ) Neither agree or disagree

   ( ) Agree

   ( ) Strongly Agree

17. **Do you have less strength in your muscles than usual?** *
   Mark only one oval.

   ( ) Strongly disagree

   ( ) Disagree

   ( ) Neither agree or disagree

   ( ) Agree

   ( ) Strongly Agree

18. **Do you feel weak?** *
   Mark only one oval.

   ( ) Strongly disagree

   ( ) Disagree

   ( ) Neither agree or disagree

   ( ) Agree

   ( ) Strongly Agree

19. **Do you have difficulty concentrating?** *
   Mark only one oval.

   ( ) Strongly disagree

   ( ) Disagree

   ( ) Neither agree or disagree

   ( ) Agree

   ( ) Strongly Agree

20. **Do you have problems thinking clearly?** *
   Mark only one oval.

   ( ) Strongly disagree

   ( ) Disagree

   ( ) Neither agree or disagree

   ( ) Agree

   ( ) Strongly Agree

Powered by

Google Forms

Colour 4: Game Preference Questionnaire
*Required

1. **Participant Number** *

   _____

2. **During game control, which of these statements applies to you?**
   Mark only one oval.

   ( ) I preferred using the white stimuli

   ( ) I preferred using the colour stimuli

   ( ) I had no preference

3. **Eye strain level (white stimuli)**
   Mark only one oval.

	1	2	3	4	5	6	7	8	9	10	
Very low	( )	( )	( )	( )	( )	( )	( )	( )	( )	( )	Very high

4. **Eye strain level (colour stimuli)**
   Mark only one oval.

	1	2	3	4	5	6	7	8	9	10	
Very low	( )	( )	( )	( )	( )	( )	( )	( )	( )	( )	Very high

5. **Feeling of Control (white stimuli)**
   Mark only one oval.

	1	2	3	4	5	6	7	8	9	10	
Very low	( )	( )	( )	( )	( )	( )	( )	( )	( )	( )	Very high

6. **Feeling of Control (colour stimuli)**
   Mark only one oval.

	1	2	3	4	5	6	7	8	9	10	
Very low	( )	( )	( )	( )	( )	( )	( )	( )	( )	( )	Very high

7. **Overall Fatigue (white stimuli)**
Mark only one oval.

	1	2	3	4	5	6	7	8	9	10	
Very low	⬭	⬭	⬭	⬭	⬭	⬭	⬭	⬭	⬭	⬭	Very high

8. **Overall Fatigue (colour stimuli)**
Mark only one oval.

	1	2	3	4	5	6	7	8	9	10	
Very low	⬭	⬭	⬭	⬭	⬭	⬭	⬭	⬭	⬭	⬭	Very high

9. **Overall Mood (white stimuli)**
Mark only one oval.

	1	2	3	4	5	6	7	8	9	10	
Very low	⬭	⬭	⬭	⬭	⬭	⬭	⬭	⬭	⬭	⬭	Very high

10. **Overall Mood (colour stimuli)**
Mark only one oval.

	1	2	3	4	5	6	7	8	9	10	
Very low	⬭	⬭	⬭	⬭	⬭	⬭	⬭	⬭	⬭	⬭	Very high

Powered by

Google Forms

Colour 6: Game Experience Questionnaire

Please complete the following questionnaire with regards to your experience while playing the BCI game

1. **Participant Number** *

_____

2. **I felt content**
   Mark only one oval.

   ⬭ Strongly disagree

   ⬭ Disagree

   ⬭ Neither agree or disagree

   ⬭ Agree

   ⬭ Strongly agree

3. **I felt skilful**
   Mark only one oval.

   ⬭ Strongly disagree

   ⬭ Disagree

   ⬭ Neither agree or disagree

   ⬭ Agree

   ⬭ Strongly agree

4. **I thought it was fun**
   Mark only one oval.

   ⬭ Strongly disagree

   ⬭ Disagree

   ⬭ Neither agree or disagree

   ⬭ Agree

   ⬭ Strongly agree

5. **I was fully occupied with the game**
   Mark only one oval.

   ⬭ Strongly disagree

   ⬭ Disagree

   ⬭ Neither agree or disagree

   ⬭ Agree

   ⬭ Strongly agree

6. **I felt happy**

   Mark only one oval.

   ( ) Strongly disagree

   ( ) Disagree

   ( ) Neither agree or disagree

   ( ) Agree

   ( ) Strongly agree

7. **I found it tiresome**

   Mark only one oval.

   ( ) Strongly disagree

   ( ) Disagree

   ( ) Neither agree or disagree

   ( ) Agree

   ( ) Strongly agree

8. **I felt competent (efficient and capable)**

   Mark only one oval.

   ( ) Strongly disagree

   ( ) Disagree

   ( ) Neither agree or disagree

   ( ) Agree

   ( ) Strongly agree

9. **I thought it was hard**

   Mark only one oval.

   ( ) Strongly disagree

   ( ) Disagree

   ( ) Neither agree or disagree

   ( ) Agree

   ( ) Strongly agree

10. **It was aesthetically pleasing**

    Mark only one oval.

    ( ) Strongly disagree

    ( ) Disagree

    ( ) Neither agree or disagree

    ( ) Agree

    ( ) Strongly agree

11. **I forgot everything around me**
Mark only one oval.

- ( ) Strongly disagree
- ( ) Disagree
- ( ) Neither agree or disagree
- ( ) Agree
- ( ) Strongly agree

12. **It felt good**
Mark only one oval.

- ( ) Strongly disagree
- ( ) Disagree
- ( ) Neither agree or disagree
- ( ) Agree
- ( ) Strongly agree

13. **I was good at it**
Mark only one oval.

- ( ) Strongly disagree
- ( ) Disagree
- ( ) Neither agree or disagree
- ( ) Agree
- ( ) Strongly agree

14. **I felt bored**
Mark only one oval.

- ( ) Strongly disagree
- ( ) Disagree
- ( ) Neither agree or disagree
- ( ) Agree
- ( ) Strongly agree

15. **I felt successful**
Mark only one oval.

- ( ) Strongly disagree
- ( ) Disagree
- ( ) Neither agree or disagree
- ( ) Agree
- ( ) Strongly agree

16. **I felt that I could explore things**

Mark only one oval.

◯ Strongly disagree

◯ Disagree

◯ Neither agree or disagree

◯ Agree

◯ Strongly agree

17. **I was fast at reaching the game's targets**

Mark only one oval.

◯ Strongly disagree

◯ Disagree

◯ Neither agree or disagree

◯ Agree

◯ Strongly agree

18. **I felt annoyed**

Mark only one oval.

◯ Strongly disagree

◯ Disagree

◯ Neither agree or disagree

◯ Agree

◯ Strongly agree

19. **I felt pressured**

Mark only one oval.

◯ Strongly disagree

◯ Disagree

◯ Neither agree or disagree

◯ Agree

◯ Strongly agree

20. **I felt irritable**

Mark only one oval.

◯ Strongly disagree

◯ Disagree

◯ Neither agree or disagree

◯ Agree

◯ Strongly agree

21. **I was deeply concentrated in the game**
    Mark only one oval.

    ◯ Strongly disagree

    ◯ Disagree

    ◯ Neither agree or disagree

    ◯ Agree

    ◯ Strongly agree

Powered by

Google Forms